Causes and Consequences of Hybrid Incompatibilities in *Arabidopsis thaliana*

Dissertation

der Mathematisch-Naturwissenschaftlichen Fakultät

der Eberhard Karls Universität Tübingen

zur Erlangung des Grades eines

Doktors der Naturwissenschaften

(Dr. rer. nat.)

vorgelegt von

Subhashini Muralidharan

aus Chennai, Indien

Tübingen

2015

Gedruckt mit Genehmigung der Mathematisch-Naturwissenschaftlichen Fakultät der Eberhard Karls Universität Tübingen.

Tag der mündlichen Qualifikation:	21.09.2015
Dekan:	Prof. Dr. Wolfgang Rosenstiel
1. Berichterstatter:	Prof. Dr. Detlef Weigel
2. Berichterstatter:	Prof. Dr. Rita Groß-Hardt

To Ajay,
in lieu of the walk in the forest
that we never went on.

ACKNOWLEDGMENTS

I would like to thank,

Detlef Weigel, for the opportunity of working in his department, for ensuring a steep climb and a great view, for his faith in my abilities in the beginning, for his concern in the middle and for his renewed faith in me towards the end.

Rita Groß-Hardt, for agreeing to be my second supervisor, along with Richard Neher and Ralf Sommer, for being part of my Thesis Advisory Committee and for the support and inputs that I have received over the years.

Beth Rowan, for her clarity of thought, positivity, encouragement and continuous support.

Roosa Laitinen, for guidance and enthusiasm when I started, for the continued interest in my career and support from far away.

Jun Cao, Eunyoung Chae, Anette Habring-Mueller, William Ho, Darya Karelina, Yasushi Kobayashi, Dan Koenig, Frank Kuettner, Christa Lanz, Chang Liu, Pablo Manavella, Josip Perkovic, Jathish Ponnu, Jens Riexinger, Ignacio Rubio, Patrice Salome, Emanuele Scacchi, Korbinian Schneeberger, Rebecca Schwab, Danelle Seymour, Lisa Smith, Marco Todesco, George Wang, Xi Wang, Norman Warthmann, Huelya Wicher and Wangsheng Zhu for asking and answering questions.

Markus Schneller, for bringing very old books from different corners of Germany to me.

Eshita Sharma, Maricris Zaidem, Johannes Kaut, Diep Tran, Dino Jolic, Patricia Lang, Vinicius Costa Galvao, Effie Symeonidi, Giovanna Capovilla, Silvio Collani, Gautam Shirsekar, Noemi Skorzinski for the fun times and the crazy times.

Joerg Hagmann, for being such a nice guy and also for going to Europa Park without me.

The developers of Google Translate, for my Zusammenfassung and Patricia Lang, for editing it.

Janani, Roopika, Ratna, Vasuki, Ruchika, Balaji, Amit, Shruthi, Prajwal, Ali, Vaishnavi, Prateek, for their friendship and for bringing along their piece of India to Tuebingen.

Amrita Mukherjee, for being my violin partner and Max Bock, for being a wonderful teacher.

Phil Wigge, Mathew Box, Emma Sedivy and all members of the Wigge group at the Sainsbury Laboratory, Cambridge, for their enthusiasm and help.

Ms. Umabai, for introducing a bunch of bored 6th-graders to Dolly.

Utpal Nath and Usha Vijayaraghavan, for getting me hooked on plant genetics, Renee Borges for the most enjoyable time I've had doing science, Pooja, Kavitha, Anusha, Mahua, Yuvi, Mainak, Prem and Sushil, for the leg up and for their friendship.

Nishad, Kalyani, Monisha, Mansi, Diptarup, Sumeet, Kajari, Ruby, Vaishnavi, Shobhna, Smrithi, Ram, Keshav, for their love and affection and for being a second family to me.

My parents, for their unconditional support for each and every thing that I do, my in-laws and my extended family, for their encouragement and their belief in my abilities.

My husband, Sridhar, to whom this thesis belongs and means as much as it does to me.

CONTENTS

LIST OF ABBREVIATIONS

2,4-D	2,4-Dichlorophenoxyacetic acid
2,4-D ME	2,4-Dichlorophenoxy acetic acid methyl ester
AEP2	*ATPase EXPRESSION 2*
AM	Axillary meristem
ARE	*ANTHOCYANIN REDUCED*
ARR	*ARABIDOPSIS RESPONSE REGULATOR*
BDM	Bateson-Dobzhansky-Muller
BP	*BREVIPEDICELLUS*
BRC1	*BRANCHED1*
BSC	Biological Species Concept
CAPS	Cleaved Amplified Polymorphic sequence
cdd1	*Constitutive defence without defect in growth and development1*
Cf-2	*Cladosporium fulvum-2*
CLV	*CLAVATA*
CK	Cytokinin
CKX	*CYTOKININ OXIDASE*
COX	*CYTOCHROME OXIDASE*
CTAB	Cetyl trimethyl ammonium bromide
CYC	*CYTOCHROME C*
CZ	Central Zone
DIG	Digoxigenin
DM	Dobzhansky-Muller
DM1/2	*DANGEROUS MIX1/2*

DPL1/2	*DOPPELGANGER1/2*
DRP	Dynamin-related protein
EDS1	*Enhanced disease susceptibility1*
EDS5	*Enhanced disease susceptibility5*
EDTA	Ethylene diamine tetra acetic acid
ERF	*Ethylene response factor*
ET	Ethylene
FLG22	Flagellin22
FLS2	*Flagellin-sensitive2*
FRK1	*Flg22-induced Receptor-like kinase1*
GA	Gibberellic acid
GUS	Glucuronidase
Hmr	*Hybrid male rescue*
HPA1/2	*HISTIDINOL-PHOSPHATE AMINO TRANSFERASE1/2*
IPT	*ISOPENTENYL TRANSFERASE*
JA	Jasmonic acid
KM hybrids	KZ-10 x Mrk-0 hybrids
KNOX	*KNOTTED1-LIKE HOMEOBOX*
Lhr	*Lethal hybrid rescue*
LOX2	*Lipoxygenase2*
MAP65-4	*Microtubule-associated protein 65-4*
MAX3/4	*MORE AXILLARY BRANCHING 3/4*
MS	Murashige-Skoog
MT	Microtubule
NBS-LRR	Nucleotide-binding site, leucine-repeat rich
OLI1	*OLIGOMYCIN RESISTANCE1*
ORF	Open Reading Frame

PAD4	*PHYTOALEXIN DEFICIENT4*
PATS	Polar auxin transport stream
PDF1.2	*PLANT DEFENSIN-LIKE 1.2*
peel-1	*Paternal-effect epistatic embryonic lethal*
PIN1	*PIN-FORMED1*
PR1	*PATHOGENESIS=RELATED 1*
PZ	Peripheral zone
qRT-PCR	quantitative reverse-transcriptase polymerase chain reaction
rcd1	*Radical-induced cell death1*
RIN4	*RPM1-Interacting Protein4*
RPM1	*Resistance to Powdery Mildew1*
RPP1	*Recognition of Peronospora parasitica 1*
RPS2	*Resistance to Pseudomonas syringae 2*
RZ	Rib zone
SA	Salicylic acid
SAM	Shoot Apical Meristem
SDS	Sodium dodecyl sulfate
SEM	Scanning electron microscopy
SG3	*SHOOT GROWTH3*
SHORE	Short Read
SL	Strigolactone
SNP	Single nucleotide polymorphism
SPRI	Solid Phase Reversible Immobilization
SRF3	*Strubbelig Receptor Family3*
SSC	Saline sodium citrate
SSLP	Single sequence length polymorphism

SSPE	Saline sodium phosphate EDTA
STM	*SHOOT MERISTEMLESS*
TB1	*TEOSINTE BRANCHED 1*
TCP	TB1 CYCLOIDEA PCNA
TT	*TRANSPARENT TESTA*
TTG-1	*TRANSPARENT TESTA GLABRA-1*
UTR	Untranslated region
UU hybrids	Uk-1 x Uk-3 hybrids
WUS	*WUSCHEL*
YUP	*YELLOW UPPER*
zeel-1	*Zygotic-effect epistatic embryonic lethal*

ABSTRACT

Gardeners, farmers, natural scientists and Augustinian monks alike have long been interested in the study of plant hybrids. And why not - the study of hybridization has taught us much about variation and the fodder that it provides for evolution. The first chapter of my thesis begins, therefore, with a brief history of the study of hybridization. I describe some of the key concepts and examples that have shaped our understanding of evolution and speciation.

Crosses between populations of the same species often uncover transgressive phenotypes in the progeny that were not present in the parents. These phenotypes may be advantageous or deleterious for the progeny, and in the latter case may serve to prevent interbreeding of the two populations. Different geographic populations may be exposed to different environments such as temperature, nutrient availability and pathogen pressure. The study of hybrid incompatibilities, therefore, helps us to determine both the mechanisms that lead to such incompatibilities and the role played by the environment in this divergence.

One such incompatibility is hybrid necrosis. It is a temperature dependent phenomenon caused by an overactive immune system. In Chapter 3 of my thesis, I describe the reaction norms of this autoimmunity with respect to temperature. Mine was the first systematic study of the molecular and morphological phenotypes associated with hybrid necrosis at a range of temperatures. Activation of the immune system usually entails a cost to growth. However, by assaying both immunity genes and plant biomass, I show that there are points in the temperature gradient where this see-saw between growth and defense can be balanced.

In Chapter 4 of my thesis, I describe a newly discovered hybrid phenotype. F1 hybrids displayed an altered shoot architecture characterized by a loss of apical dominance and a bushy habit. Hybrids of the F2 generation showed an additional, segregating phenotype of increased anthocyanin accumulation and small stature. I describe the genetic basis of this hybrid incompatibility in part and show that the

two seemingly different phenotypes are linked genetically. One of the genes that I identified to be involved in this hybrid incompatibility is a microtubule-associated protein. This family of proteins has never before been associated with the phenotypes that I describe. Therefore, further study of this incompatibility is expected to detail new pathways regulating shoot architecture and anthocyanin accumulation.

ZUSAMMENFASSUNG

Gärtner, Landwirte, Naturwissenschaftler und Augustinermönche gleichermaßen hegen seit langem ein Interesse für das Studium von Pflanzenhybriden. Und warum nicht - die Erforschung der Hybridisierung hat uns viel gelehrt über Variation und das Material, das sie für Evolution birgt. Das erste Kapitel meine Dissertation beginnt daher mit einer kurzen Geschichte des Studiums der Hybridisierung. Ich beschreibe einige der wichtigsten Konzepte und Beispiele, die unser Verständnis der Evolution und Artbildung geprägt haben.

Kreuzungen zwischen Populationen der gleichen Art decken oft transgressive Phänotypen in den Nachkommen auf, die in der Elterngeneration nicht vorhanden waren. Diese Phänotypen können vorteilhaft oder nachteilig für die Nachkommen sein, und im letzteren Fall dazu dienen, die Kreuzung der beiden Populationen zu verhindern. Verschiedene geographische Populationen können unterschiedlichen Umgebungen ausgesetzt sein, wie Temperatur, Nährstoffverfügbarkeit sowie Druck von Krankheitserregern und Schädlingen. Die Studie von Hybrid Unverträglichkeiten hilft uns daher, sowohl die Mechanismen, die zu derartigen Unverträglichkeiten führen, als auch die Rolle, die die Umwelt bei dieser Divergenz spielt, zu bestimmen.

Eine dieser Inkompatibilitäten ist die Hybrid-Nekrose. Sie ist ein temperaturabhängiges Phänomen, das durch ein überaktives Immunsystem verursacht wird. In Kapitel 3 meiner Dissertation beschreibe ich die Reaktions-Normen dieser Autoimmunität in Bezug auf die Temperatur. Meine Studie war die erste systematische Untersuchung der mit Hybrid-Nekrose assoziierten molekularen und morphologischen Phänotypen über einen Temperaturbereich. Die Aktivierung des Immunsystems bringt in der Regel Kosten für das Wachstum mit sich. Doch durch Testen von Immunitäts-Genen und pflanzlicher Biomasse zeige ich, dass es Punkte im Temperaturgradienten gibt, an denen diese Wippe zwischen Wachstum und Verteidigung ausbalanciert sein kann.

In Kapitel 4 meiner Dissertation beschreibe ich einen neu entdeckten Hybrid Phänotyp. F1-Hybriden zeigen eine veränderte Spross-

Architektur, die durch einen Verlust von Apikaldominanz und buschigen Wuchs gekennzeichnet ist. Hybride aus der F2-Generation zeigten einen zusätzlichen, segregierenden Phänotyp erhöhter Ansammlung von Anthocyanen und kleiner Statur. Ich beschreibe teilweise die genetische Basis dieser Hybrid-Inkompatibilität und zeige, dass die beiden scheinbar unterschiedlichen Phänotypen genetisch verknüpft sind. Eines der Gene, die ich als in diese Hybrid-Inkompatibilität involviert identifiziert habe, ist ein Mikrotubuli-assoziiertes Protein. Diese Familie von Proteinen wurde bisher noch nie mit den Phänotypen, die ich beschreibe, in Verbindung gebracht. Daher ist zu erwarten, dass weitere Erforschung dieser Inkompatibilität neue Wege der Regulierung von Spross-Architektur und Anthocyan-Ansammlung genau beschreiben wird.

PUBLICATIONS

Ideas and figures in Chapter 3 have appeared previously in the following publication:
Muralidharan, S., Box, M. S., Sedivy, E. L., Wigge, P. A., Weigel, D., Rowan, B. A. (2014), Different mechanisms for Arabidopsis thaliana hybrid necrosis cases inferred from temperature responses. Plant Biology, 16: 1033–1041. doi: 10.1111/plb.12164

1

INTRODUCTION

1.1 HYBRIDS: A HISTORY

Hybrids are the progeny of two individuals that belong to different varieties, populations, species or genera. Although hybridisation in plant and in animal species has been important throughout the history of human civilisation and has greatly facilitated domestication of various species (Roberts, 1929), systematic studies of hybridisation did not take place until the 18th century. Rudolph Jacob Camerarius, Professor of Natural Philosophy in the University of Tübingen, discovered in 1694, that pollen is indispensable for fertilization and wondered if female flowers of one species could be fertilized by pollen from another species (Roberts, 1929). Thomas Fairchild, in 1719, conducted the very first instance of intentional hybridisation between two species, when he crossed *Dianthus caryophyllus* (carnation) and *Dianthus barbatus* (sweet William; Roberts, 1929).

One of the first botanists to conduct hybridisation experiments in plants was Joseph Gottlieb Kölreuter, who had incidentally studied at the University of Tübingen. He successfully generated a hybrid between *Nicotiana paniculat*a and *N. rustica*, following which he proceeded to hybridise 54 species across 13 genera. He found that hybrids produced by crossing two species were often intermediate in appearance to their parents, that they were mostly sterile and that the offspring produced from back-crosses resembled one parent or the other (Stebbins, 1950; Roberts, 1929).

Carl Friedrich von Gärtner, who was a professor of botany at the University of Tübingen, followed up on Kölreuter's work by performing hybridisations in 700 different species belonging to 80 genera (Roberts, 1919) and classified hybrids into "intermediate types" with features that were in between those of the parents, "commingled types" with different features resembling those of one of the parents or the other and "decided types" with features that entirely

resembled only one of the parents. He also made observations about what we today call "segregation":

> *"Other hybrids, and in fact the most of them which are fertile, present from the seeds of the second and further generations, different forms, i.e. varieties varying from the normal types, which in part are unlike the original hybrid mother, or deviate from the same, now more, now less.... Among many fertile hybrids, this change in the second and succeeding generations affects not only the flowers but also the entire habit, even to the exclusion of the flowers, whereby the majority of the individuals from a single cross ordinarily retain the form of the hybrid mother, a few others have become more like the original mother parent, and finally, here and there an individual more nearly reverted to the original father."*

The work of Kölreuter and Gärtner was carried forward in the 19th century by many botanists, such as Naudin, Godron, Lecoq and Wichura, with the principal aim of establishing the validity of hybrid sterility as a criterion for the definition of a species (Roberts, 1929; Stebbins, 1959; Rieseberg and Carney, 1998). Focke (1881) summarized this work and reached the conclusion that plants tended to hybridise easily, but that this tendency varied across taxonomic groups (Stebbins, 1959; Rieseberg and Carney, 1998). He also made the suggestion that interspecific hybridisation in nature was more likely to occur when one of the species is a minority in the area of overlap, or when the breeding seasons are so different that one of the species only begins to flower when the other is at its peak of flowering. If both species were obligate outcrossers, then the probability of the rarer species being pollinated by the more abundant one would be higher than the probability that it would be pollinated by a conspecific.

Charles Darwin, in his Origin of Species (Darwin, 1859), drew on both Kölreuter's and Gärtner's work in the context of species distinctness. He pointed out that while hybrid sterility seemed to be a general result of hybridisation, it was not a universal phenomenon. He also noted that all gradations of features could be found in hybrids, ranging from perfect sterility to perfect fertility and in some cases, higher fertility than either of the hybridising parents. He used the examples of hybrids in the genus *Verbascum*, which hybridised relatively easily, but which produced only sterile hybrids, and examples of *Dianthus*

species, which did not hybridise easily, but produced very fertile hybrids, to show that hybrid sterility could not be used as an argument against the gradual evolution of new species from pre-existing ones.

In dealing with hybrids between varieties of the same species, Darwin cited examples from Gärtner's work on maize, de Buzareingues' work on gourd and Kölreuter's work on tobacco, to illustrate that not all varieties, when crossed, are invariably fertile. In the summary of this chapter, Darwin made a very important observation, which we will allude to later in the importance of hybridisation's role in evolution:

> *"...yet the facts given in this chapter do not seem to me opposed to the belief that species aboriginally existed as varieties."*

The work of Gregor Mendel in plant hybridisation needs no introduction. In stating his objectives for conducting the experiments that he did (Bateson and Mendel, 1909), he cites the work of Kölreuter, Herbert, Lecoq, Wichura and of Gärtner especially, concluding that while their observations had proved valuable, there appeared, from these studies, no general laws governing the behavior of hybrid progeny, particularly in a statistical sense. In his concluding remarks, he pays attention to the question of how one species could be transformed into another by artificial fertilisation. The following excerpt makes it clear that Mendel was referring to the process of introgression of certain defining characteristics between two species, which he and others before him called "transformation":

> *"If a species A is to be transformed into a species B, both must be united by fertilisation and the resulting hybrids then be fertilised with the pollen of B; then, out of the various offspring resulting, that form would be selected which stood in nearest relation to B and once more be fertilised with B pollen, and so continuously until finally a form is arrived at which is like B and constant in its progeny. By this process the species A would change into the species B."*

By the 20th century, hybrids were known in at least 150 plant genera (Roberts, 1929). The rediscovery of Mendel's work by Hugo de Vries, Carl Correns and Erik von Tschermak (Roberts, 1929) and their own confirmation of his laws of inheritance set off a large body of work in genetics and hybridisation. This, combined with T.H.Morgan's dis-

covery that genes on chromosomes are the units of heredity (Morgan, 1915), set the stage for the rapid progression of knowledge concerning hybridisation and how it shapes the evolution of species.

1.2 HYBRIDISATION AND EVOLUTION: THE 20TH CENTURY

The modern study of the role of hybridisation in evolution was stimulated by the following discoveries. First, Winge (1917) discovered that by doubling chromosome number, new, true-breeding hybrid species could be formed. Second, Müntzing, in his study of *Galeopsis* species, proposed that chromosomal rearrangements in hybrids could lead to the formation of new species which would then be at least partially isolated from their parents ((Müntzing, 1930; Rieseberg and Carney, 1998)). Third, studies by Edgar Anderson on natural hybrid populations suggested that selection could act on hybrid progeny and result in adaptive evolution within populations (Anderson and Hubricht, 1938; Anderson, 1936).

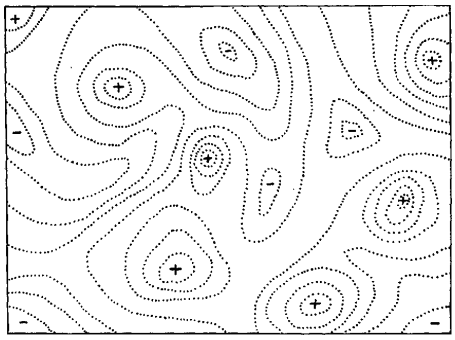

Figure 1: *Two-dimensional representation of the fitness landscape, as imagined by Wright (1932, Figure 2)*

.

At the same time that these studies on plant hybridisation were being conducted, great strides were made to unite Mendel's laws of heredity with Darwin's theory of evolution by natural selection. The works of Fisher (1918), Wright (1932) and Haldane (1932) showed that several independent Mendelian factors (genes) could have a cumulative effect as predicted by Darwin, i.e. a gradual distribution of phenotypes, upon which natural selection could have differential effects. Wright introduced the concept of fitness landscapes as a metaphor for the varying amounts of fitness contributed by different loci. In a

fitness landscape, gene combinations that increased fitness occupied adaptive peaks or hills, whereas those that lowered fitness occupied valleys (see Figure 1). Peaks shifted with changes in environment and natural selection would move populations to the closest peaks.

Further work by Dobzhansky (1937), Mayr (1942), Huxley (1942), Simpson (1944) and Stebbins (1950) resulted in what we call today the Modern Synthesis of Evolution, as it brought together statistical and population genetics with botany and zoology. There was now a theoretical framework against which to test the various predictions of the role of hybridisation in evolution.

Early work on the role of hybridisation in evolution focused mainly on its creative outcomes, for e.g., evolution of phenotypic novelties that could allow a hybrid to occupy new ecological or geographical niches that the parental species could not, which often, but not always, led to invasiveness of the hybrid species and its rapid spread in the new environment (Stebbins, 1950). Later interest in the role of hybridisation extended to its negative, or inhibitory outcomes, such as hybrid sterility, or the incapacitation of hybrid progeny, when produced. It was this work that eventually led to the formulation of the Bateson-Dobzhansky-Muller theory, which explained how variation in populations separated over long periods of time could lead to incipient speciation.

Darwin (1859), had already speculated that causes of sterility in first crosses may be due to fundamentally different reproductive organs in the mother and father plants, and in hybrids, due to imperfect development of the sexual organs. However, Bateson (1909) was the first to think about the mechanisms that lead to hybrid incompatibilities, which he called "interracial sterility". He proposed that the decreased viability of some hybrids could be due to the meeting of two distinct factors in the hybrid that had been acquired independently by two diverging parental lineages. He recognized that if sterility were due only to one factor, then the lineage that had acquired it would have died out. He went so far as to say that the factors causing hybrid sterility need not lead to any noticeable effects in the parents and would not even come into play until the cross was made. This seminal essay remained largely unread for many years and Bateson himself is said to have had doubts about his theory during later years (Orr, 1996).

In the 1930s, working with two strains of *Drosophila*, *D. pseudoobscura* races A and B (race B is now known to be a sister species, *D. persimilis*), Dobzhansky (1937) discovered that interbreeding between them was hampered by geographical, ecological and sexual isolation. In addition, he observed sterility of hybrid males and lowered viability of the offspring of back-crosses. He inferred that the two races of *D. pseudoobscura* must have already differed in certain characteristics that were a consequence of their geographical isolation, which led to each of the races becoming increasingly genetically distinct. Each of the "isolating mechanisms", as he called them, could not have on their own had a remarkable effect on the ability of the two races to interbreed, but together, they could reinforce the effects of one another.

Muller (1942), in his paper on "Isolating mechanisms, evolution and temperature", meticulously laid down the evidence for the theory of two-gene interactions causing hybrid sterility. He divided isolating mechanisms into two classes: obstacles to crossing and incapacitation of hybrids, which today are called pre- and post-zygotic barriers. Bars to crossing were factors that conserved the reproductive energy of a species by disallowing any attempts at cross-breeding between groups. These were further divided into two subtypes: first, geographical barriers and conditioned behaviour, which prevented access to other groups despite possible genetic similarity and second, influences that depended on genetic differences that led to more frequent intra-group than inter-group mating, today called assortative mating. Incapacitation of hybrids included mechanisms that rendered hybrid zygotes inviable or infertile in the first or later generations. He also made it patently clear that hybrid incompatibility must arise due to the interaction of at least two genes:

> *"But since practically all mutant genes must exist in heterozygous condition in the first individuals which inherit them, it is evident that any such lethal or sterilizing effect on the heterozygote would* ipso facto *incapacitate the very individuals necessary for the perpetuation of these genes. For this reason individual mutations causing complete hybrid incapacitation at one bound cannot become established."*

Citing the work of Dobzhansky and others, he stressed the fact that, in animals at least, hybrid incapacitation seemed to be caused by genic incompatibilities and not by chromosomal differences (as was believed by some at the time). From the work carried out by Spencer,

Patterson and Sturtevant, he concluded that the same factors that caused differences between species, also caused the differences between races and between sub-species:

> *"..it* [all this work] *has demonstrated that in this genus at least no sharp line can be drawn between sub-divisions of one rank, such as races or sub-species, and of another rank, such as species. For although published analyses of the actual genetic bases of the phenomena here concerned have necessarily been very limited as yet (we have already cited most of those so far reported in* Drosophila*), it is clear that the same kinds of taxonomic, physiological, and cytological differences, and the same general characteristics of crossability, which differentiate so-called species, also differentiate the lesser sub-divisions, although of course to a lesser degree."*

This, as we have already seen, was also the view held by Darwin.

In the years since these hypotheses were proposed, the Bateson-Dobzhansky-Muller (BDM) theory of hybrid incompatibility has come to be understood as follows: a population of individuals with a certain amount of variation becomes divided by an initial barrier, such as geography, change in feeding strategy or timing of reproduction (see Figure 2). Over time, due to drift or selection, some genetic variants that were segregating in the original population become differentially fixed in the two diverging lineages, and each population gradually accumulates further genetic changes. Bateson, Dobzhansky and Muller showed that there need to be two such differences, one in each population, which have developed in the absence of contact with the other population, in order for them to interact and cause hybrid incompatibility.

In the development of this theory, Bateson, Dobzhansky and Muller had solved Darwin's paradox of the origin of species. Darwin wanted his readers to believe both that evolution occurred by means of natural selection, and also that the origin of new species required the evolution of hybrid sterility, which, by definition, could not have been targets of natural selection; these were seemingly opposing facts that he could not reconcile in his Origin of Species. He, however, concluded that hybrid sterility must have been an accidental consequence of evo-

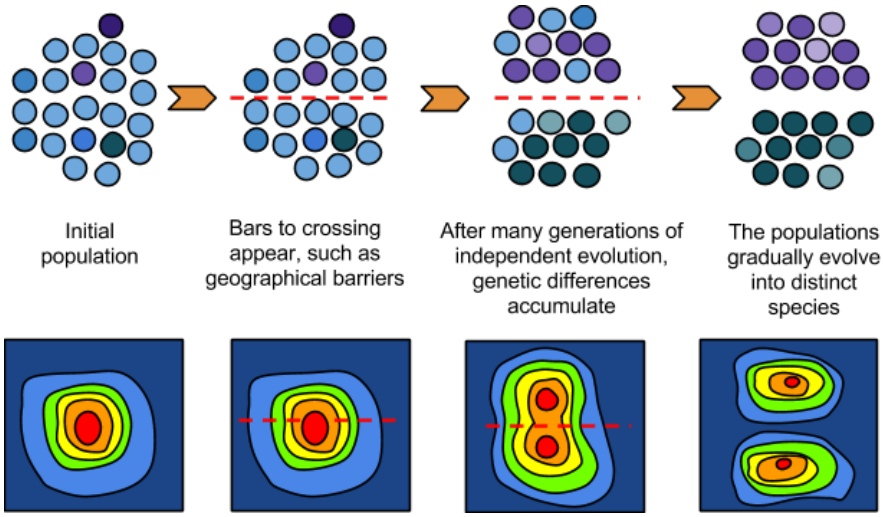

Figure 2: *Upper panel: Schematic representation of origin of new species by means of Bateson-Dobzhansky-Muller incompatibilities. Lower panel: Fitness landscapes corresponding to each stage of the upper panel, to represent the process in which diverging populations can reach different adaptive peaks without crossing a valley of low fitness. Red indicates high fitness, blue indicates low fitness and the dashed line represents a geographical barrier. The upper panel was modified from evolution.berkeley.edu/evolibrary/article/o_o_o/history_20; adaptive landscapes in the lower panel are my own interpretations.*

lution, "incidental on other acquired differences". The simple explanation afforded by the presence of a two-gene interaction in diverging populations/species took care of this apparent paradox. It also explained how diverging populations (or incipient species) were able to find new adaptive peaks without having to go through adaptive valleys.

In 1942, Ernst Mayr, an ornithologist working in Papua New Guinea, published his influential book "Systematics and the Origin of Species", in which he laid out wide-ranging examples of geographic variation among and between populations of organisms and how this reflected on speciation processes. He acknowledged the difference between how systematists viewed species (as a static categorizing device) and how geneticists and evolutionists viewed it (as a constantly changing stage in the evolutionary process). He insisted that a definition of species was therefore required, which could be used practically in categorizing, without a doubt, all members that belong to the same group, and that could also capture the dynamism of that group's continued evolution. Although Dobzhansky came up with a definition of a biological species in his Critique of Species Concepts (1935), Mayr was the one who refined the definition and is the one who is usu-

ally credited for it. Species, according to the Biological Species Concept (BSC), are "groups of actually or potentially interbreeding natural populations, which are reproductively isolated from other such groups" (Mayr, 1942). Other species concepts have been proposed and are reviewed in Coyne (1994) and Coyne and Orr (2004). Despite the absence of a consensus for the definition of a species, the BSC has come to dominate most discussions of speciation and is relevant for the purposes of this thesis.

1.3 ISOLATING MECHANISMS

In order to understand how reproductive barriers between species arise, it is essential to recognize the isolating mechanisms that are at play and whether they were consequences of adaptation to different lifestyles or habitats. Over several decades, many lines of evidence corroborating the two-locus epistasis model of Bateson, Dobzhansky and Muller have been found across a broad taxonomic range: plants, flies, yeast, fish and mice (Rieseberg and Blackman, 2010; Presgraves, 2010; Maheshwari and Barbash, 2011). Many of the mechanisms for these cases have not yet been elucidated. Over the last few years, however, studies in several plant species have shed light on the processes acting in plant evolution and hybridisation.

I present first a brief overview of some of the examples from monkeyflower, rice, tomato, *Phlox* and *Arabidopsis* that have helped us understand the kinds of molecular mechanisms that have acted to keep lineages separate at both the inter- and intra-species levels. Next, I touch on some of the hybrid incompatibilities that have been investigated in yeast and in animals such as copepods, flies and nematodes. Some of the examples deal with lineages that have diverged in geographically separate regions (allopatry), whereas other cases deal with species or populations that have diverged while in the same geographic region (sympatry). Most of the examples represent BDM-type incompatibilities, whereas others represent variations of this theory.

1.3.1 *Interspecific hybrid incompatibilities in plants*

Mimulus

Studies of hybrids between closely related species have provided a glimpse into the ways in which they have diverged from each other. Species complexes of the monkeyflower, such as *Mimulus cardinalis*, *M.lewisii* and *M. guttatus*, have been used to study the diversity within this genus and the factors that contribute to its adaptive divergence and modes of speciation. *Mimulus* species display a wide variety of floral morphologies (Wu et al., 2008) that affect pollinator visitation. In a landmark study, Schemske and Bradshaw (1999) showed that crosses between the closely related *M. cardinalis* and *M. lewisii* species produced fertile hybrids. *M. cardinalis* plants have red flowers that are pollinated by hummingbirds (*Osmia* sp.), whereas *M. lewisii* plants have pink flowers that are pollinated by bumblebees (*Bombus vosnesenski*). This pollinator-specificity is very high in the areas where both species grow. In the F_2 generation, the hybrids displayed the entire range of phenotypes between the two parental species, allowing the authors to identify causal relationships. Divergence in one locus, *YELLOW UPPER (YUP*), affected anthocyanin and carotenoid concentrations in petals, largely determining which pollinator would visit the flowers. This divergence promoted pollinator-mediated assortative mating and drove the differentiation and isolation of *M. cardinalis* from an *M.lewisii* -like ancestral species (Beardsley et al., 2003). Thus, reproductive isolation between these two species occurs before the formation of hybrids.

Mimulus is also a model system for studying the effects of chromosomal rearrangements on adaptive divergence and speciation. A recent study used synthetic tetraploids to show that chromosomal inversions and translocations between *M. lewisii* and *M. cardinalis* directly caused F_1 underdominance by decreasing pollen fertility (Stathos and Fishman, 2014).

Oryza

In rice, pollen sterility in hybrids between the domesticated strain *Oryza sativa ssp. japonica* var. Taichung 65 and a wild relative, *O. glumaepatula* is caused by an epistatic interaction between the duplicated loci *S27* and *S28*, which encode isoforms of the mitochondrial ribosomal protein L27 (Yamagata et al., 2010). The *O. sativa* allele of *S28* fails to express in the *O. sativa* variety T65 and *O. glumaepatula* has lost its copy of *S27*. This is an example of a situation in which reciprocal loss of duplicated genes in divergent species leads to a hybrid

incompatibility. This kind of duplication and sub-functionalization is a variation of the BDM-type of incompatibilities.

Solanum

Orr and Turelli (2001) predicted that the number of two-locus hybrid incompatibilities would increase non-linearly, with the square of the time separating two species. This follows from the assumption that potentially incompatible alleles arise at the same rate in the two lineages. Therefore, the complexity of the genetics behind postzygotic isolation would accelerate over time and would be very different from the pace of evolution of other traits in each of the lineages. This sort of "snowballing" of incompatibilities was recently tested in *Solanum* species and found to be true for seed sterility but did not hold for pollen sterility (Moyle and Nakazato, 2010). However, this study did not have the power to detect incompatibilities due to multi-locus interactions, which may have been one of the reasons that the snowballing effect for pollen sterility was not apparent.

Arabidopsis

Burkart-Waco et al. (2012) determined the loci in different *Arabidopsis thaliana* ecotypes that affect interspecific incompatibility with the closely related species *A. arenosa*. They used a RIL population of Col-0 x C-24 since these accessions differed in the degree of hybrid sterility with *A. arenosa* (0% and 17% respectively). They identified seven different QTL that affected F_1 seed viability. Thus, multiple loci of small effect from the maternal genome modulated hybrid growth and viability at various stages of development. This agrees with the snowball effect expected from lineages that have been diverging for long periods of time. It is possible that *A. thaliana* populations have a network of different Dobzhansky-Muller gene pairs and an associated network of modifiers that act to prevent inter-specific hybridisation.

Phlox

While several studies have looked at traits that are by-products of adaptive divergence between geographically isolated populations, very few studies have looked at the processes that keep sympatric populations from interbreeding. The process by which selection directly acts on hybrids by reducing their fitness, thus favouring speciation even in sympatry, is called reinforcement. The most well-characterised

example of this process in plants comes from studies of Texas wildflowers (*Phlox* species).

Divergence in flower colour between related species in sympatry (termed character displacement) has been recorded in many plant genera: *Clarkia*, *Phlox*, *Fuchsia* and *Rudbeckia* (Levin, 1985). The question of whether this is caused by the presence of the other species was addressed in Levin's study (1985) of *Phlox drummondii* (an outcrosser), and *P. cuspidata* (a selfer), annuals that grow in Texas' prairies. Both species produce light blue flowers in allopatry, but, *P. drummondii* produces dark-red flowers in the overlapping regions. Both species are pollinated by the same array of Lepidopterans and are cross-compatible. Hybrids between them display strong, but incomplete, male and female sterility. Thus, there is a strong expectation for selection to reduce the possibility of hybridisation and prevent wasting gametes.

Levin (1985) showed that the shift from blue to red flowers decreased hybridisation between the red-flowered *P. drummondii* morph and *P.cuspidata* by 66% in the wild, despite the higher cross-compatibility of the red-flowered morph. In the cases where hybridisation did take place, seed set was drastically reduced in *P. drummondii*. Sympatric populations of *P. drummondii* also showed higher levels of self-compatibility than allopatric populations, which could be a byproduct of selection against hybridisation.

Hopkins and Rausher (2011) demonstrated that this character shift from blue to red morphs was controlled by two loci of large effect that functioned in anthocyanin biosynthesis and controlled the hue and intensity of flower colour. Expression levels of a *Flavonoid 3′5′-hydroxylase* controlled variation in hue, whereas expression levels of an *R2R3-Myb* transcription factor controlled the variation in intensity of flower colour.

Hopkins et al. (2014) estimated the relative fitnesses of each of the colour morphs of *P.drummondii* in the wild, in both allopatry and sympatry. They discovered that the blue morphs suffered a large reduction in fitness in sympatry, while possessing the highest fitness among all morphs in allopatry. The red morph showed the highest relative fitness in sympatry with *P. cuspidata*.

Thus, the flower colours controlled by the two loci are under differential selection in sympatry and in allopatry, allowing each of the morphs to be maintained in the different environments. The different flower colouration ensures that there is minimal interspecific hybridisation, reinforcing the existing differences between the two species, allowing them to diverge further.

1.3.2 *Intraspecific hybrid incompatibilities in plants*

Mimulus

Mimulus species have a wide distribution in Western North America and in Australia and can be found in various habitats, such as coastal regions, grasslands, deserts and mountainous areas. A study by Macnair and Christie (1983) and a follow-up study by Wright et al. (2013) showed that high copper content in soils drove the adaptation of copper tolerance in certain populations of *M. guttatus*, which displayed hybrid sterility when crossed to other populations of the same species that were not exposed to high levels of copper. Initially, the locus controlling copper tolerance was thought to produce hybrid sterility as a pleiotropic effect (Macnair and Christie, 1983). However, a recent study showed that the two phenotypes were caused by two distinct, but tightly linked loci. Due to selection imposed by the copper-rich soil, the hybrid lethality gene hitchhiked to high frequency on the back of the copper tolerance locus (Wright et al., 2013). This represents a variation of the idea that hybrid incompatibilities generally arise as an accidental by-product of adaptation to new environments. This particular case involved selection imposed by the environment, followed by hitchhiking of a genetic element that was unrelated to the trait being selected for.

Oryza

Some of the well-studied examples of hybrid sterility in plants come from the hybrids between the *indica* and *japonica* subspecies of cultivated rice, *Oryza sativa*. At least 50 loci controlling hybrid fertility have been identified in *indica* x *japonica* hybrids and have been classified into those that cause female gamete abortion, those that cause pollen sterility and those that cause both (Ouyang and Zhang, 2013).

One of the loci that decreases embryo-sac fertility, *S5*, exists as three alleles: an *indica* allele, *S5-i*; a *japonica* allele, *S5-j*; and a neutral allele, *S5-n* (Chen et al., 2008). Hybrids that bring together the *S5-i* and the *S5-j* alleles are sterile, whereas either of these alleles is fertile when combined in a hybrid with the *S5-n* allele. The *S5* locus was delimited to a 40 kb fragment containing five open reading frames (QRFs; Qiu et al., 2005). One of the genes encoded an aspartic protease (called ORF5), expressed mainly in ovule tissues. The *ORF5* alleles of *indica* (referred to as ORF5+) and *japonica* (referred to as ORF5-) differ by two nucleotides resulting in non-synonymous substitutions. However, ORF5 was not sufficient to explain the hybrid sterility and segregation distortion observed in successive generations. Therefore, the roles of the other genes in the locus were also determined.

ORF3 and *ORF4*, which encode a heat shock protein and a transmembrane-domain containing protein, also differ in sequence between the *indica*, *japonica* and neutral alleles and both were required for the action of *ORF5* in hybrid sterility. An *ORF3+ORF4-ORF5+* combination of alleles was found in *indica* varieties, whereas the *ORF3-ORF4+ORF5-* combination was found in the *japonica* varieties. When *ORF5+* and *ORF4+* were combined in a hybrid, they acted as a "killer" combination, selectively killing female gametes that did not possess the *ORF3+* allele, which acted as a "protector". Thus, progeny that contained ORF3+ were disproportionately represented in the progeny, explaining the segregation distortion. In the mechanism that has been proposed (Yang et al., 2012), *ORF5+* produces a signal that is recognized by the *ORF4+* protein on the membrane. This triggers ER-stress in the cell, which would induce programmed cell death unless it is kept in check by *ORF3+*.

In an independent case of hybrid male sterility in *indica* x *japonica* hybrids, two adjacent genes at a single locus, *SaF* and *SaM*, were found to be causal (Long et al., 2008). *SaM* encodes a ubiquitin-like modifier E3 ligase and *SaF* encodes an F-box protein. The *indica* varieties carry the SaM^{+} SaF^{+} genotype, whereas the *japonica* varieties carry the SaM^{-} SaF^{-} genotype. The SaM^{-} gene has a single nucleotide polymorphism that results in a truncated protein, whereas the SaF^{-} gene differs from SaF^{+} by a single amino acid change. Pollen carrying SaM^{-} and SaF^{+} are selectively aborted, leading to semi-sterility of the hybrid and segregation distortion in successive generations.

A third case of hybrid pollen sterility was characterised in a cross between the *indica* variety of Kasalath and the *japonica* variety of Nipponbare (Mizuta et al., 2010). Pollen sterility due to non-germination of pollen was caused by two paralogous genes, *DOPPELGANGER1* (*DPL1*) and *DOPPELGANGER2* (*DPL2*). The *indica* allele of *DPL1* is disrupted by a transposable element, whereas the *japonica* allele of *DPL2* contains a mutation that renders the protein nonfunctional. In hybrids, those pollen that carried the defective copies of both genes, i.e. *DPL1* of *indica* and *DPL2* of *japonica* were unable to germinate, since at least one of the genes is needed for normal pollen function (Mizuta et al., 2010).

To summarise the findings from rice, in the first two examples, two or three genes acting in a single locus contributed to hybrid incompatibility, whereas in the third example, two loci that contained duplicated genes with reciprocal loss of function contributed to incompatibility. These examples represent variations of the Bateson-Dobzhansky-Muller model, in that there are still two or more genetic factors required for the incompatibility, but they can be linked together in a single locus, or the same factors duplicated and sub-functionalized.

Arabidopsis

Despite the ubiquity of *A. thaliana* for studies of plant genetics, there are relatively few studies looking at inter- or intraspecific hybrid incompatibilities in *Arabidopsis*. The first characterised hybrid incompatibility phenotype was discovered in a cross between the *A. thaliana* accessions Uk-1 and Uk-3 (Bomblies et al., 2007). Hybrid progeny of the F_1 generation displayed necrotic lesions on leaves at 16°C, that disappeared when the plants were shifted to a higher temperature regime (23°C). The genetic basis of this phenotype was mapped to two loci, *DANGEROUS MIX1* (*DM1*) and *DM2*. The causal allele in *DM1* encoded an NBS-LRR (*n*ucleotide-*b*inding *s*ite, *l*eucine-*r*epeat *r*ich) protein, that is normally involved in recognizing plant pathogens and mounting an immune response. In the hybrids, defence responses were ectopically activated, leading to autoimmunity and decreased fecundity of hybrids.

Interactions between incompatible R proteins have been repeatedly found to cause hybrid incompatibilities in many species (Krüger et al., 2002; Jeuken et al., 2009; Alcazar et al., 2010; Yamamoto et al., 2010; Al-

cazar et al., 2014; Chae et al., 2014). Reduced hybrid performance has also been attributed to single gene incompatibilities causing either abnormal growth phenotypes (Smith et al., 2011) or hybrid necrosis (Todesco et al., 2014).

There are also hybrid incompatibilities in *Arabidopsis* that are caused by gene duplication followed by reciprocal loss of function. This results in a proportion of the F2 hybrids inheriting two non-functional copies of the causative loci. Such a case was recorded in a cross between Col-0 and Cvi accessions (Bikard et al., 2009); when F2 progeny were homozygous for the Col-0 allele of *HPA1* (*HISTIDINOL-PHOSPHATE AMINO-TRANSFERASE1*), which was not transcriptionally active, and the Cvi allele of *HPA2*, which contained a 6.4kb deletion, the embryos died and were aborted.

A similar mechanism was also found to cause growth defects in Bur-0 and Col-0 hybrids (Vlad et al., 2010). Due to duplication and loss of divergent paralogues of the *SG3* (*SHOOT GROWTH-3*) gene, those plants that inherited neither functional copy of this gene were small, had a reduced chlorophyll content, flowered later and produced fewer seeds. In yet another case, hybrid incompatibility between Col-0 and Sha accessions was caused by reciprocal DNA methylation and transcriptional silencing of a pair of duplicated genes that encode folate transporters (Durand et al., 2012).

Thus, there are at least three instances in *Arabidopsis* (Bikard et al., 2009; Vlad et al., 2010; Durand et al., 2012) and one in rice (Yamagata et al., 2010), in which duplication of genes followed by subfunctionalization led to hybrid incompatibilities in progeny that received both the non-functional copies of the gene.

1.3.3 *Hybrid incompatibilities in Fungi and Animals*

Yeast

Crosses between *Saccharomyces cerevisiae* and *S. bayanus* gave rise to hybrids that were sterile (Lee et al., 2008). The cause of this sterility was attributed to divergence between two genes, AEP2 (*ATPase expression2)* in the nuclear genome and OLI1 (*Oligomycin Resistance1*) in the mitochondrial genome (Lee et al., 2008). The Aep2 protein

binds to the 5'UTR of the OLI1 mRNA and promotes its translation. However, the *S. bayanus* copy of Aep2 does not bind to the *S. cerevisiae copy* of OLI1 mRNA. This loss of function resulted in a defect in respiration and sporulation, leading to hybrid incompatibility when these two copies were inherited in the homozygous state. The sequence divergence in OLI1 mRNA may have arisen due to differences in the preferred growth medium between the two yeast strains. Alternatively, the shift away from respiration towards fermentation for *Saccharomyces* may have relaxed the constraints on the mitochondrial genome, leading to accelerated rates of substitution (Presgraves, 2010).

Hybrid sterility between *S. cerevisiae* and the more closely-related *S. paradoxus* was found to be caused not by nuclear DM pairs of incompatible alleles, but by multiple complex incompatibilities of weak effect (Kao et al., 2010). Hybrid infertility between the recently diverged *Schizosaccharomyces pombe* and *S. kambucha* was found to be caused by a combination of genome rearrangements and meiotic drive alleles on each of the chromosomes of *S. kambucha* (Zanders et al., 2014). Reciprocal translocations between chromosomes 2 and 3 rendered certain hybrid chromosomal combinations unviable. Of the three meiotic drive alleles, two were linked by a translocation between two chromosomes, forming a paired meiotic drive complex. Thus, non-BDM mechanisms such as genome rearrangements and meiotic drive can also cause reproductive isolation between species.

Copepods

Cytonuclear incompatibilities have also been found to cause hybrid dysfunction between isolated copepod populations (*Tigriopus californicus*; Willett and Burton, 2001; Ellison and Burton, 2006). Cytochrome c (*CYC*) variants demonstrated a reduced rate of oxidation when tested with mitochondrial extracts of other populations. The hybrid breakdown between two populations could be attributed to a natural variant of *CYC* encoding a single amino acid change (Harrison and Burton, 2006). This suggests that the nuclear-encoded *CYC* genes and the mitochondrial-encoded cytochrome oxidase (*COX*) genes are coevolving within each population, similar to the coevolution of the mitochondrial and nuclear genome described above in yeast.

Flies

Genes contributing to F_1 hybrid male lethality between *Drosophila melanogaster* females and *D. simulans* males were identified when suppressor mutations in *Hmr* (*Hybrid male rescue*; Watanabe and Kawanishi, 1979) and *Lhr* (*Lethal hybrid rescue*; Barbash and Ashburner, 2003) rescued the incompatibility. The *Hmr* and *Lhr* genes encode proteins that form a heterochromatic complex with Heterochromatin Protein 1a (HP1a; Brideau et al., 2006; Satyaki et al., 2014). They repress transcription of transposable elements and satellite DNAs and control telomere lengths (Satyaki et al., 2014). The sequence divergence between the *Hmr* and *Lhr* and the interactions between them supported a BDM-model of incompatibility (Brideau et al., 2006). However, these two genes are not sufficient to cause incompatibility in the other parent. This suggests the action of additional genetic factors of minor effect, as expected from earlier experiments with these species (Muller and Pontecorvo, 1940; Pontecorvo, 1943; Brideau et al., 2006). Cuykendall et al. (2014) screened the entire autosomal genome of Drosophila and did not find any additional major-effect loci contributing to this incompatibility. They found many weak-effect loci, but could not easily test candidate genes due to technical difficulties.

At the same time that the study of snowballing incompatibilities in *Solanum* was conducted, Matute et al. (2010) investigated this phenomenon in *Drosophila* species. Using synonymous substitutions as a proxy for divergence time and by looking at hybrid progeny of mutated *D. melanogaster* lines with *D. simulans* and *D. santomea*, they were able to show that deleterious epistatic interactions accumulate faster than linearly with time since divergence.

Nematodes

When F_1 hybrids between the Bristol and Hawai'i strains of *C.elegans* were crossed back to the Hawai'ian parent, embryo lethality was observed in the next generation in a direction-dependent manner. Fifty percent of the embryos died when the hybrids were sperm donors, whereas no lethality was observed when the Hawaiian strain was the sperm donor. A paternally acting factor, *peel-1* and a zygotically expressed factor *zeel-1* were found to be responsible for this incompatibility (Seidel et al., 2008). The *zeel-1* gene product is necessary to counteract the toxic effects of the PEEL-1 protein derived from the Bristol strain. When an egg with the Hawai'i allele of the *zeel-1* gene (that carries a deletion) is fertilized by a sperm carrying the Bristol

allele of PEEL-1, the harmful effects of PEEL-1 are not negated, leading to embryo lethality. These two genes are located on a 62 kb stretch of the genome and do not segregate independently. This tight linkage between the "toxin" and its "antidote" has allowed these two genes to act as a selfish genetic element, causing transmission ratio distortion in hybrids, and favouring the Bristol over the Hawaii haplotype.

1.3.4 *Variable Reproductive Isolation*

An important concept that has emerged recently is that there is genetic variability in the degree of isolation between populations or species, due to incompatible alleles that are segregating within a lineage (Cutter, 2012). Studies in plants (Rieseberg, 2000; Burkart-Waco et al., 2012), nematodes (Kozlowska et al., 2012), arthropods (Wade et al., 1997; Gerard and Presgraves, 2012), mice (Good et al., 2008) and yeast (Charron et al., 2014) have indicated that polymorphisms within diverging lineages contribute to the variability in reproductive isolation between populations or species. This variability might also account for the "missing snowball": if alleles involved in a Bateson-Dobzhansky-Muller (BDM) interaction are polymorphic and unaccounted for, then the estimate for the number of "fixed" BDM interactions between two species would be inflated, contributing to the appearance of a linear, rather than a non-linear increase, in the accumulation of such interactions, especially between more closely-related species (Cutter, 2012).

1.3.5 *"Speciation" genetics*

The recent surge in speciation research has largely focused on the genetics of postzygotic isolation in diverging lineages. Genes identified in such studies are are not necessarily "speciation" genes. It is unclear if the incompatibilities that are observed today contributed directly to the reproductive isolation of two lineages; the differences that led to incompatibilities may also have accumulated after the speciation process was completed. To address this problem, Nosil and Schluter (2011) suggested that a speciation gene meet certain criteria: one, that it affected reproductive isolation; two, divergence at its locus preceded the divergence of the two lineages and three, its ef-

fect on total reproductive isolation between the two lineages could be quantified. Studying incompatibilities between species that are already separate and between incipient species will provide a more balanced view of such speciation genes.

1.4 SUMMARY

The BDM theory of hybrid incompatibilities has been demonstrated in a wide range of species, in both interspecific and intraspecific crosses. Variations of the BDM model of incompatibilities have also been observed as well as mechanisms that keep species apart that are not described by the BDM model. These examples have shown us that adaptation to the local environment plays a large role in the evolutionary trajectories of organisms (such as in Phlox, Mimulus and *Arabidopsis*). Adaptations to the external environment can lead to reproductive isolation if the loci under selection are linked to the loci involved in isolation. Mutations of large effect also play an important role in isolating populations of the same species (such as in rice, yeast, copepods and nematodes). Non-BDM mechanisms such as chromosomal rearrangements (Rieseberg, 2001; Kirkpatrick and Barton, 2006; Widmer et al., 2009), mismatch repair (Greig, 2009) and changes to ploidy levels (Otto and Whitton, 2000; Mallet, 2007; Rieseberg and Willis, 2007) are additional ways in which species get isolated from one another.

Studying intraspecific incompatibilities between divergent populations gives us insights into both the kinds of mechanisms and pathways that are likely to be involved in the isolation of incipient species and into the role played by the environmental conditions in this divergence.

1.5 AIMS OF THE THESIS

The mechanisms that keep species separate are probably not different from the mechanisms that lead to the divergence of species in the first place. Thus, studying intraspecific hybrid incompatibility allows us to get a sense of the isolating mechanisms involved in incipient speciation. It also allows us to identify the environmental conditions

that are most important to the success of the different populations. *Arabidopsis thaliana* provides just such a system (Weigel, 2012): its different populations are spread across a wide geographic region in the temperate zones of the world. It has both native and introduced stands, with many sequenced genomes and genetic manipulation is facile. Studying synthetic hybrids and their incompatibilities will give us information about the differentiation between populations and how the local environment shaped these differences.

In my thesis, I describe two lines of investigation, with two different aims: one descriptive and the other explanatory. The first study details the effects of different temperature regimes on hybrid necrosis phenotypes. Hybrid necrosis is a temperature dependent phenomenon and temperature control of immunity is an important theme of research in current plant biology. My study is the first to describe reaction norms of auto-immunity with respect to temperature, using both morphological phenotypes such as appearance of necrosis and shoot biomass and molecular phenotypes such as transcript levels of various immunity-related genes. The second study describes the genetic basis of a newly discovered hybrid phenotype. Hybrids displayed a loss of apical dominance and increased anthocyanin accumulation compared to their parents. I identified one of the genes responsible for this phenotype and carried out several experiments to tease out how this phenotype could be produced in hybrids.

2

MATERIALS AND METHODS

2.1 PLANT GROWTH CONDITIONS AT THE MPI, TÜBINGEN, GERMANY

Plants were grown on soil in growth chambers maintained at temperatures of either 23°C or 16°C, a relative humidity of 65%, and light fluence rate of 125-175 μmol m^{-2} s^{-1} (1:2 cool:warm Cool White and Warm White De Luxe fluorescent lights, Sylvania, USA) under long day conditions (16 hours light, 8 hours dark).

2.2 PLANT GROWTH CONDITIONS AT THE SAINSBURY LABORATORY, CAMBRIDGE, UNITED KINGDOM

Plants were grown in Conviron BDW150 Controlled Environment Rooms. Seeds were sown out on soil in 40-pot trays and grown under long day conditions, 65% humidity, 150 μmol m^{-2} s^{-1}. Temperatures were maintained at 12, 14, 16, 18, 20, 22, 24 and 26°C. Plants belonging to different biological replicates were sown out on different days. Trays were rotated every alternate day and moved to a different location in the rack to avoid positional effects. Plant material for gene expression was harvested at the same time of day to avoid circadian effects. Each of the three biological replicates collected for RNA extraction was a pooled sample of 20 plants.

2.3 ACCESSIONS

The accessions used in this study are:

Accession Name	Alternative ID
Kro-0	CS6766
BG-5	CS22345
Col-0	CS1094
ICE49	CS76347
Uk-1	N1575
Uk-3	N1577
KZ-10	N22442
Mrk-0	N1375

The accession name is a reference to the geographical location from where the seeds were collected. The Alternative ID indicates the pedigree of the germplasm in the seeds stock center.

2.4 DNA EXTRACTION USING CTAB

Frozen tissue was homogenized either with micropestles (in case of single tube extractions) or in a bead mill (Retsch MM 300, Retsch GmbH, Haan, Germany) for 96-well plate formats. The powdered tissue was resuspended in 500 µL CTAB (0.1M Tris-HCl, pH 8.0, 2% CTAB, 0.7M NaCl, 0.02M EDTA pH 8.0, 1 % b-Mercaptoethanol and 1% sodium bisulfite) and incubated at 65°C for 1 hour. After cooling the tubes for 5 minutes, 500 µL of 24:1:: chloroform:isoamyl alcohol were added and mixed by inversion. The aqueous phase was separated by centrifugation at 4000 g for 20 minutes. The supernatant was transferred to fresh tubes containing 0.7 volumes isopropanol. Nucleic acids were precipitated by centrifugation at maximum speed for 30 minutes. The supernatant was discarded and the pellet was washed with 70% ethanol. The pellet was air dried and resuspended in 30-100 µL of milliQ water. The DNA was quantified on a Nanodrop spectrophotometer (Nanodrop 2000, Peqlab Biotechonologie GmbH, Erlangen, Germany) and quality was examined using the 260/280 and 260/230 absorbance ratios.

2.5.1 *RNA extraction*

RNA was extracted according to the high-throughput 96-well protocol developed by Box et al. (2011). I describe in brief how it was used for both the 96-well format and the single tube format.

Ninety six-well collection tubes with clean steel beads were cooled in dry ice for twenty minutes before collection of tissue. Upto 200 mg of fresh tissue was harvested on dry ice into each tube and frozen at -80°C. The tissue was homogenized on a bead mill (Retsch MM 300 Homogenizer, Retsch GmbH, Haan, Germany) in four rounds, for 30 seconds each time, at 20 cycles/second. The 96-well plate was frozen at -80°C between each round of grinding to prevent the tissue from thawing. To each tube 300 µL of RNA Extraction buffer (0.1M Tris pH 8.0, 5mM EDTA pH 8.0, 0.1M NaCl, 0.5% SDS, 1% β-Mercaptoethanol added just before use) were added and mixed by inversion. To this, 300 µL of 1:1::Acid phenol:chloroform were added and mixed by inversion, making sure that the tubes were tightly sealed. The aqueous and organic phases were separated by centrifugation at 6000 x g at 4°C for 15 minutes. The upper aqueous phase was transferred into fresh tubes containing 240 µL isopropanol and 30 µL 3M sodium acetate. The RNA was precipitated at -80°C for 15 minutes, followed by centrifugation for 30 minutes at 6000 x g at 4°C. The supernatant was discarded and the pellet was washed twice with 70% ethanol. The pellet was allowed to air dry and was resuspended in 30 µL double distilled H_2O.

2.5.2 *Quantitative RT-PCRs*

RNA samples were treated with DNase (Thermo Scientific GmbH, Karlsruhe, Germany) to remove genomic DNA contamination. One unit of DNase was added to 2 µg of total RNA in a total volume of 10 µL. First strand cDNA synthesis primed with oligo-$(dT)_{18}$ was carried out on 1 µg of DNase-treated RNA using RevertAid First Strand cDNA Synthesis Kit (Thermo Scientific, Karlsruhe, Germany)

in a total volume of 10 µL. The cDNA was diluted 2x before being used in quantitative PCR. Primers for qPCR were designed using Primer3 (http://bioinfo.ut.ee/primer3-0.4.0/) or Roche UPL Assay Design Centre (http://lifescience.roche.com/shop/products/universal-probelibrary-system-assay-design). Reactions were carried out on a Bio-Rad CFX384 C1000 Touch qPCR machine (Bio-Rad Laboratories GmbH, Munich, Germany) using SYBR Green I to monitor PCR product formation. Melting curves for all primer pairs were analyzed to ensure the presence of a single amplicon.

2.6 FINE MAPPING

This section refers to fine mapping efforts for the chromosome 3 interval. Rough mapping of both loci and fine mapping of the chromosome 2 interval were carried out by Roosa Laitinen and Helena Boldt (Boldt, 2009).

Plants of the BG-5 x Kro-0 F_2 generation were grown at 16°C and plants that were either bushy or small and purple were collected. Genomic DNA from all plants was extracted by the CTAB protocol adapted for the 96-well format. Genotyping was carried out using SSLP (simple sequence length polymorphisms) markers that were designed at the ends of the intervals obtained from rough mapping. When recombinant samples were identified, the mapping interval was further narrowed down using SNP markers between Kro-0 and BG-5; i.e. short PCR amplicons containing the SNP(s) were sequenced by Sanger sequencing and the chromatogram peaks were analyzed using the SeqMan software (DNASTAR Inc., Madison, USA; see Appendix A.2 for details).

2.7 CANDIDATE GENE TESTING

2.7.1 *Construction of artificial microRNA constructs against candidate genes*

Oligonucleotide primers corresponding to sense, antisense, sense* and antisense* were designed for each candidate gene as described earlier using the WebMicroRNADesigner (WMD3.0) tool (Schwab et al.,

2006, see Appendix A.2 for further details;). Artificial microRNA were generated by overlapping PCRs with the plasmid pRS300. PCR products of the correct size were excised from an agarose gel, purified and cloned into pJLBlue (rev) vector by restriction digestion with EcoRI and BamHI and ligation by T4 DNA ligase. Correct clones were confirmed by sequencing of the plasmids with vector-specific primers G-4041 and G-4042 to ensure that the artificial microRNA sequences matched the expected sequences. The construct was then subcloned by recombination using LR Clonase (Invitrogen) into pFK210, a pGreen-IIS based plasmid that contains the Cauliflower mosaic virus (CaMV) 35S overexpression promoter upstream of the multiple cloning site and genes conferring Spectinomycin resistance in bacteria and BASTA resistance in plants. The insert was sequenced with vector-specific primers G-0474 or G-0463. The construct was then co-transformed with the helper plasmid pSOUP into *Agrobacterium tumefaciens* strain ASE. The *Agrobacterium* clones were tested by culture PCR and were transformed into *Arabidopsis* as described earlier (Clough and Bent, 1994).

2.7.2 *Genomic complementation with candidate genes*

Genomic constructs were made using the Greengate system as described (Lampropoulos et al., 2013). In brief, I designed oligos that removed Eco31I sites from within the PCR amplicons. Overlapping PCRs were then carried out to obtain the full length gene, or UTR or promoter with Eco31I sites removed. When Eco31I sites were mutated in exons, synonymous changes to amino acid sequence were made. These fragments were then cloned into "entry" vectors: pGGA000 for promoter modules, pGGC000 for CDS modules and pGGD000 for UTR modules. Entry modules were sequenced completely to select clones that had the correct sequence. The modules were brought together in destination vector pGGZ000 by using the Eco31I restriction endonuclease together with a high concentration T4 DNA ligase (30U/µL) in a "one-pot" reaction. Destination clones were sequenced across ligation junctions to ensure that all modules had been stitched together in the correct order. These clones were then transformed into Agrobacterium and then into plants as described above.

2.8 PHENOTYPIC CHARACTERIZATION OF KZ-10 X MRK-0 AND UK-1 X UK-3 HYBRIDS

Measurement of growth and necrotic phenotypes

The cotyledons of KZ-10 x Mrk-0 hybrids, Uk-1 x Uk-3 hybrids and their parents were examined for the appearance of necrotic spots each day. The proportion of plants that were necrotic was calculated relative to the total number of plants in the replicate. Each replicate consisted of 20 plants on average with a range of sample sizes from 16 to 25. Growth was measured by weighing the dry shoot biomass of the aerial parts of plants at 42 DAS. For each genotype, pools of 8 plants were weighed from two biological replicates.

2.9 PHENOTYPIC CHARACTERIZATION OF BG-5 X KRO-0 HYBRIDS

2.9.1 *Measurement of anthocyanin content*

Plants were grown at 16°C for 4 weeks. Aerial parts were collected and frozen at -80°C and roots were collected separately for genotyping. Frozen tissue was homogenized with steel beads and 1 mL of 1%(v/v) hydrochloric acid in methanol was added in Eppendorf tubes. The tissue was mixed thoroughly and left overnight at 4°C. The mixture was centrifuged (Eppendorf centrifuge, 5417R) at 18000 g for 5 minutes. The supernatant was transferred to a fresh tube and its absorbance was measured at 530nm and 657nm (μQuant, Bio-Tek Instruments Inc., Bad Friedrichshall, Germany). Anthocyanin content was calculated according to the following formula:

$$\text{Relative anthocyanin content} = \frac{(A_{530} - 0.25 * A_{657})}{\text{Fresh weight of tissue}}$$

2.9.2 *Shoot dry biomass*

Plants were collected after 6 weeks of growth at 16°C. Aerial parts were collected in paper bags and roots were collected for genotyp-

ing. Shoot dry biomass was measured for individual plants (Rauch XA 52/2X Radwag, Graz, Austria) after drying the tissue at 85°C overnight.

2.9.3 *Other phenotypic characteristics*

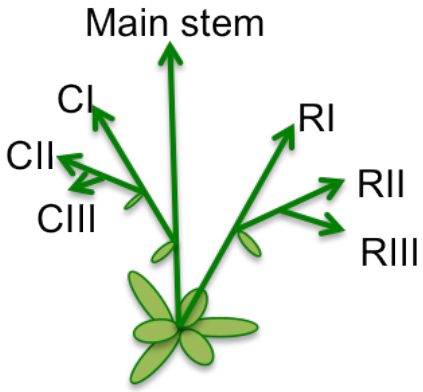

Figure 3: *Schematic representation of Arabidopsis thaliana branching pattern. RI, RII and RIII refer to primary, secondary and tertiary branches arising from the axils of rosette leaves. CI, CII and CIII refer to primary, secondary and tertiary branches arising from the axils of cauline leaves of the main stem.*

Lifetime traits such as main stem height, silique number and number of branches were measured when the plants were senescent, or when the oldest siliques had turned brown. Rosette and cauline branches were assigned according to Figure 3 (adapted from Aguilar-Martinez et al., 2007, Plant Cell). In all of the above experiments, F2 plants of all genotypes were analysed, including normal, bushy and purple plants.

2.10 STATISTICAL ANALYSES

The R software program version 2.15.2 was used to conduct all statistical analyses. For the temperature sensitivity experiments, comparisons were made between the F_1 hybrids grown at different temperatures. The phenotypes of the parents were used only to highlight the change in the hybrids. They were not included in the multiple comparisons since the aim was to monitor change specifically in the hybrid phenotype with temperature. The aov function was used followed by Tukey's HSD for post-hoc multiple comparisons. For the BG-

5 x Kro-0 hybrids, Fligner-Killeen tests revealed non-homogeneous variance for most datasets. Therefore, Kruskal-Wallis rank sum tests were carried out followed by a post-hoc Tukey's HSD (using the npar-comp library) to determine significant differences between groups.

2.11 SCANNING ELECTRON MICROSCOPY

Inflorescence meristems were collected from samples when the plant had made 5-6 siliques. Surrounding buds and flowers were removed prior to collection. Samples were fixed in 2.5% glutaraldehyde. All downstream techniques from critical point drying to image collection were carried out by Jürgen Berger of the Electron Microscopy Facility of the Max Planck Institute of Developmental Biology, Tübingen.

2.12 GRAFTING

Plants were grown on half-strength Murashige-Skoog medium containing 1% sucrose, with the plates placed vertically in a growth chamber. When the seedlings were 5 days old, they were placed on a fresh MS plate on a Millipore nitrocellulose filter. Both the cotyledons were removed to enable the seedling to be placed flat on the filter. A cut was made perpendicular to the hypocotyl with a scalpel blade. Both scion and stock plants were cut together and their shoot and root parts exchanged. Grafts were aligned visually and the plates were sealed with Parafilm and left vertically for 7 days. Before transferring grafted plants to soil, any adventitious roots growing from scions were cut.

2.13 TREATMENT WITH AUXIN

Plants were grown at 16°C on soil in a randomized design within each treatment. Flats containing control plants were separate from, but adjacent to flats containing treated plants to reduce contamination by aerosol particles. After three weeks, plants were sprayed every four days with either 5µM 2,4-D or 5µM 2,4-D methyl ester (ME) prepared in DMSO. Control plants were sprayed with the equivalent concentration of DMSO. One plant in each genotype was not sprayed

with anything to ensure that there were no effects on plants due to aerosol contamination. The spraying continued until the plants had bolted to at least 2 cm. At the start of the experiment, there were six biological replicates for each genotype and treatment combination. However, stem heights were only measured for the plants that bolted and produced siliques. The final numbers of replicates were six for all genotype-treatment combinations except Kro-0 (2,4-D), Kro-0 (2,4-DME), Kro-0 (control) and BG-5 (2,4-D).

2.14 WHOLE-GENOME RESEQUENCING

2.14.1 *Preparation of BG-5 genomic DNA*

One gram of tissue was ground to a fine powder in liquid nitrogen using a mortar and pestle and transferred to a 15-mL polyethylene centrifuge tube containing 10 mL of ice-cold Nuclei Extraction buffer (10mM Tris-HCl pH 9.5, 10mM EDTA pH 8.0, 100mM KCl, 500mM sucrose, 4mM spermidine, 1mM spermine, 0.1% ß-mercaptoethanol). The tissue was mixed with a wide-bore pipette and filtered through two layers of Miracloth (Merck Millipore, Darmstadt, Germany) into an ice-cold 50-mL polyethylene centrifuge tube. It was then gently mixed with 2 mL of Lysis buffer (10% Triton X-100 in Nuclei extraction buffer) for 2 minutes on ice. The nuclei were pelleted by centrifugation at 2000 x g for 10 minutes at 4°C. The supernatant was discarded and 500 µL of CTAB extraction buffer (100mM Tris pH 7.5, 0.7M NaCl, 10mM EDTA pH 8.0, 1% (w/v) CTAB, 1% ß-mercaptoethanol) were added to the pelleted nuclei. This mixture was transferred to a 1.5 mL microcentrifuge tube and was mixed by inversion. It was incubated at 60°C for 30 minutes and then cooled to room temperature for 5 minutes. 350 µL of 24:1 :: chloroform:isoamyl alcohol were added and mixed by inversion for about 5 minutes, followed by centrifugation at 6000rpm (5796 g in a Sigma centrifuge, model 4K15) for 10 minutes. The upper phase was transferred to a fresh tube containing equal volume of isopropanol and mixed by inversion. The DNA was pelleted by centrifugation at 13000 rpm for 3 minutes and the pellet was washed with 75% ethanol. The DNA was resuspended in 50-100 µL of DNase-free water (containing 10 µg/mL RNaseA).

2.14.2 *Library Preparation for Illumina sequencing*

The genomic DNA (500 ng) was fragmented enzymatically with the help of dsDNA Shearase^{TM} (Zymo Research, Freiburg, Germany) in a total volume of 25 µL, containing 500ng of genomic DNA, 3x shearase buffer and 1.25µL of Shearase^{TM} enzyme. The reaction was incubated at 37°C for 30 minutes and was terminated by the addition of 1.25 µL of 0.5M EDTA. The fragmented DNA was cleaned up by using SPRI magnetic beads (Ampure XP, Brea, CA, USA). In brief, 1.8x volume of SPRI beads were added to the DNA sample, vortexed and left to stand at room temperature for 5 minutes. The tubes were then placed in the magnetic rack for 5 minutes or until the sample cleared up. The solution was removed from the tube while the tube was still in the magnetic rack. Two ethanol washes were carried out with 700 µL of 70% ethanol, with the tubes in the magnetic rack. The sample was dried on a heat block at 37°C for 5-10 minutes, or until the ethanol had evaporated. The sample was then incubated at room temperature for 5 minutes with 35 µL of water. The tube was placed in the magnetic rack to clear the solution and the supernatant containing the purified DNA was transferred to a fresh tube. The purified DNA was profiled for size and quantity on an Agilent Bioanalyzer 2100 (Agilent Technologies, Germany).

The DNA was A-tailed using Klenow exonuclease and dATP at 37°C for 30 minutes, followed by a SPRI clean-up as described earlier. Adapters were ligated for 15 minutes at 20°C, followed by 15 minutes at 65°C. The DNA was cleaned again using SPRI beads and then PCR-amplified using Phusion polymerase. PCR products were cleaned up using QiaQuick PCR Cleanup according to manufacturer's instructions. The library was then measured on Qubit (Qubit 2.0, Life Technologies, Germany) and Bioanalyzer.

The library was sequenced on an Illumina GA IIX sequencer to an average depth of 6.4 x coverage of the *A. thaliana* genome with 2 x 100-bp reads. The raw reads were aligned to the reference genome (Schneeberger et al., 2009) using SHORE, allowing for 10% mismatches and 7% gaps. After paired-end correction, SNPs and small (1-3 bp) indels were called using SHORE consensus, requiring a minimum allele fre-

quency of 51% for an alternative call, and excluding reads that cover a position only with the first or last 4 bases of the read. Further filtering of the polymorphisms was achieved using custom scripts to select only those with quality scores above 25, a read count of at least 3 to support an alternative call, and non-repetitive mapping. Large structural variants (deletions, insertions, translocations, inversions) were called using SHORE structure with an estimated insert size of 400 bp.

2.15 FOSMID LIBRARY CONSTRUCTION AND SCREENING

2.15.1 *Construction of the fosmid library*

Genomic DNA was isolated by the CTAB method from several inflorescences and run on a gel to examine quality and size. Lambda phage DNA was used as a size control. The genomic DNA was then sheared to approximately 40kb fragments by repeatedly passing it through a 200uL pipette tip.

The sheared DNA was end-repaired to generate blunt-ended and 5′-phosphorylated DNA. It was then ligated overnight with the Copy-Control vector pCC1FOS (Epicentre Biotechnologies, Madison, USA) and packaged into MaxPlax Lambda Packaging Extracts. Serial dilutions of the packaging reaction were made to determine the titer of the packaged fosmid clones. Each dilution was infected into 100uL of EPI300-T1^{R} host cells and these were spread on a plate containing 0.5X chloramphenicol and incubated at 37°C overnight. Colonies were counted the following morning and the titre was determined according to the following equation:

$$\text{Titre} = \frac{(\#\ \text{of colonies}) * (\text{dilution factor}) * (1000\ \mu\text{l/ml})}{\text{volume of phage plated } (\mu\text{l})}$$

The titre of the BG-5 fosmid library was approximately 90,000, indicating that the coverage of the BG-5 genome in this library was 5X, based on the 125Mb *Arabidopsis thaliana* genome.

2.15.2 *Screening of the fosmid library*

Approximately 70,000 clones were then packaged and infected into EPI300-T1^R cells and plated on LB plates containing 12.5µg/mL chloramphenicol. The plates (referred to as "master plates") were incubated at 37°C for 12-16 hours or until the colonies were ~3mm in diameter and well separated. A Hybond-N nylon filter (GE Healthcare Life Sciences, Freiburg, Germany) was placed on the colonies. The filter was then transferred colony side up onto an LB plate and the replica colonies were grown for 4 hours at 37°C.

At the end of 4 hours, the replica colonies on the filters were lysed by transferring them between Whatman papers soaked with the following solutions:

1. 10% SDS 2 min
2. 1.5M NaCl, 0.5M NaOH 5 min
3. 0.5M Tris-Cl pH7.4, 1.5M NaCl 5 min x2

Filters that had been processed through the above solutions were stored in 2X SSPE (20X SSPE stock contains 3M NaCl, 200mM NaH_2PO_4.H2O, 20mM EDTA, pH adjusted to 7.4 with NaOH) until all filters were processed. The filters were then blotted out on paper towels and cross-linked using UV light.

The filters were floated on the surface of 2x SSC solution until completely wet from below and then submerged in the same solution for 5 minutes. They were then transferred to a dish containing 6x SSC (preheated at 65°C; 20X SSC contains 3M NaCl, 0.3M sodium citrate, pH adjusted to 7.0) for 30 minutes on a shaking platform. Cell debris was gently scraped off using a paper towel soaked in 6x SSC.

Probes corresponding to different regions in the mapping interval were constructed and labeled with DIG in a PCR reaction, according to manufacturer's instructions (Roche PCR DIG labeling mix, for moderately labeled probes). The probes were purified by precipitating with ethanol and LiCl. Two or three different probes were used together in a single hybridisation event.

Filters were soaked in prewarmed prehybridisation solution (5X SSC, 0.1% (w/v) N-laurylsarcosine, 0.02% SDS, 1% Blocking solution) at 57°C for 5-6 hours in a rolling glass bottle. Denatured probes were then added and hybridised at 57°C overnight. The filters were washed once in 2x SSC, 0.1% SDS for 30 minutes. They were then transferred to new rolling glass bottles and washed in 2x SSC, 0.1% SDS at 57°C for 30 minutes. This wash was repeated three more times, followed by 4 washes with 0.1X SSC, 0.1% SDS for 30 minutes each at 57°C. The filters were then placed in 1x maleic acid buffer (100 mM maleic acid, 150 mM NaCl, pH adjusted to 7.5 with NaOH); after 1 minute, the maleic acid buffer was replaced with fresh buffer for another minute.

The filters were placed facing each other in a tray with 10 mL of 1x Blocking solution (10% (w/v) blocking reagent, 1x maleic acid buffer) between each pair. They were left gently shaking for 30-60 minutes at room temperature before adding the alkaline phosphatase-conjugated anti-DIG antibody (5 µL antibody in 50 mL blocking solution). At the end of 30 minutes at room temperature, the antibody solution was discarded and the filters were washed in 1x Washing buffer (100 mM maleic acid, 150 mM NaCl, 0.3% Tween 20) twice for 15 minutes each.

The filters were equilibrated in detection buffer (100 mM Tris-Hcl, 100mM NaCl, pH adjusted to 9.5) for 5 minutes. CSPD, a chemiluminescent substrate that acts as a substrate for alkaline phosphatase, was added all over the surface of the filter and emission was recorded on an X-ray film for 15-30 minutes.

The spots on the film were then compared to the master plates and the corresponding colonies were streaked out on fresh LB plates to propagate them further and to ensure that the positive colonies are not a mix of two clones. Several individual colonies from each plate were tested by colony PCR with the same primers that were used for probe construction and positive clones were propagated in large culture media. Copy numbers of the fosmids were increased by addition of the CopyControl Fosmid Autoinduction Solution. The cells were spun down and fosmid DNA was extracted with the help of a Qiagen Large Construct Kit according to manufacturer's instructions. The fosmids were then end-sequenced using T7 promoter-specific and T3 promoter-specific primers. If fosmids had similar end sequences, then

only one of them was selected for further shotgun sequencing such that the selected clone overlapped other fosmid end sequences.

2.15.3 *Shotgun subcloning of fosmid DNA*

Fosmid DNA was sheared acoustically using a Covaris S2 ultrasonicator (Covaris Inc., Brighton, UK). The sheared DNA was examined on an agarose gel and DNA in the size range 800-2000 bp was excised from the gel and used for subsequent subcloning steps. Blunt end repair and dephosphorylation were carried out on approximately 3 µg of sheared DNA according to manufacturer's instructions (TOPO Shotgun Subcloning Kit, Life Technologies). About 100ng of blunt-end DNA was then ligated into the pCR4Blunt-TOPO vector and the reaction was purified by dialysis on a Millipore filter. The ligation reactions were then transformed into OneShot TOP10 cells by electroporation. A fraction of the electroporated cells were plated out on LB plates containing Ampicillin and X-Gal; TOPO clones containing the fosmid inserts were selected by blue-white screening. Positive clones were propagated in liquid LB-Ampicillin media in a 96-well format and plasmid DNA was extracted using the Qiagen MagAttract 96 Miniprep kit with the help of a liquid handling robot (Qiagen Biorobot 8000). Clones were sequenced with T7 and T3 primers and the sequences were assembled using DNAStar's Seqman software.

3

PATTERNS OF TEMPERATURE DEPENDENCE IN NECROTIC HYBRIDS

3.1 BACKGROUND

Dobzhansky-Muller incompatibilities in several plant species have been shown to cause ectopic immune activation in hybrids due to interaction between genes from independently evolving lineages. To illustrate how widespread this phenomenon is, I briefly introduce some of the well-characterized hybrids in tomato, lettuce, rice and *Arabidopsis*. In all the examples, genes that normally function in disease resistance, interact epistatically to give rise to autoimmunity.

One of the earliest identified cases that was also characterised at the molecular level comes from tomato. In tomato, the R-gene *Cf-2* confers resistance to the fungus *Cladosporium fulvum* (Krüger et al., 2002). This gene interacts with certain alleles of the *RCR3* gene to produce necrotic hybrids. In hybrids of the F_2 generation after a cross of *Solanum lycopersicon* (domesticated tomato) with *S. pimpinellifolium* (a wild relative), necrotic lesions were produced in progeny that carried the *Cf-2* gene from *S. pimpinellifolium* and that were homozygous for the *RCR3* allele of *S. lycopersicon*. *Cf-2* is a transmembrane protein that monitors the integrity of the *RCR3* cysteine protease, which is a target of the avirulence factor *Avr2* of *C. fulvum* (Rooney et al., 2005). Necrosis is caused by activation of *Cf-2*, which in turn can be caused by inhibition of *RCR3* by *Avr2*, or by inactivation of the *RCR3* protein by mutation or changes in its protein sequence, as in the *S. lycopersicon* allele.

In interspecific lettuce hybrids of the cross *Lactuca saligna* x *L. sativa*, hybrids containing the *RIN4* (*RPM1-INTERACTING PROTEIN4*) allele of *L. saligna* interact with a locus on chromosome 6 of *L. sativa* to produce necrosis (Jeuken et al., 2009). These hybrids are resistant to *Bremia lactucae*, the fungus that causes downy mildew in lettuce. RIN4 in *Arabidopsis thaliana* is targeted by several effectors of the bacterial pathogen *Pseudomonas syringae* and is guarded by two R pro-

teins, RPM1 and RPS2 (Axtell and Staskawicz, 2003; Mackey et al., 2003; Kim et al., 2005b,a).

In crosses between the *japonica* variety of Koshihikari and the *indica* variety of Habataki of *Oryza sativa* (domesticated rice), a casein kinase interacts with a highly diversified gene cluster of NB-LRR proteins to induce hybrid necrosis. NB-LRR genes form a large family of resistance proteins and are often found in complex gene clusters that are formed by gene rearrangements and duplications.

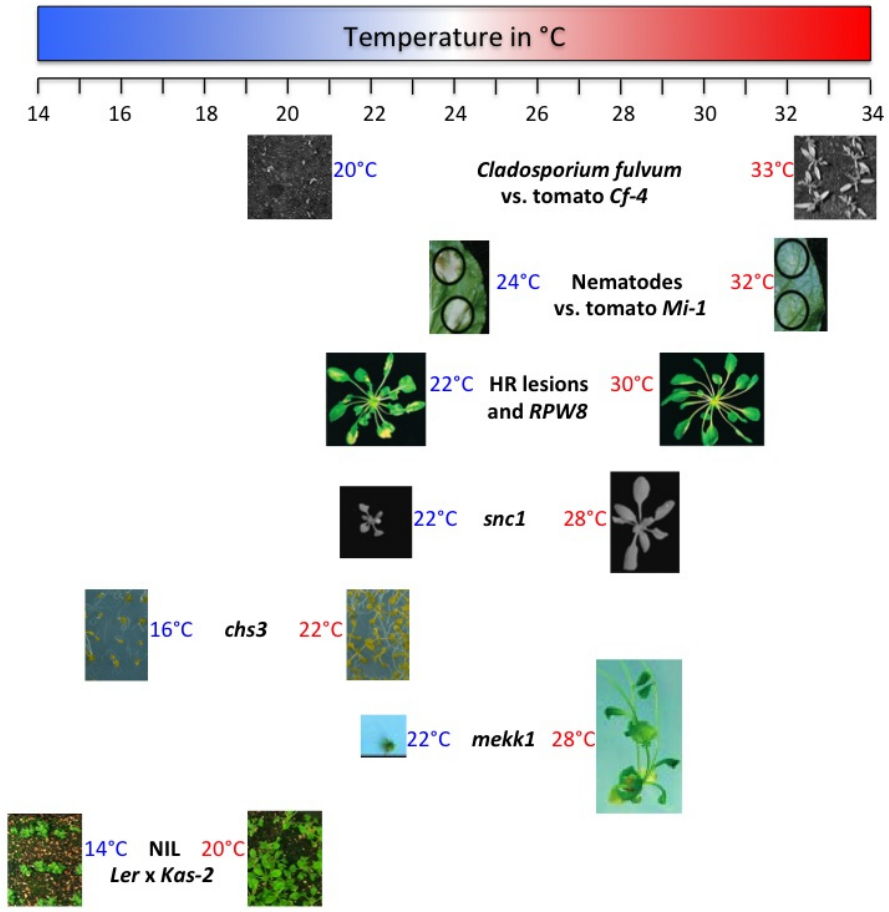

Figure 4: *Examples of cases involving different plant-patho systems and autoimmune mutants, where the temperature sensitivity of the immune response was observed.*

NB-LRR genes are also involved in intraspecific hybrid necrosis cases in *Arabidopsis thaliana*. In the first such case identified, an NB-LRR gene from one locus (*DM1*) interacted with *DM2* (an *RPP1*-like gene cluster) to induce autoimmunity in Uk-1 x Uk-3 hybrids. *RPP1* is also responsible for causing incompatibilities between Ler and a group of

Asian accessions that carry a specific allele of a receptor-like kinase, *SRF3* (*STRUBBELIG RECEPTOR FAMILY*; Alcazar et al., 2010).

Most cases of hybrid necrosis are suppressed when the plants are grown at elevated temperatures. This is similar to the temperature sensitivity of defence responses during pathogen infection and ectopic activation of the immune system of mutants in the absence of pathogen pressure (see Fig. 4).

Despite intense interest in the effect of environmental changes on plant defence status, there exist no systematic studies so far that elucidate the effect of small changes in temperature on the various readouts of plant fitness. Most studies focus their efforts on temperatures that are far apart, losing the information about reaction norms for these phenotypes. This is the first study that takes a detailed look at how temperature exerts different effects on morphological and molecular phenotypes of activated defence responses. We use autoimmune hybrids as a useful tool in studying this phenomenon as it gives additional insights into how environmental changes at very small scales can dramatically affect epistatic interactions between genes. This has implications for the effect of climate change on adaptation and speciation.

3.2 RESULTS

Previously, several *A. thaliana* intraspecific hybrids were shown to display necrotic symptoms at 16°C, which disappeared when the plants were grown at 23°C (Bomblies et al., 2007). I studied the appearance of necrotic symptoms in the Uk-1 x Uk-3 F1 (UU) hybrids and the KZ-10 x Mrk-0 F1 (KM) hybrids in more detail over a continuous range of temperatures in 2°C increments between 12 and 26°C. Both hybrids displayed severe symptoms of necrosis at low temperatures, but their genetic causes were different. This allowed me to determine whether patterns of temperature sensitivity were distinct in necrotic hybrids with different causes.

3.2.1 *Onset of necrotic symptoms*

Both UU and KM hybrids were necrotic only in the temperatures between 12 and 22°C, but the proportion of plants that displayed the symptoms in this range differed between the two. In the case of the UU hybrids, appearance of necrotic lesions at 10 and 16 days after sowing (DAS) increased with temperature and peaked at 16-18°C. Further increases in temperature led to a gradual decrease in the proportion of plants displaying symptoms, until there were no plants displaying necrosis at 24°C.

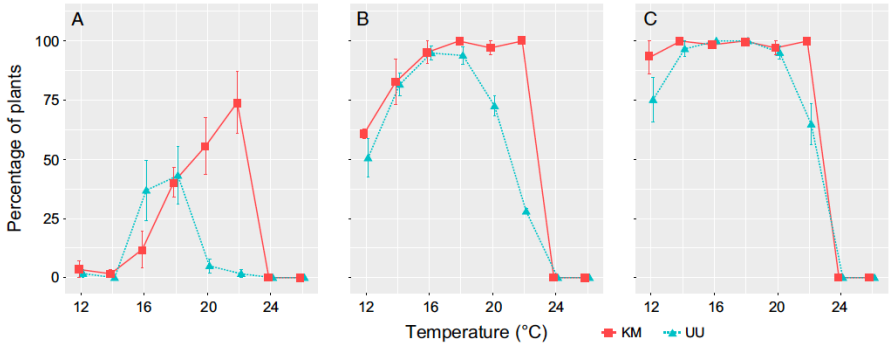

Figure 5: *Appearance of necrosis in F1 hybrids of Uk-1 x Uk-3 (UU) and KZ-10 x Mrk-0 (KM) at 10 (A), 16(B) and 42(C) days after sowing (DAS). UU hybrids showed a steady decrease in the share of necrotic plants, while KM hybrids displayed an abrupt decline from 22 to 24°C (B,C). Means ± SE are shown for three biological replicates. Each replicate consisted of 20 plants on average (range 16-25 plants).*

In KM hybrids, necrotic lesions increased with temperature at 10 and 16 DAS and reached a maximum at 22°C. With an increase in temperature of 2°C, there were no necrotic hybrids at 24°C. These differences in the patterns of temperature sensitivity between the UU and KM hybrids were very obvious at 16 DAS and at 42 DAS. There were higher proportions of KM hybrids displaying necrotic symptoms than UU hybrids, indicating that the defence responses in KM hybrids were either induced earlier or to a stronger degree than they were for UU hybrids.

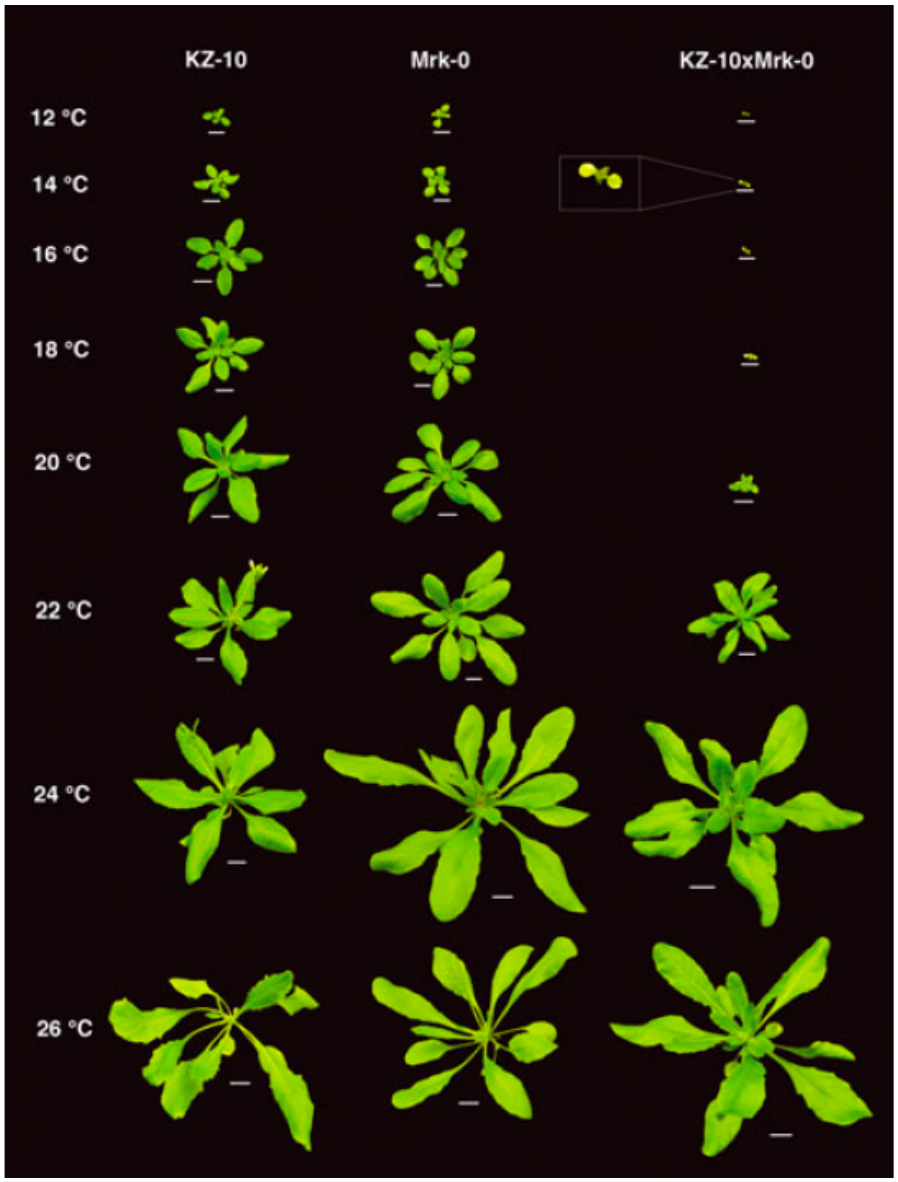

Figure 6: *Representative images of KM hybrids alongwith the parental accessions, grown at different temperatures. Photographs were taken at 42 DAS. Scale bars are 1cm.*

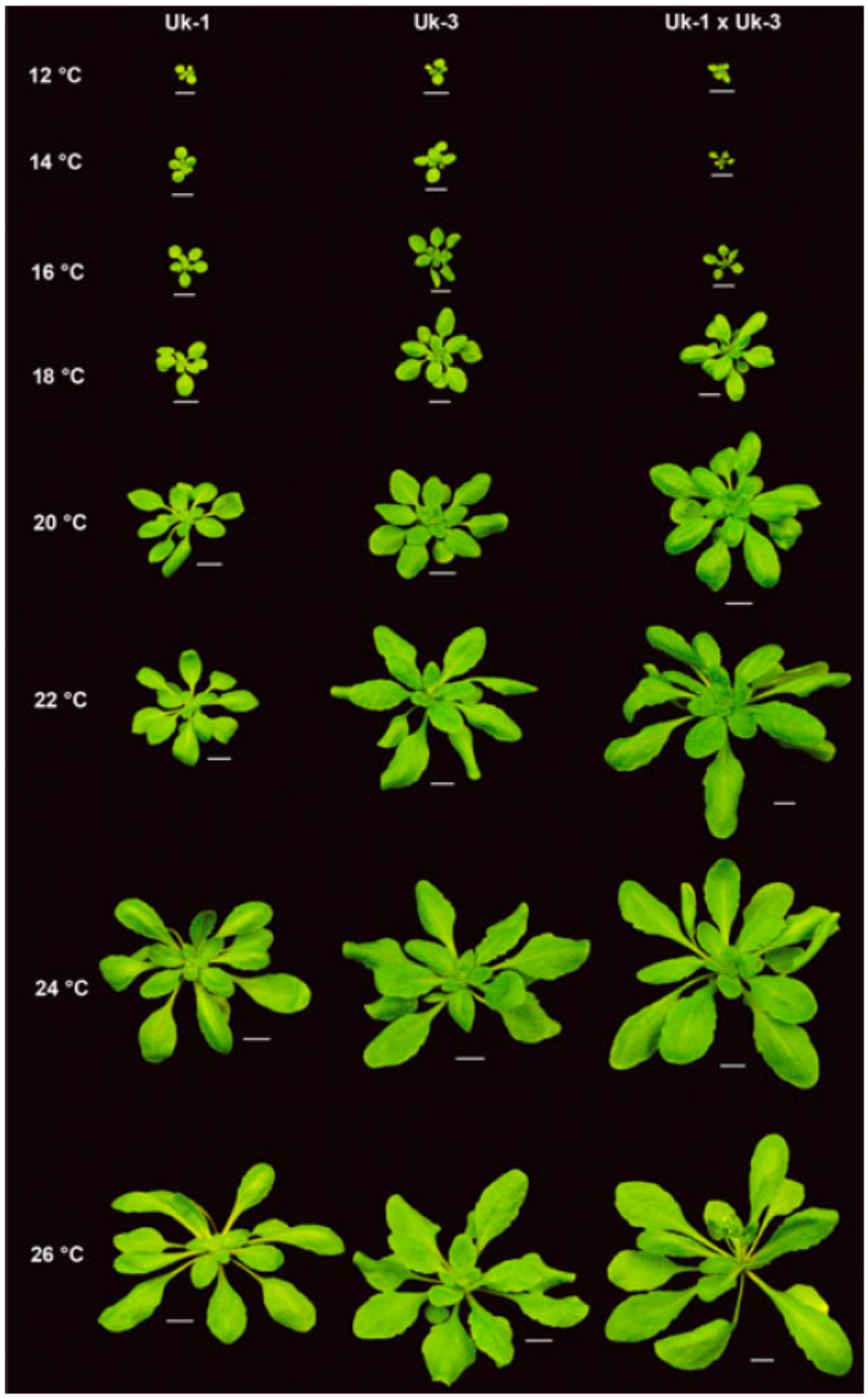

Figure 7: *Specimens of UU hybrids and parents grown at different temperatures and photographed at 42 DAS. Scale bars are 1cm.*

3.2.2 *Temperature-dependent change in shoot biomass*

The antagonistic effects of immune activation on growth are well-documented (Tian et al., 2003; Yang and Hua, 2004; Todesco et al., 2010; Alcazar and Parker, 2011; Hua, 2013). To assess whether the decrease in necrotic lesions in hybrids was reflected by an increase in growth, I measured the dry shoot biomass of plants at 42 DAS (expressed as a proportion of the mid-parent biomass). For the KM hybrids, relative biomass was low from 12 to 20°C, then increased steeply from 20 to 22°C and once again from 24 to 26°C. At 24 and 26°C, the KM hybrids performed better than the parents. The UU hybrids were smaller than the parents from 12-18°C, except one replicate at 12°C. At 20°C and above, they had higher biomass than the parents, but with no additional increase proportional to temperature.

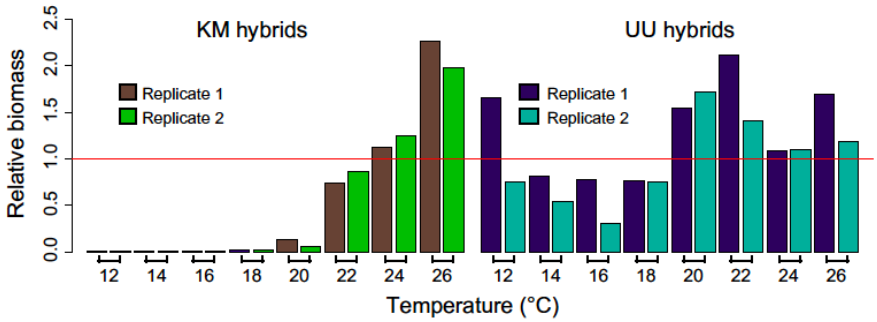

Figure 8: *Relative biomass of KM and UU hybrids at different temperatures. Relative biomass was calculated as a ratio of the hybrid's dry biomass to the mid-parent biomass. Plants from two biological replicates were weighed in pools of 8 plants each.*

In both the hybrids, the greatest increases in biomass took place at temperatures where necrosis was still apparent: 20°C for UU hybrids and 22°C for KM hybrids. This indicates that the antagonism between growth and defence is complex and can have different outcomes based on the temperature at which it is being investigated. Since both the growth and necrosis phenotypes of the two hybrids showed different temperature profiles, they may possibly be governed by different mechanisms.

3.2.3 *Immunity gene expression profiles*

To determine whether the morphological phenotypes observed in the hybrids are mirrored by the molecular phenotypes, I assayed expression levels of the *PATHOGENESIS-RELATED1* (*PR1*) immunity marker gene. *PR1* gene expression is mediated by salicylic acid (SA) and is upregulated in response to pathogen attack (Yalpani et al., 1991; Uknes et al., 1992). It was previously shown to have increased expression in the UU and KM hybrids, along with other defence-related genes (Bomblies et al., 2007).

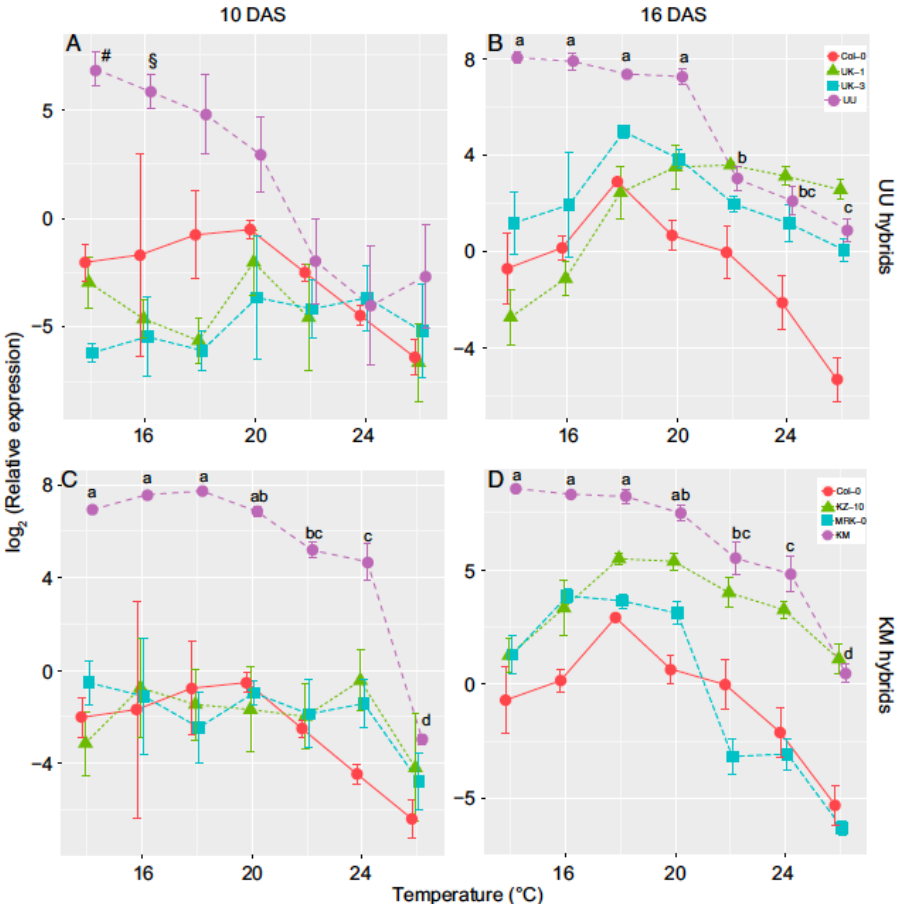

Figure 9: *PR1 expression is similar among UU hybrids grown at different temperatures at 10DAS(A). At 16DAS, PR1 expression shows a threshold change from 20 to 22°C (B). PR1 levels in KM hybrids are similar from 14 to 18°C and decrease gradually from 20 to 24°C with a sharp decline at 26°C, at 10 and 16DAS (C,D). Means ±SE are shown for three biological replicates containing pools of 20 plants each. Different letters denote significant differences between groups in a post-hoc Tukey's test. In UU hybrids, at 10 DAS, PR1 transcript levels at 14 and 16°C were different from some of the other temperatures. This is indicated by the symbols # and §. The legend for both A and B is shown in B; the legend for both C and D is shown in D.*

PR1 expression was not significantly different in UU hybrids at 10 DAS among most of the temperature regimes, but there was a steep decline in expression at 16 DAS between 20 and 22°C. *PR1* expression in KM hybrids was high from 14 to 18°C and decreased gradually from 20°C onwards. The decrease in PR1 expression levels at 26°C was sharp at both 10 and 16 DAS.

Thus, *PR1* expression decreased non-linearly in UU hybrids even though the necrosis phenotypes decreased linearly with temperature from 18 to 24°C. On the other hand, *PR1* expression in KM hybrids decreased linearly and gradually even though the necrotic phenotypes changed sharply from 22 to 24°C. I focused on the KM hybrids for further investigation of temperature-dependence since the morphological phenotypes changed non-linearly with temperature. At the time of experimentation, the causal genes for this hybrid were not yet known. Therefore, I assayed some of the intermediate signaling genes required for immune activation.

SA-mediated signaling increases *PR1* gene expression dependent on several signaling components, including *EDS1*, *PAD4* and *EDS5* (Rogers and Ausubel, 1997; Zhou et al., 1998; Falk et al., 1999). I quantified the transcript levels of these genes to evaluate if their temperature profiles were similar to that of PR1.

The KM hybrids showed higher transcript levels for all three genes compared to their parents at all temperatures other than 26°C. *EDS1* transcript levels were similar between 14 and 20°C and then declined steadily with further increase in temperature. A similar pattern was observed for *EDS5* and *PAD4* transcript levels.

To determine whether there were gene expression differences in other immunity pathways, I measured transcript levels of three other genes: *FRK1* (*FLG22-INDUCED RECEPTOR-LIKE KINASE1*), a marker for pattern-triggered immunity that acts downstream of the flagellin-induced responses, and *LOX2* (*LIPOXYGENASE 2*) and *PDF1.2* (*PLANT DEFENSIN-LIKE1.2*), which are both markers for defence related to JA or ET signaling.

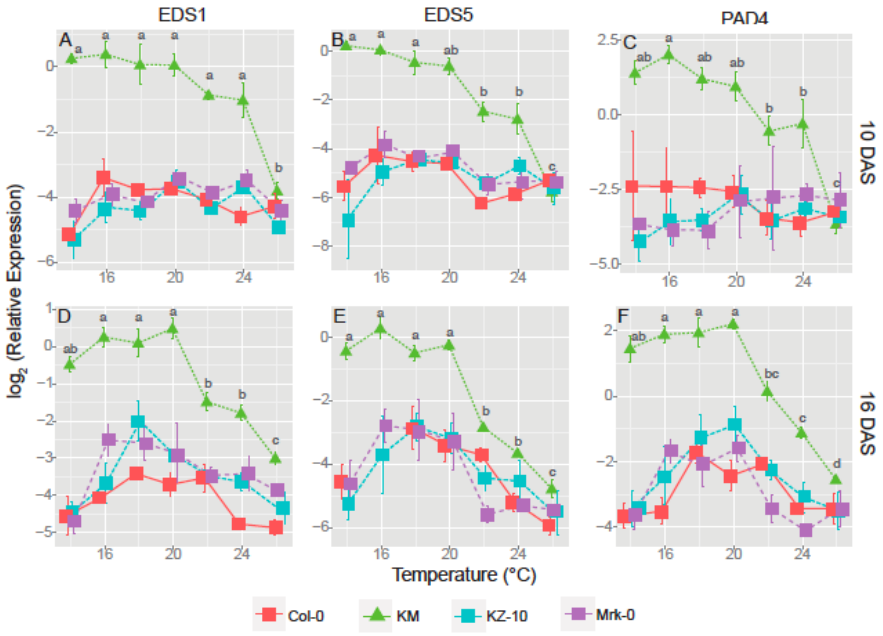

Figure 10: *Expression levels of EDS1, EDS5 and PAD4 reduce gradually with temperature at 10 (A-C) and 16 DAS (D-F). Means±SE for three biological replicates are presented.*

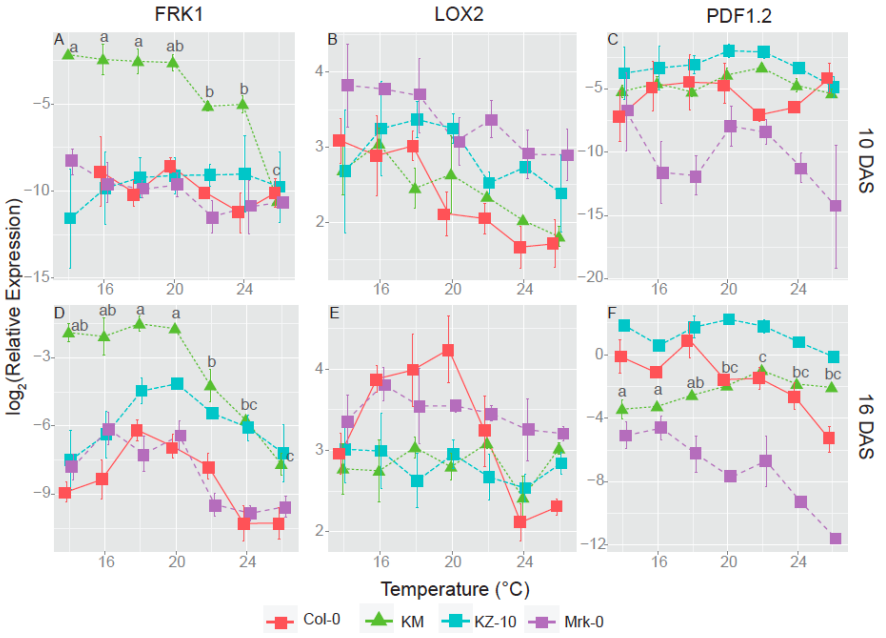

Figure 11: *Transcript levels of FRK1 decrease gradually with temperature at 10 (A) and 16 DAS (D). LOX2 (B, E) and PDF1.2 (C, F) levels do not show significant differences in expression with temperature. Means ± SE for three biological replicates are displayed.*

FRK1 gene expression followed a similar pattern to PR1 gene expression in the hybrids. *LOX2* and *PDF1.2*, however, did not have any temperature-dependent gene expression differences.

3.3 DISCUSSION

Temperature influences many key factors affecting plant success, including immunity against pathogens. Defence mediated by R genes is commonly suppressed at higher temperatures, but it is not known whether a specific critical temperature acts as a switch for increased immunity. The nature of the change in immunity - whether it is linear or nonlinear with temperature - is also not known. Since many different plant-pathogen systems share a set of common components in the immune activation cascade, another interesting question to ask would be whether these shared components are what give the immune system its sensitivity to temperature.

Since the ectopic immune activation in necrotic hybrids can be studied at different temperatures independent of the confounding effect that temperature may have on the pathogens causing the disease, the hybrids present us with a useful tool to address the questions specifically related to plant defence components. I investigated the temperature responses of two different necrotic hybrids: Uk-1 x Uk-3 (UU) hybrids and KZ-10 x Mrk-0 (KM) hybrids. They have different genetic bases, but appear to be similarly affected by temperature (Bomblies et al). I discovered that the different necrosis phenotypes showed both linear and nonlinear responses to temperature.

Defence response activation is costly and several studies have investigated this trade-off between growth and defence (Mauricio, 1998; Heil and Baldwin, 2002; Tian et al., 2003; Korves and Bergelson, 2004; van Hulten et al., 2006; Todesco et al., 2010). Mutants that displayed constitutively active defences had stunted growth (Bowling et al., 1997; Shah et al., 1999; Li et al., 2001a; Shirano et al., 2002; Yang and Hua, 2004; Wang et al., 2009). Plants that had reduced levels of SA or glucosinolates were larger in size (Scott et al., 2004; Zust et al., 2011), whereas plants that had constitutive SA signaling and PR1 expression

were reduced in size (Bowling et al., 1997; Shah et al., 1999; Du et al., 2009). This growth vs. immunity trade-off needs to be mitigated so that disease resistance can be engineered into plants without affecting their yield.

In this study, I discovered that it is possible at certain temperatures, to have both increased immune activation (indicated by *PR1* levels) and high biomass. In both the hybrids studied, there was at least one environmental condition under which plants expressed relatively high levels of *PR1* without a loss of biomass. This may be due to a greater boost to growth at these temperatures or due to a decreased cost of defence on growth. Despite the fact that it is not possible to distinguish between these hypotheses from the current data, it is evident that growth and *PR1* expression reveal different responses to temperature.

The changes in molecular and morphological traits in both hybrids occurred at different temperatures, suggesting that their temperature-sensitivities and growth-defence trade-offs are probably driven by different mechanisms. Data from the KM hybrids indicate the presence of a *PR1* expression level threshold that triggers the formation of necrotic lesions. The UU hybrids did not demonstrate a similar threshold for *PR1* expression in relation to necrosis phenotypes. The absence of covariance between *PR1* expression, biomass and necrotic lesions with temperature indicates that it is possible to uncouple the morphological attributes of a defence response from its molecular phenotypes.

Other studies investigating suppressors or enhancers of immunity-related genes have pinpointed *Arabidopsis* mutants that show a similar uncoupling of growth from defence. One example is the *cdd1* (*constitutive defence without defect in growth and development1*) mutant which has increased SA signaling and immune activation without the associated costs to growth (Swain et al., 2011). However, this study looked at the mutant phenotypes at only one temperature (22°C), so I cannot infer a role for this gene in temperature-dependent uncoupling of the growth-defence trade-off.

Another example is the *rcd1* mutant, in which the growth defect of the *snc1* mutation is enhanced, without increasing defence responses

(Zhu et al., 2013). The *snc1* mutant displays a growth defect at 22°C, which is normally rescued at 28°C. When it is combined with an *rcd1* mutation, the growth defect is sustained even at 28°C. The role of the *RCD1* (*RADICAL-INDUCED CELL DEATH1*) gene in maintaining homeostasis of reactive oxygen species indicates a split in signaling pathways following PAD4- and SA-dependent signaling. Both *snc1* and *rcd1* display their phenotypes at temperatures higher than those relevant to my study. Therefore, I cannot speculate if this could be a universal mechanism applicable to the hybrids' temperature response.

In spite of the slower growth from 14 to 20°C, *PR1* transcript levels at these temperatures did not vary significantly. This may be due to a greater effect of the metabolic slowdown on growth than on immune activity at lower temperatures.

PR1 expression is downstream of many signaling cascades involved in activating defences. Its temperature sensitivity likely depends on one or more of the upstream components. Therefore, I assayed transcript levels of *EDS1*, *PAD4* and *EDS5*, which are all involved in amplification of SA signaling, contributing to an increase in *PR1* expression levels. All these genes had temperature-dependent expression levels, implying that the temperature-sensitive step occurs upstream of these molecules in KM hybrids. This is similar to the *bon1* mutant which has reduced expression of *EDS1* and *PAD4* at higher temperatures. Further investigation of *bon1* revealed that there may be additional factors downstream of *EDS1*/*PAD4* that contribute to its temperature-sensitivity, since constitutive expression of *EDS1* and *PAD4* did not alter its temperature sensitive defects. The decline of *EDS1*, *PAD4* and *EDS5* transcript levels in the KM hybrids mirrored that of *PR1* expression, suggesting that if there are any other downstream factors contributing to temperature sensitivity, they must follow activation of *PR1* expression.

Defense responses involving SA-signaling often antagonise those mediated by JA (Vlot et al., 2009). Since the two pathways of defence are targeted at different types of organisms (SA-mediated response against bacterial and fungal pathogens and JA-mediated response against herbivores), it is predicted that the up-regulation of SA-mediated defences may contribute to the susceptibility of plants to her-

bivore attacks. In fact, natural hybrid zones tend to have a higher diversity and abundance of herbivores (Fritz et al., 1999; Traw and Bergelson, 2010). It has been suggested that this is due to down-regulation of JA in hybrids driven by SA-mediated hybrid incompatibilities (Traw and Bergelson, 2010).

To test this hypothesis, I assayed markers for pathways that would indicate JA-mediated immune activity. *LOX2* is an enzyme that acts in the JA biosynthesis pathway and *PDF1.2* is a JA-responsive marker that is suppressed by elevated SA levels (Leon-Reyes et al., 2010). The *PDF1.2* promoter also contains ERF (ETHYLENE RESPONSE FACTOR) binding sites; ERFs are transcription factors that up-regulate its transcription in response to synergistic action of JA and ET (Brown et al., 2003; Lorenzo et al., 2003). I anticipated that the transcript levels of these genes would show the inverse temperature response as the SA-dependent pathway genes. However, I found that *LOX2* and *PDF1.2* levels were similar or intermediate to that of the parents and did not vary significantly with temperature. This is different from the hybrid necrosis case in Ler x Kas-2 F_1 hybrids that show decreased *PDF1.2* levels relative to the parental accessions at 14-16°C. This suggests that the antagonism between the SA and JA pathways may differ for each case, determined by the specific pathways involved.

FRK1 is an LRR receptor kinase necessary for broad-spectrum resistance to bacterial pathogens. The flagellin epitope on bacteria, flg22, is recognized by the receptor FLS2, following which the transcription of *FRK1* is increased. I found that *FRK1* levels decreased gradually with temperature, similar to that of *PR1*. This indicates that KM hybrids have an elevated basal defence response that is also sensitive to temperature. Further investigation may reveal whether this increased basal resistance contributes to the severity of the phenotype of KM hybrids.

3.4 CONCLUSION

To summarise, I found that the underlying genetic cause, rather than the downstream signaling components, determined the nature of the suppression of hybrid necrosis with temperature. The molecular and morphological phenotypes displayed both linear and nonlinear re-

sponses to temperature and it was possible to uncouple the effects of one on the other. This signifies that growth and defence can be modulated in such a way that biomass and yield are affected as slightly as possible in plants with active immune responses.

4

CAUSES OF AN ATYPICAL HYBRID INCOMPATIBILITY: THE KRO-0 X BG-5 DWARVES

4.1 BACKGROUND

A majority of F_1 hybrid incompatibility phenotypes studied in *Arabidopsis* are due to autoimmunity (Chae et al., 2014; Phadnis and Malik, 2014). This likely reflects that the immune system and the arms race between plants and their pathogens have played a central role in shaping the genomes of *Arabidopsis* accessions. However, different populations of *Arabidopsis* grow in very diverse environmental conditions, which is also a driver for many other traits that are affected by environment-dependent factors such as daylength, temperature, soil composition, water availability, humidity and light quality and quantity. Studying hybrids that do not express autoimmune, but other deleterious phenotypes may provide insights into such environmental factors and their evolutionary consequences.

One such case that does not relate to autoimmunity involves the accessions Kro-0 (from Germany) and BG-5 (from Seattle, USA). The F_1 hybrids between these accessions display temperature-dependent loss of apical dominance and increased shoot branching while the F_2 hybrids segregate an additional phenotype of increased anthocyanin accumulation and small stature. These phenotypes have not yet been studied either in the context of hybrid incompatibilities or in the context of temperature-dependent plasticity. Their study should reveal a new set of genes or pathways involved in the control of shoot branching and anthocyanin accumulation. It may also help in elucidating the reason behind their temperature-sensitive phenotypic plasticity and how these seemingly different phenotypes are linked.

In order to place this study in the context of previous work, I will first provide a brief introduction to what is already known about the control of shoot growth and apical dominance and how the regulation of anthocyanin synthesis is connected with this process.

4.1.1 *How does the main stem grow?*

The *Arabidopsis* shoot apical meristem (SAM) contains a group of stem cells that are required for the continuation of growth and the initiation of new organs (Sussex, 1989). They are organized into three cell layers: L1 and L2, that form the two topmost layers of cells called *tunica* and L3, which includes all interior cells below the L2, called *corpus* (Fig. 12). (Fletcher, 2002)

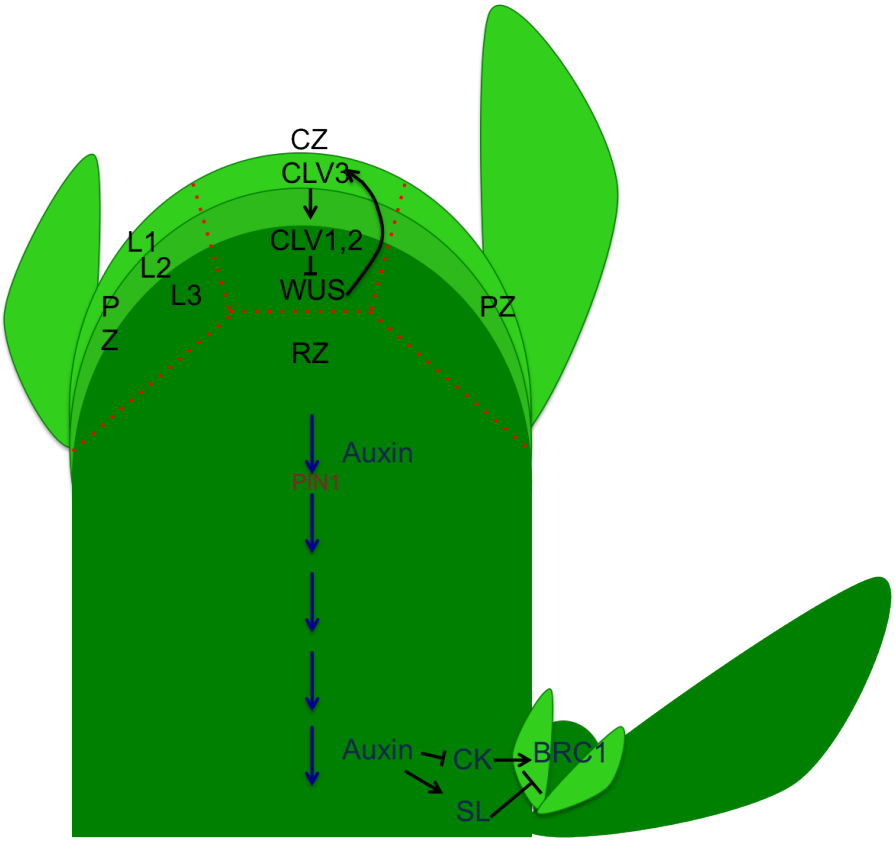

Figure 12: *A simplified schematic representation of the shoot apical meristem (SAM) and the control of axillary meristem outgrowth.*

The stem cells are also classified into three zones according to their position in the SAM: the central zone (CZ), the peripheral zone (PZ) and the rib zone (RZ). The CZ contains pluripotent cells that divide slowly and support the indeterminate growth of the main stem. The PZ contains actively dividing multipotent cells that differentiate into leaf and flower primordia. The RZ contains multipotent cells that give rise to the pith and vasculature.

The L3 layer that coincides with the CZ acts as the organizing centre (OC) that has an instructive role in imparting stem cell identity to the cells that are above it. The maintenance of the SAM is dependent on a feedback loop among the *CLAVATA* (*CLV*) genes and a transcription factor, *WUSCHEL* (*WUS*; Schoof et al., 2000). CLV1 encodes an extracellular serine/threonine kinase (Clark et al., 1997), CLV2 encodes a receptor-like protein (Jeong et al., 1999) with a short cytoplasmic tail and CLV3 encodes a secreted peptide (Fletcher et al., 1999) that can move between cells.

The cells in the RZ express *WUS*, which indirectly activates the expression of *CLV3* in stem cells (Mayer et al., 1998; Schoof et al., 2000). CLV3 is perceived by the CLV1-CLV2 receptor complex (Trotochaud et al., 2000). This signal activation leads to repression of WUS transcription, restricting the expression of the *CLV* genes to a small region that marks the organizing centre (Schoof et al., 2000).

The SAM is also developed and maintained by a homeodomain family protein called *SHOOT MERISTEMLESS* (*STM*; Barton and Poethig, 1993), which prevents cells from becoming differentiated (Clark et al., 1996; Endrizzi et al., 1996; Long et al., 1996). The absence of *STM* expression is a marker for future lateral organs (Long and Barton, 1998).

4.1.2 *Hormonal control of shoot growth*

Several hormones also affect SAM activity and shoot branching (Domagalska and Leyser, 2011). Cytokinins stimulate *WUS* expression in the RZ (Gordon et al., 2009, PNAS). *WUS* expression in turn represses the transcription of *ARR* (*ARABIDOPSIS RESPONSE REGULATOR*) genes which act as negative regulators of cytokinin signaling (Leibfried et al., 2005). This results in the promotion of the stem cell fate in the apex, resulting in a positive feedback loop. In addition, *STM* and other *KNOX* (*KNOTTED1*-like) genes such as *BREVIPEDICELLUS* (*BP*) induce cytokinin biosynthesis in the CZ by upregulating transcription of *ISOPENTENYL TRANSFERASE5* (*IPT5*) and *IPT7* (Jasinski et al., 2005; Rupp et al., 1999; Yanai et al., 2005). This in turn pushes stem cells towards division rather than differentiation. *KNOX* genes also lower the levels of GA (gibberellic acid) in the CZ

by repressing *GA2oox* and promoting *GA2ox* levels (Hay et al., 2002; Jasinski et al., 2005). These genes are responsible for the synthesis and degradation of GA. GA promotes the lengthening of internodes, contributing to the final height of a plant.

Auxin is transported from cell to cell in a polar manner along the shoot to root axis (Lomax et al., 1995; Estelle, 1998). Many influx and efflux carriers of auxin have been identified, with *PIN1* (*PIN-FORMED1*) being the best-studied (Gälweiler et al., 1998). *PIN1* is localized to the epidermis, vasculature and the L1 and L2 layers(Reinhardt et al., 2003).

Lateral organs are initiated in the PZ by an auxin trigger (Reinhardt et al., 2003). When a new primordium is initiated, *PIN1* protein expression and localization are redirected towards the tip of the new primordium so that a new local auxin maximum is created at the tip (Heisler et al., 2005). This leads to reduced *STM* expression, which in turn lowers the levels of cytokinins and increases the GA levels at the PZ (Hamant et al., 2002). Then, in the inner cells that will form the future vasculature of the lateral organ, *PIN1* gets localized to the basal membranes. This allows auxin to eventually be transported out of the tip basally, similar to the mechanism of transport in the main stem.

4.1.3 *Hormonal control of axillary meristem outgrowth*

Shoot branching patterns are determined by the spatial and temporal regulation of axillary bud outgrowth. Axillary meristems (AMs) are initiated at the axils of leaves and can either grow and become a branch or remain dormant. The dormancy of AMs is not permanent; it can be reversed upon damage to the apex or upon flowering initiation. The decision to grow or to remain dormant depends on the integration of several signals, both endogenous and environmental and depends on the developmental stage of the plant. Hormones play a decisive role in the control of shoot branching and axillary bud outgrowth.

Auxin transport in the main stem is entirely basipetal, i.e., it moves away from the apex. It does not enter axillary buds from the polar

auxin transport stream (PATS). There are two hypotheses to explain how auxin controls axillary bud outgrowth without entering the axillary buds.

The first model posits that auxin acts upstream of a secondary messenger that enters the axillary buds and controls their outgrowth (Sachs and Thimann, 1967). Cytokinins (CKs) and strigolactones (SLs) are good contenders for the role of secondary messengers (Tucker and Mansfield, 1971; Cline, 1991; Tanaka et al., 2006; Brewer et al., 2009). Cytokinins move acropetally (towards the apex) into the bud and trigger its outgrowth (Faiss et al., 1997). Auxin can inhibit bud outgrowth by inhibiting the biosynthesis of CKs (Nordstrom et al., 2004) locally in the nodal stem (Tanaka et al., 2006), leading to decreased levels of CK in the axillary bud. Auxin also increases expression of the *CYTOKININ OXIDASE* (*CKX*) gene in the nodal stem, leading to degradation of CK (Shimizu-Sato et al., 2009). Strigolactones, on the other hand, act by inhibiting bud outgrowth. Auxin stimulates the production of SLs by promoting the transcription of the biosynthetic genes, *MAX3* (*MORE AXILLARY BRANCHING3*) and *MAX4* (Hayward et al., 2009). CKs and SLs regulate the expression of the *BRANCHED1* (*BRC1*) transcription factor in an antagonistic manner (Dun et al., 2012). The expression of *BRC1* is necessary to inhibit shoot branching in both *Arabidopsis* and pea (Aguilar-Martinez et al., 2007). Decapitation of the main stem drives down auxin levels, leading to an increase in CK (Turnbull et al., 1997) and a decrease in SL (Sorefan et al., 2003), contributing to bud outgrowth. Therefore, auxin may exert its effect indirectly on bud outgrowth by modulating the levels of CKs as well as SLs.

The second model, called the canalization theory, proposes that auxin export from axillary buds to the main stem is necessary for bud outgrowth (Li and Bangerth, 1999). This export is inhibited by the PATS of the main stem, due to the weaker sink strength of the PATS at the internodes compared to the apex. In support of this theory, auxin transport inhibitors have been shown to decrease apical dominance (Chatfield et al., 2000). Additionally, *PIN1* localization correlates with auxin export and bud outgrowth in the axillary buds (Balla et al., 2011).

The two models are not mutually exclusive; the actions of the secondary messengers often intersect with the canalization model. For instance, SLs decrease *PIN1* levels in a *MAX2*-dependent manner on the basal membranes of xylem parenchyma cells in the axillary buds, bringing down auxin transport levels (Crawford et al., 2010). Thus, they enhance the competition between the main stem and the axillary buds for access to the PATS. Similarly, exogenous application of CKs to dormant buds leads to an increase in the expression and polarization of *PIN1* (Kalousek et al., 2010). This may in turn stimulate auxin export out of the buds into the main stem. Thus, both models likely function in different stages to coordinate the activities of the axillary meristem.

4.1.4 *Anthocyanins and auxin*

Anthocyanins are naturally occurring secondary metabolites that belong to a class of chemicals called flavonoids. The different types of anthocyanins constitute the various red, pink, yellow and blue pigments found in plants. Apart from their important function in flowers for the attraction of pollinators, anthocyanins are also found to play different roles in other tissues, such as in pollen tube germination in maize, as phytotoxins secreted by invasive plants and in signaling to symbionts in leguminous plant roots (Taylor and Grotewold, 2005).

They also play developmental roles: mutants with defects in flavonoid biosynthesis genes, *ttg-1* (*transparent testa glabra-1*), *tt8-1*(*transparent testa8-1*) and *tt10-1* have increased shoot branching (Buer and Djordjevic, 2009). The *ttg-1* mutant also has shorter stems (Buer and Djordjevic, 2009). The gene *TT4* encodes chalcone synthase, the first enzyme in the synthesis of flavonoids. *tt4* mutants cannot make flavonoids and display two-fold increased auxin transport in inflorescences leading to a loss of apical dominance (Murphy et al., 2000; Brown et al., 2001). Similarly, in the tomato *anthocyanin reduced* (*are*) mutant, auxin transport in the root is increased in both speed and quantity (Maloney et al., 2014).

Anthocyanin accumulation in the Kro-0 x BG-5 hybrid and the lack of apical dominance may be due to common genetic defects. Finding the causes of this hybrid phenotype will give us insights into

possible novel players in the control of both shoot architecture and anthocyanin production. Thus, the Kro-0 x BG-5 hybrids pose some interesting questions:

1. Are the F_1 and F_2 hybrid phenotypes quantitatively different and therefore transgressive?
2. If yes, what is the genetic basis of these transgressive phenotypes?
3. Are the two different phenotypes of bushy habit and increased anthocyanin accumulation linked to the same genetic basis, or are they caused by different sets of genes?
4. Are the genes involved in these phenotypes already known to be involved in processes affecting these phenotypes? If not, what are the new insights that we can gain from studying these hybrids?

4.2 RESULTS

Figure 13: *Comparison of the shoot architecture of Kro-0 (left), BG-5 x Kro-0 F_1 hybrid (centre) and BG-5 (right), grown at 16°C.*

Kro-0 x BG-5 hybrids of the F_1 generation lost apical dominance, had shorter stems resulting in a bushy habit. These phenotypes are expressed at 16°C (Fig. 13), but not at 23°C, indicating temperature sensitivity (Boldt, 2009). The F_2 generation included normal-looking and bushy F_1-like plants, plus small purple plants, which showed a gradient of rosette sizes (Fig. 14). The larger purple plants bolted and produced siliques when shifted to a higher growth temperature. However, the smallest, most severely affected plants could not be rescued

at higher temperatures. The purple colouration of the F_2s was due to an increased accumulation of anthocyanins in these plants (Fig. 15).

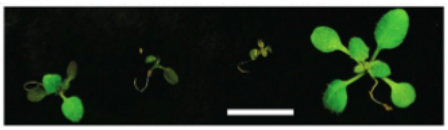

Figure 14: *Additional segregating phenotype in F_2 generation of plants with reduced growth and increased anthocyanin biosynthesis. The plant on the extreme right is a "normal" looking plant. The plants from the extreme left to the centre represent varying degrees of severity of the purple phenotype. The scale bar is 1 cm long.*

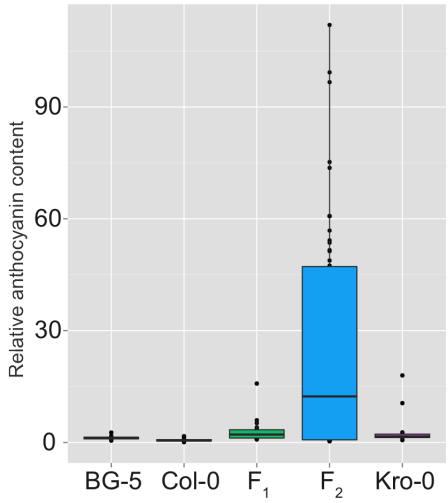

Figure 15: *The F_2 generation has increased anthocyanin content compared to the parents or the F_1 hybrids. F_1 hybrids also displayed a slight increase in anthocyanin content compared to the parents. The F_2 generation consists of all F_2 genotypes irrespective of phenotype.*

4.2.1 *Phenotypic characterization*

To characterize the F_1 and F_2 hybrid phenotypes in a more quantitative manner, I measured various traits of the parents and hybrids grown at 16°C. The parents and hybrids differed from one another with regard to inflorescence stem height (Fig. 16A; Kruskal-Wallis rank sum test, X^2 = 16.3063, df = 3, p-value = 0.0009813), shoot dry biomass (Fig. 16C; Kruskal-Wallis rank sum test, X^2 = 28.316, df = 3, p-value = 3.118e-06) and silique number (Fig. 16B; Kruskal-Wallis rank sum test, X^2 = 11.7945, df = 3, p-value = 0.008121).

For each trait measured, the F_2 population deviated from a normal distribution. Purple plants in the F_2 generation typically did not reach reproductive maturity, causing them to have no bolting shoots (these were therefore recorded as having a stem height of zero) and no siliques. These plants also had very low shoot biomass.

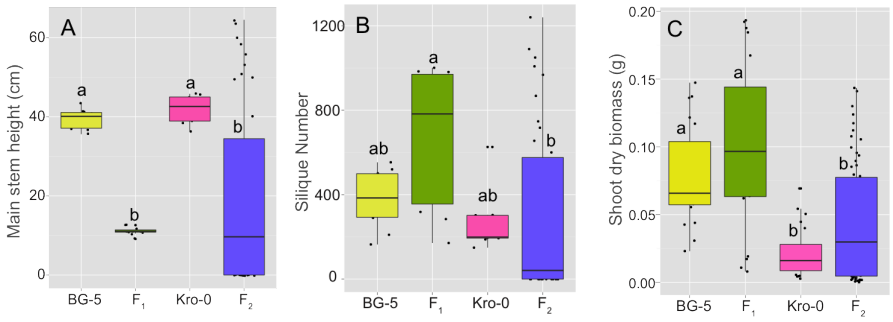

Figure 16: ***A.*** *Box plot comparing the main stem heights of BG-5, Kro-0 and their F_1 and F_2 hybrids.* ***B.****Comparison of silique numbers produced by the parents and hybrids.****C.*** *Comparison of shoot dry biomass of the parents and hybrids. Different letters denote significant differences between the groups. For A and B, 10 biological replicates were measured for the parents and F_1 hybrids and 40 plants from the F_2 generation were measured. For C, 20 replicates of the parents and F_1 hybrids and 63 plants of the F_2 generation were weighed. In all cases, the F_2 generation included plants that showed normal, bushy and purple phenotypes.*

The bushy habit of the F_1 hybrids is evident in the number of rosette and cauline branches produced relative to the parents. The number of CI branches (see Methods for definitions) produced in the F_1 hybrid was intermediate between the two parents and significantly different from the F_2 generation (Fig. 17A; Kruskal-Wallis rank sum test, X^2 = 40.1316, df = 3, p-value = 9.992e-09). F_1 hybrids produced more CII (Fig. 17B; Kruskal-Wallis rank sum test, X^2 = 32.1157, df = 3, p-value = 4.948e-07) and CIII branches (Fig. 17C; Kruskal-Wallis rank sum test, X^2 = 33.2684, df = 3, p-value = 2.827e-07).

The number of rosette branches was significantly higher for the F_1 hybrids than for any other genotype; RI (Kruskal-Wallis rank sum test, X^2 = 17.3854, df = 3, p-value = 0.0005888), RII (Kruskal-Wallis rank sum test, X^2 = 26.7001, df = 3, p-value = 6.804e-06) and RIII (Kruskal-Wallis rank sum test, X^2 = 22.6907, df = 3, p-value = 4.684e-05) all exhibited higher branch numbers in F_1 plants.

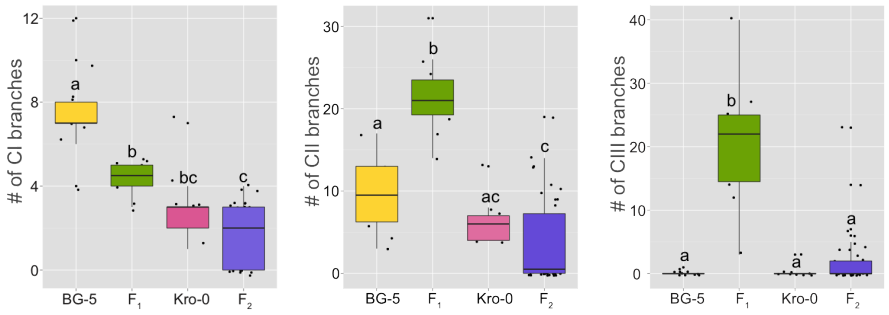

Figure 17: ***A.****Comparison of the number of primary cauline branches arising from the main stem among parents and hybrids.****B.****Comparison of the total number of secondary cauline branches originating from primary cauline branches.* ***C.****Comparison of the number of tertiary branches arising from secondary cauline branches. In all plots, different letters indicate significant differences between groups. Numbers of samples is the same as in Fig. 16A and B.*

For each of the traits studied, the F_1 and F_2 phenotypes were quantitatively different from each other and in many cases, different from the parents as well. Therefore, these are transgressive phenotypes that display increased vigour in the F_1 generation, which breaks down in the F_2 generation.

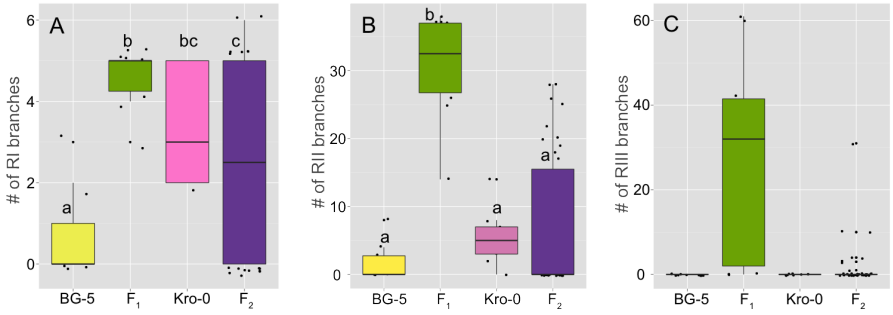

Figure 18: *Differences between parents and hybrids in the number of primary (A), secondary (B) and tertiary (C) rosette branches. Different letters specify significant differences between groups. Numbers of samples is the same as in Fig. 16A and B.*

4.2.2 *Genetic basis of the transgressive phenotypes*

In order to investigate the basis of the transgressive phenotypes, Roosa Laitinen carried out genetic mapping of the bushy phenotype. From an F_2 population grown at 16°C, 200 normal plants and 200 F_1-like plants were collected and genotyped (Roosa Laitinen, personal communication). The rough mapping indicated a relatively simple genetic basis for the bushy phenotype. Two loci, one on chromosome 2 and

the other on chromosome 3 were found to be associated with the F_1-like phenotype (Fig. 19).

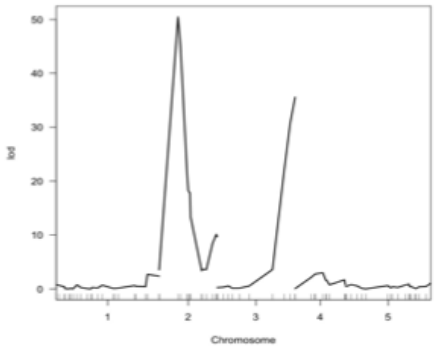

Figure 19: *Rough mapping was carried out using a 149 SNP marker set by Sequenom. Two loci were identified to be associated with the bushy phenotype with peaks mapping to chromosomes two and three (Boldt, 2009).*

A large number of F_2 plants were then analysed for their segregation ratios (Boldt, 2009). The purple plants in the F_2 generation were genotyped at the two loci to determine if the same loci that were associated with the bushy phenotype were also linked to the purple phenotype. From the genotyping and segregation ratios, a two-gene model appeared to best fit the data.

The F_1-like plants were heterozygous for both the chromosome 2 and chromosome 3 loci (Fig. 20, highlighted in green in the Punnett square). The purple plants fell into three genotypic categories: (i) Kro-0 homozygous on chromosome 2 with a heterozygous chromosome 3 locus, or (ii) heterozygous at the chromosome 2 locus along with a homozygous BG-5 allele on chromosome 3, or (iii) Kro-0 homozygous on chromosome 2 and BG-5 homozygous on chromosome 3 (Fig. 20, highlighted in purple). Normal looking plants resulted either from parental combinations at the two loci, or combinations that did not involve the "harmful" alleles from Kro-0 and BG-5 (Fig. 20, no highlights). Therefore, the causal allele on chromosome 2 comes from Kro-0 and the causal allele on chromosome 3 comes from BG-5. I hypothesized that the hybrid phenotypes in both F_1 and F_2 arise from an epistatic interaction between two semi-dominant alleles.

If this hypothesis is true, then the plants with higher levels of anthocyanin content should contain more copies of the causal alleles than other segregants. Corroborating this hypothesis, when I assayed

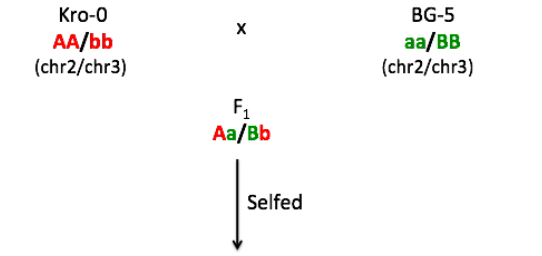

	A/B	A/b	a/B	a/b
A/B	AA/BB	AA/Bb	Aa/BB	Aa/Bb
A/b	AA/Bb	AA/bb	Aa/Bb	Aa/bb
a/B	Aa/BB	Aa/Bb	aa/BB	aa/Bb
a/b	Aa/Bb	Aa/bb	aa/Bb	aa/bb

Figure 20: *Punnett square depicting the segregation of the different hybrid phenotypes according to a two-locus model. A,a and B,b represent the different alleles on chromosomes 2 and 3 respectively. Squares highlighted in green represent genotypes of plants with the F_1-like bushy phenotype, those highlighted in purple represent purple plants and those with no highlights represent normal looking plants.*

relative anthocyanin contents of F_2 generation plants and genotyped them, I found that the plants with the causal alleles displayed higher levels of anthocyanin than those without (Fig. 21). Some of the purple plants that displayed very high levels of anthocyanin levels (see Fig. 15) could not be assigned a genotype, because I used shoots to measure anthocyanin content and had to use roots for genotyping. The most severe class of purple plants had markedly stunted roots, resulting in very small quantities of genomic DNA that were insufficient for genotyping PCR reactions. Plants of the F_2 generation with the H/H genotype displayed significantly higher levels of anthocyanin than did the F_1 hybrids. This may be due to other segregating factors in the background that contribute to increased stress.

4.2.3 *Previous work on the chromosome 2 locus*

Previously, efforts had been made to identify the causal gene on chromosome 2 by using artificial microRNAs against candidate genes in the parents and looking for a rescue of the F_1 phenotype (Boldt, 2009). This approach indicated that a gene encoding a methylmalonate semialdehyde dehydrogenase (*MMSDH*: AT2G14170, 5977356-5981899 bp on chromosome 2) was necessary for the F_1 bushy phenotype (Boldt, 2009). However, when I attempted to reproduce these experiments using the previously generated artificial microRNA constructs with my own test crosses, I was not able to rescue the hybrid phenotype.

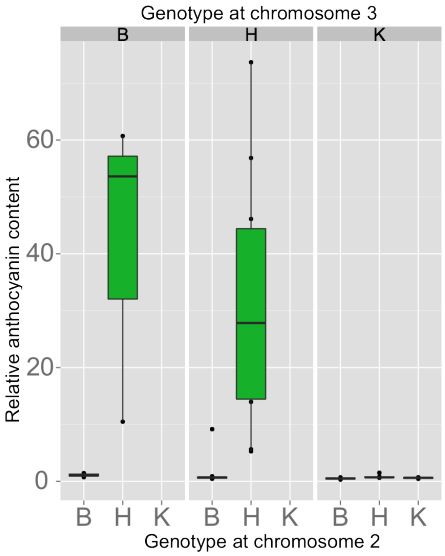

Figure 21: *Anthocyanin content of the different genotypes in an F_2 population; Plants with genotypes K/H, H/B or K/B at chromosomes two and three display the purple phenotype.*

Upon further investigation of the transgenic plants used to arrive at the original conclusion, I found out that the apparent rescue of the hybrid phenotype was due to an accidental selfing. I confirmed that this gene was not necessary for the phenotype by repeating the experiment using independent transgenic lines and crosses that I generated (data not shown).

I also introduced the genomic fragment of the Kro-0 *MMSDH* allele as a transgene into BG-5 to look for recapitulation of the F_1 bushy phenotype. Out of a total of 60 independent T_1 lines, 52 lines showed the wildtype phenotype, 5 showed a bushy phenotype and 3 lines showed a phenotype that was bushy at the beginning of the life cycle, but looked more similar to wild-type as development progressed. Moreover, the 5 lines that did display a bushy phenotype in the T_1 generation did not reproduce this phenotype in the next generation. I conclude that the minor proportion of lines that showed the bushy phenotype in the T_1 generation occurred either by chance or due to environmental fluctuations in the growth chambers, and that the *MMSDH* gene is not responsible for the hybrid phenotype.

4.2.4 *Genetic mapping of the chromosome 3 locus*

I attempted to narrow down the chromosome 3 locus by conventional fine-mapping. I used a combination of CAPS, SSLP and SNP markers to delineate the mapping interval (see Appendix). In plants with the bushy phenotype in the F_2 generation, any recombination that occurred inside the mapping interval is expected to have changed the genotype of that marker from heterozygous to homozygous (either Kro-0 or BG-5). In a population of 950 bushy plants, 9 contained a recombination event within the mapping interval, bringing its size down to 520 kb.

I then used F_2 plants that had the purple phenotype to limit the interval further; this phenotype can be identified earlier in the life cycle than the bushy phenotype, making it possible to screen larger numbers of plants in a shorter time period. Purple plants can fall into one of the following genotypic categories: (i) Kro-0 at chromosome 2 and BG-5 at chromosome 3 (K,B), or (ii) Kro-0 at chromosome 2 and heterozygous at chromosome 3, (K,H), or (iii) heterozygous at chromosome 2 and BG-5 at chromosome 3, (H,B). Therefore, plants homozygous for Kro-0 at chromosome 3 should be recombinants. Out of a total of 4750 purple plants genotyped, only 3 had recombination events inside the mapping interval, restricting the region of interest to about 160 kb.

Within this mapping interval, there were 38 protein-coding loci (Fig. 22a). In order to gain insights into which genes are more likely to be involved in the phenotype, I performed whole-genome resequencing of the BG-5 accession and Beth Rowan determined the variants in this region. Figure 22b indicates the positions of non-synonymous SNPs in the mapping interval.

Because there were only 3/4750 recombinants in an approximately 500kb region, the relationship of genetic to physical map is 0.1 cM/Mb, which is about 50 times lower than the genome average (Salome et al., 2012). This suppression of recombination suggested the possibility of genome rearrangements in this region. Despite the availability of next-generation sequencing analysis tools to predict structural rearrangements from short read resequencing data, accurate and precise identification of such variants remains difficult and imprecise (Lin

et al., 2014). Therefore, I constructed a fosmid library from BG-5 genomic DNA and screened for clones containing the region of interest. I then carried out shotgun Sanger sequencing of these clones and assembled the fosmid sequences independent of the Col-0 reference sequence.

I discovered a large transposition that moved a fragment of about 70kb in length from within the mapping interval (22.51 - 22.59 Mb) to a location about 4Mb further North on chromosome 3 at 17.33 Mb. This was identical to a translocation reported for the Ler genome (Wijnker et al., 2013). Because accessions sharing this transposition do not exhibit the hybrid phenotype when crossed to Kro-0, I could rule out the possibility that the transposition itself is responsible for the phenotype. This substantially reduced the length of the mapping interval and the number of genes under consideration as candidates (Fig. 22c).

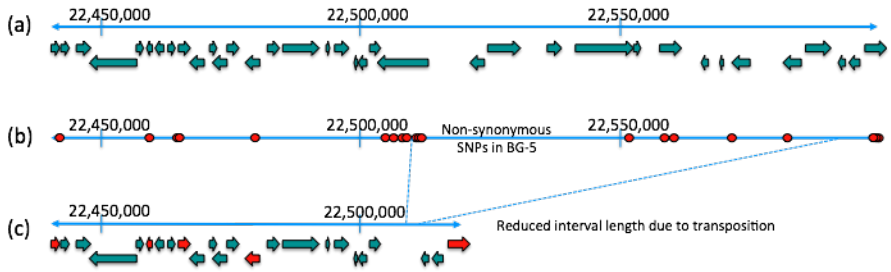

Figure 22: *Schematic representation of the chromosome 3 mapping interval with (a) protein coding genes of the interval, (b) non-synonymous SNPs found in the BG-5 genome, (c) reduced mapping interval due to a transposition. In (c), the proteins containing non-synonymous SNPs are coloured red.*

4.2.5 *Candidate gene approach*

I constructed artificial miRNAs (amiRNA; Schwab et al., 2006) for the genes in the mapping interval, prioritizing those candidates containing non-synonymous changes (relative to the Col-0 reference genome) in their protein sequence. In this approach, I transformed BG-5 plants with individual constructs containing different artificial miRNAs. I then crossed four to six independent T_1 lines to Kro-0, using the transgenic lines as pollen donors. Since the T_1s that are used in the cross are not homozygous, they segregate the amiRNA transgene such that only half of the pollen carry the amiRNA. If the gene

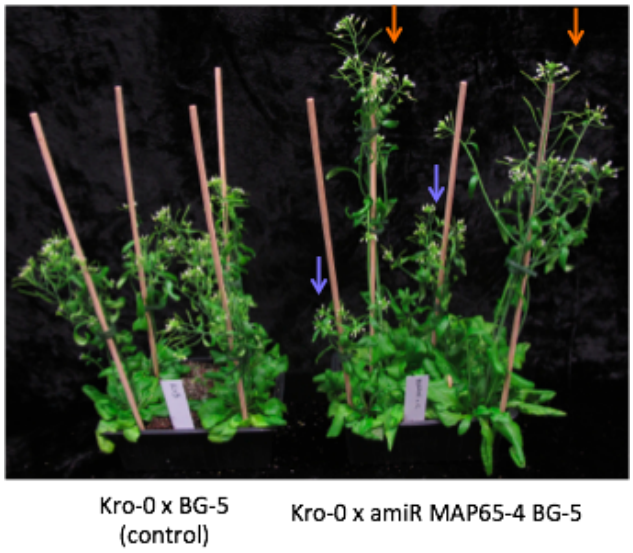

(a)

(b)

Figure 23: ***a*** *The plants on the left are F_1 hybrids that do not contain the amiRNA against MAP65-4. The plants on the right are hybrids segregating for the amiRNA; half of them display the bushy phenotype (purple arrows) and half are rescued (orange arrows).* ***b*** *The plants that were rescued were genotyped for the presence of the amiRNA transgene (lanes 2-7) whereas the plants that remained bushy did not contain this transgene (lanes 8-13). This PCR amplified the transgene using primers for the 35S promoter and the rbcs terminator.*

that is knocked down is responsible for producing the phenotype, I would expect half of the F_1 progeny (ami*Gene*-BG-5 x Kro-0) not to show the F_1-like bushy phenotype anymore. Lines containing the amiRNA against AT3G60840 displayed such a rescue of phenotype (Fig. 23a). The transgene carrying the amiRNA against the gene co-segregated with the phenotypic rescue (Fig. 23b). Thus, At3g60840, encoding *MICROTUBULE-ASSOCIATED PROTEIN65-4* (*MAP65-4*) is necessary for the phenotype.

4.2.6 *MAP65-4 and the F_2 purple phenotype*

To determine whether the knock-down of this gene could also rescue the purple phenotype in the F_2 generation, I collected selfed seeds

from those F_1 plants that exhibited the rescued phenotype and propagated the F_2 population at 16°C, again without selection for the transgene. The ratio of the plants with the transgene to those without was close to 3:1 (data not shown). This indicates that each of the T_1 lines that the F_2 populations are derived from most likely contained a single insertion of the transgene.

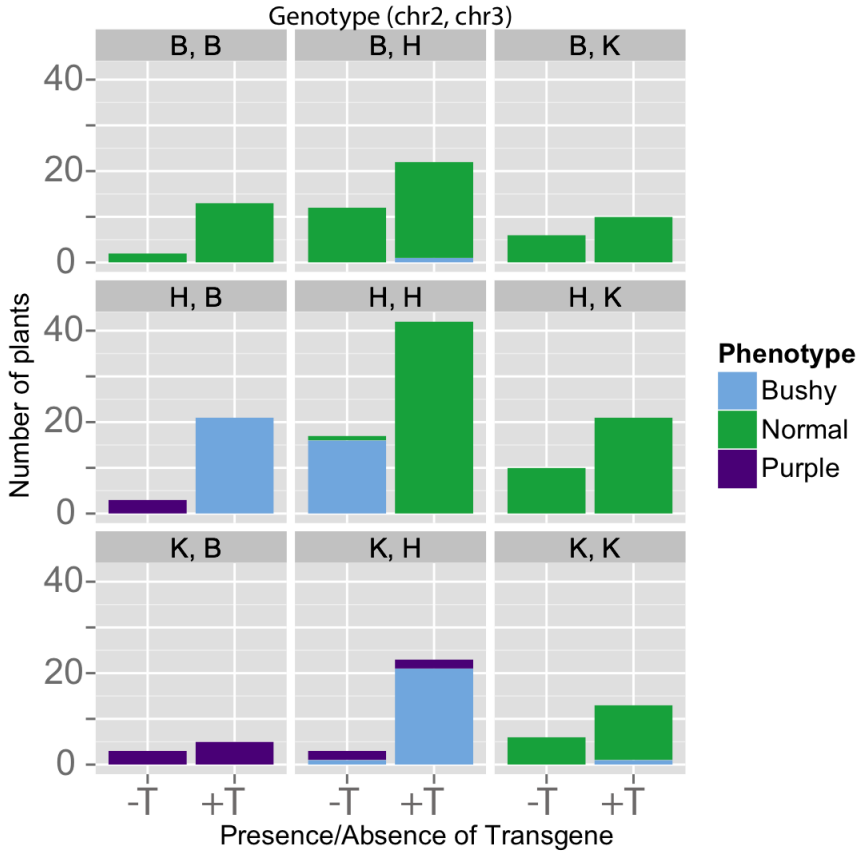

Figure 24: *Numbers of plants in each phenotypic class of F_2 populations that contain the amiRNA against the MAP65-4 gene. Data from three different F_2 populations were collated. The total number of plants genotyped was 232, with 89, 75 and 68 plants from each of the three populations.*

As seen in the F_1 generation, transgenic plants that were heterozygous at both loci showed the normal phenotype (Fig. 24: H,H +T), whereas the non-transgenic doubly heterozygous plants remained bushy (Fig. 24: H,H -T). The small purple plants displayed a partial rescue of phenotype when they carried the amiRNA transgene. This was dependent on the genotype of the purple plants: those that were doubly homozygous for the causal loci were not rescued (Fig. 24: K,B +T), whereas those that were homozygous for only one of the loci now displayed a bushy F_1-like phenotype (Fig. 24: K,H +T and H,B+T).

For the plants that did not inherit the transgene, the various phenotypic classes largely corresponded to the different genotypic classes for the chr 2 and chr 3 loci, as expected. The few cases where the phenotypes did not fit with the expected genotype might have been due to either recombination in the region or sample contamination during preparation of genomic DNA.

Apart from the visual scoring of the phenotypes, I also measured stem heights for all categories of plants to obtain a more quantitative measure of the phenotypic rescue. As before, purple plants that did not have inflorescence shoots were recorded as having a stem height of zero. The plants that had the double heterozygous genotype in conjunction with the amiRNA had stem heights similar to those of the wildtype (Fig. 25: H,H +T), in agreement with visual scoring of the phenotypic classes.

Among the plants that had either the (K,H) or the (H,B) genotype, the non-transgenic plants had the purple phenotype and mostly did not bolt, but nearly all of the plants containing the transgene bolted (Fig. 25: H,B +T and K,H +T) and their final stem heights were similar to the (H,H) plants without the transgene.

The axillary branches for the (K,H) and (H,B) plants with the transgene grew much taller than the main stem, resembling the bushy phenotype of the F_1 plants and the (H,H) plants of the F_2 generation. This suggests that the presence of the transgene converts the purple phenotype to a slightly more severe version of the F_1-like bushy phenotype. The plants that had the (K,B) genotype had similar stem heights irrespective of the presence of the amiRNA-containing transgene (Fig. 25: K,B $\pm$T). Plants that did not inherit the incompatible combinations of BG-5 and Kro-0 alleles exhibited no differences in stem height in the presence or absence of the transgene (Fig. 25: all other genotypes).

From the visual scoring of the phenotype and the measurement of stem heights, it appears that the artificial miRNA against the *MAP65-4* gene rescued the hybrid phenotypes in a dose-dependent manner. In the most severe class of purple plants, it did not rescue the phenotype (Fig. 26A). In purple plants of the genotype (K,H) or (H,B), it conferred a bushy phenotype (Fig. 26B), whereas in the (H,H) back-

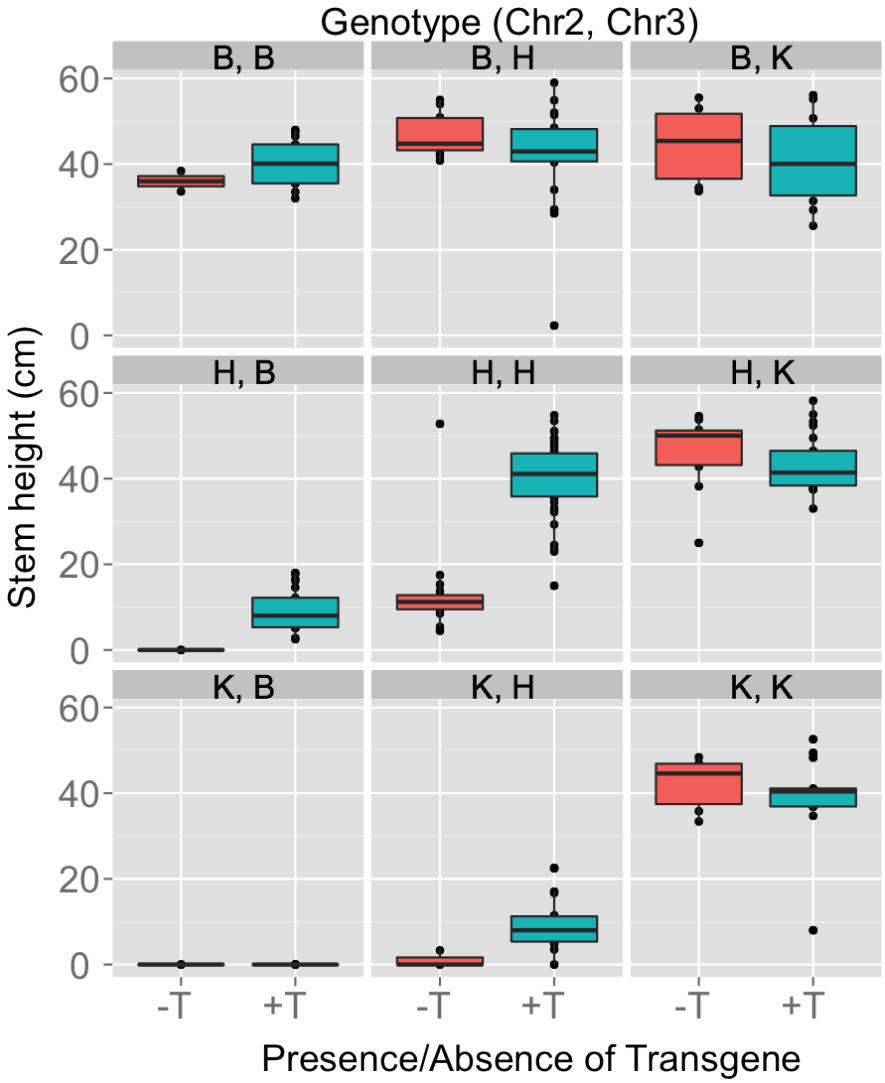

Figure 25: *Main stem height of the different genotypic classes of F_2 populations that were segregating for the amiRNA against MAP65-4 in addition to the causal loci. Further details about these populations are the same as in Figure 24.*

ground (Fig. 14C), it rescued the hybrid phenotype completely (Fig. 26D). Therefore, I conclude that *MAP65-4* is necessary for both the bushy phenotype and the purple phenotype.

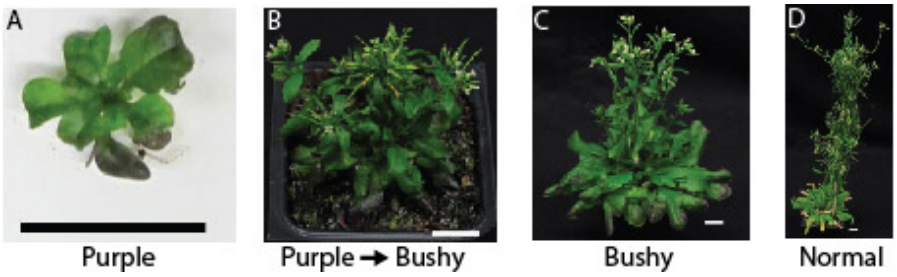

Figure 26: ***A.****Plants that are double homozygotes for the causal loci and that did not carry a transgene that knocks out the MAP65-4 gene, remained purple.****B*** *Plants containing the amiRNA transgene, that are heterozygous at one locus and homozygous at the other locus for the causal allele are purple as well as bushy, albeit much smaller than the F_1 plants.****C*** *Double heterozygotes that did not carry the transgene remained bushy.****D*** *Double heterozygotes that carried the transgene and all other categories of genotypes displayed the normal phenotype. All scale bars are 1 cm.*

To confirm that the amiRNA against *MAP65-4* had the intended effect of lowering transcript levels and that this led to the observed rescue of phenotypes, I assayed *MAP65-4* gene expression in the 6th leaf of all the F_2 generation plants from the previous experiments. In all genotypes, the expression of *MAP65-4* is lowered by the amiRNA. In the absence of the amiRNA (Fig. 27: orange bars), *MAP65-4* levels increase with the number of Kro-0 alleles on chromosome 3, except in the case of the double heterozygote. This indicates that the Kro-0 *MAP65-4* allele is expressed at higher levels than the BG-5 allele, at least in leaf tissue. The genotypes with the causal loci do not show any obvious relationships between expression levels of *MAP65-4* and severity of phenotype. This indicates that the expression levels of *MAP65-4* in leaves possibly had no influence on how *MAP65-4* acts to produce the hybrid phenotypes in these plants.

In the presence of the amiRNA (Fig. 27: turquoise bars) *MAP65-4* expression levels were uniformly low, indicating that the amiRNA targets both alleles equally. Even though the difference in expression between the (H,B), (K,H) and (K,B) genotypes are not great, this seems to be sufficient for the widely different phenotypes seen in these plants. This further indicates that the spatial or temporal expression of *MAP65-4* may be important in explaining its mechanism of action.

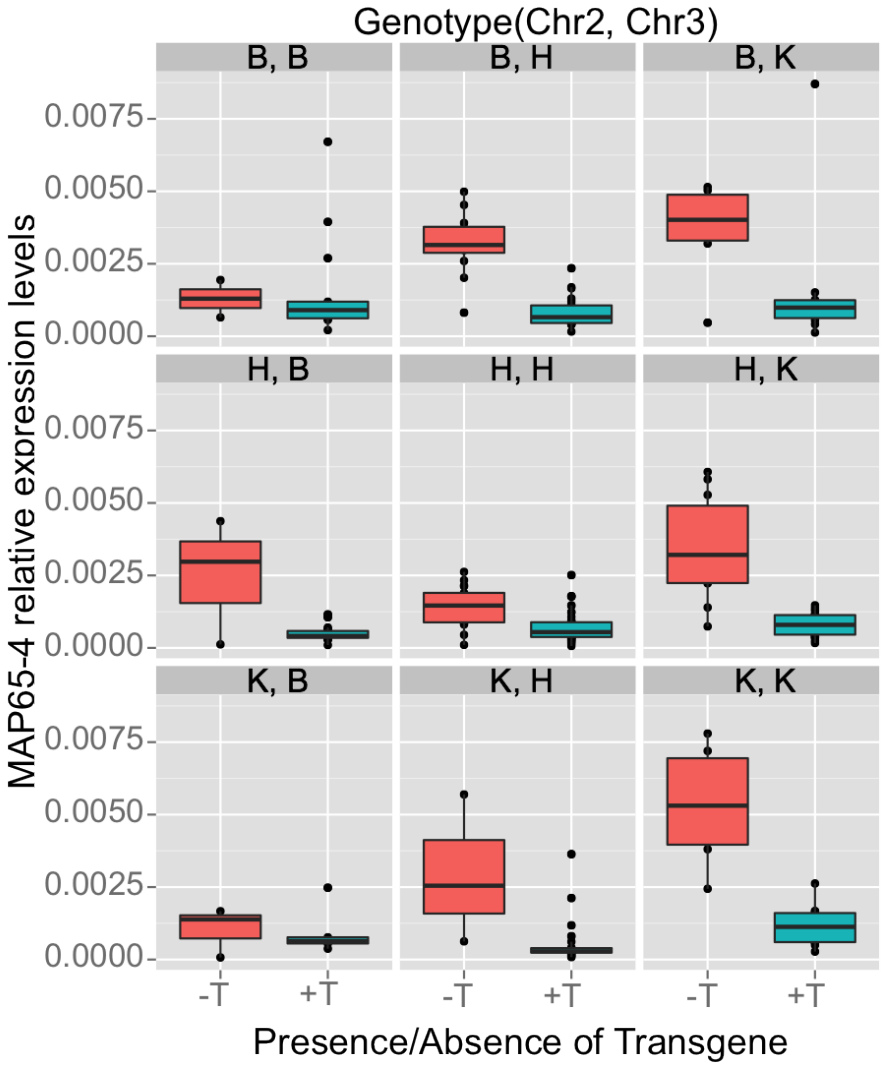

Figure 27: *Relative transcript levels of MAP65-4 in the F_2 population containing the amiRNA against MAP65-4. ACTIN2 gene expression levels were used as internal controls. Further details about these populations are the same as in Figure 24.*

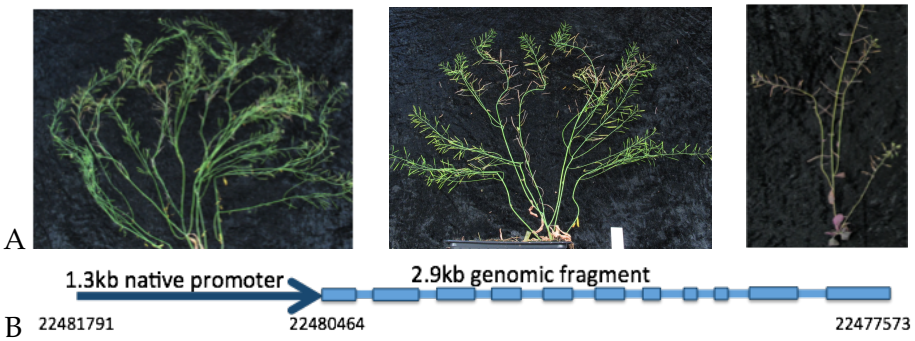

Figure 28: ***A***. *Representative pictures of transgenic lines of Kro-0 carrying the BG-5 allele of MAP65-4 as a genomic construct.* ***B***. *Schematic diagram of the construct used; the dark blue arrow represents the native promoter of BG-5 MAP65-4, the light blue boxes represent exons and the light blue lines between the boxes represent introns. The numbers indicate nucleotide positions on chromosome 3, according to TAIR10.*

Overall, these results indicate that the F_1 bushy phenotype and the F_2 purple phenotype have a common genetic basis. They also suggest that the purple phenotype is a more severe form of the bushy phenotype, because *MAP65-4* expression is necessary for both the bushy phenotype and the purple phenotype. However, the most severe class of purple plants could not be rescued with the artificial miRNA. This points to dosage sensitivity, with transgene knockdown of *MAP65-4* expression not being complete, or the contribution of another gene in the same mapping interval to the severe purple phenotype.

4.2.7 *Genomic complementation*

To find out if *MAP65-4* is sufficient to produce the F_1-like phenotype, I introduced the BG-5 allele of *MAP65-4* into Kro-0 as a genomic fragment. This construct contained the entire coding sequence along with 1.3kb of the endogenous promoter from BG-5 (Fig. 28B). If a majority of the transgenics recapitulate the bushy phenotype, then this would indicate both necessity and sufficiency of this gene.

Out of 30 independent transgenic lines analysed, none displayed the F_1-like bushy phenotype, indicating that this gene is either not sufficient to induce the hybrid phenotype or that the transgene does not produce the desired effects due to silencing or that the resulting protein is not properly made or not expressed because the complete regulatory elements were not included.

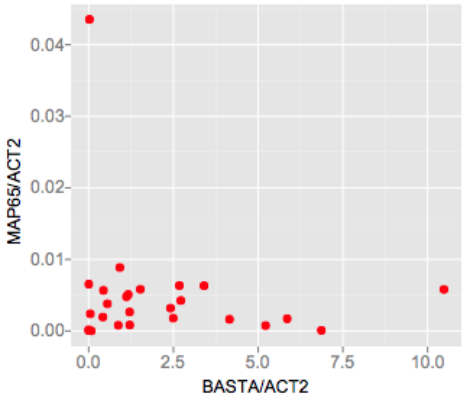

A

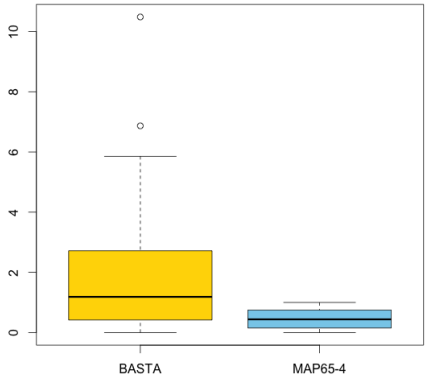

B

Figure 29: *Transcript levels of MAP65-4 and the bar gene that confers BASTA resistance. Expression levels were calculated from three technical replicates for each transgenic line. Each red dot in A represents the expression level of MAP65-4 and BASTA for each transgenic line. B shows the variation in expression in these two genes for all transgenic lines. The box-whisker plot displays the median and range of expression levels for all transgenic lines. Since individual T_1s were used in this experiment, there are no biological replicates.*

To ensure that the lack of phenotype was not due to transgene suppression, I assayed transcript levels of *MAP65-4* in the transgenic lines (Fig. 24) and compared it to expression of the gene that confers resistance to BASTA, both of which were carried on the same T-DNA fragment. The BASTA resistance gene displayed a wide range of expression levels, indicating that the transgene was not suppressed. The *MAP65-4* gene, however, was expressed at relatively low levels in all the transgenic lines. This may be a reason why none of the lines displayed a bushy phenotype.

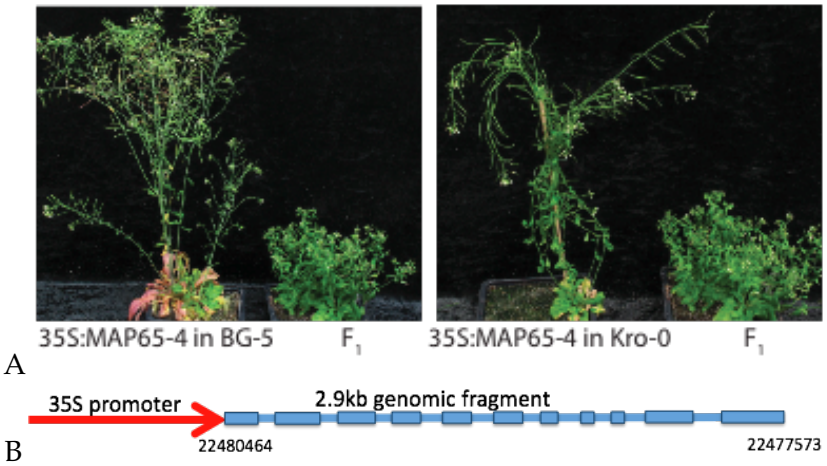

Figure 30: ***A***. *Transgenic lines in BG-5 and Kro-0 backgrounds containing constructs that constitutively express the BG-5 allele of MAP65-4.* ***B***. *Schematic diagram of the construct used; the red arrow represents the constitutive 35S promoter, the light blue boxes represent exons and the light blue lines between the boxes represent introns. The numbers indicate nucleotide positions on chromosome 3, according to TAIR10.*

4.2.8 *Constitutive expression*

To determine if over-expression of the BG-5 allele of *MAP65-4* can produce either the F_1-like bushy phenotype or the purple phenotype, I expressed the *MAP65-4* CDS under the constitutively expressed 35S promoter (Fig. 30B). There were very few transformants generated for this construct and none of them displayed a bushy or purple phenotype (Fig. 30A).

4.2.9 *Expression analyses*

In transgenic F_2 populations in which *MAP65-4* was knocked down, the expression levels of *MAP65-4* measured in leaf tissue did not display any specific patterns correlating with the severity of the phenotypes. Therefore, I measured *MAP65-4* transcript levels in 4-week old vegetative shoot tissue of Kro-0, BG-5, F_1 and F_2 plants grown at 16°C, in order to determine whether expression levels and phenotype correlated. There were no differences between F_1 and BG-5 expression levels (Kruskal-Wallis rank-sum test, p-value = 7.857e-01) , whereas Kro-0 had higher levels of expression than both F_1 (p-value = 6.661e-16) and BG-5 (p-value = 6.661e-16). Similar to this, in the F_2 generation, increasing the number of Kro-0 alleles of *MAP65-4*

increased its expression levels in every background. In an opposite pattern, increasing the number of BG-5 dosage at the chromosome 2 locus increased *MAP65-4* gene expression. The double heterozygotes were an exception to these patterns. This is the opposite of what I expected based on the expression patterns of the F_1 hybrids. The only explanation for why the F_1 hybrids and the F_2 double heterozygotes, which resemble the F_1 hybrids at the two causal loci, differ in their expression patterns is that there may be other segregating factors in the F_2 population that also affect *MAP65-4* expression.

In this tissue, as in the amiRNA experiments, the *MAP65-4* gene expression levels did not correlate with the severity of the hybrid phenotypes. One possible explanation is that the age or tissue that I assayed did not correlate well with the function of this gene in this hybrid phenotype. Another explanation is that the transcript levels of *MAP65-4* may not be decisive for the hybrid phenotype; the protein function in terms of localisation or tissue-specific protein expression may be more important. It is also possible that the spatial or temporal difference in expression between the parents and hybrids is not captured in a qPCR assay. A more fine-scale study using RNA in situ hybridisation or protein immunolocalisation may reveal the true differences in *MAP65-4* expression.

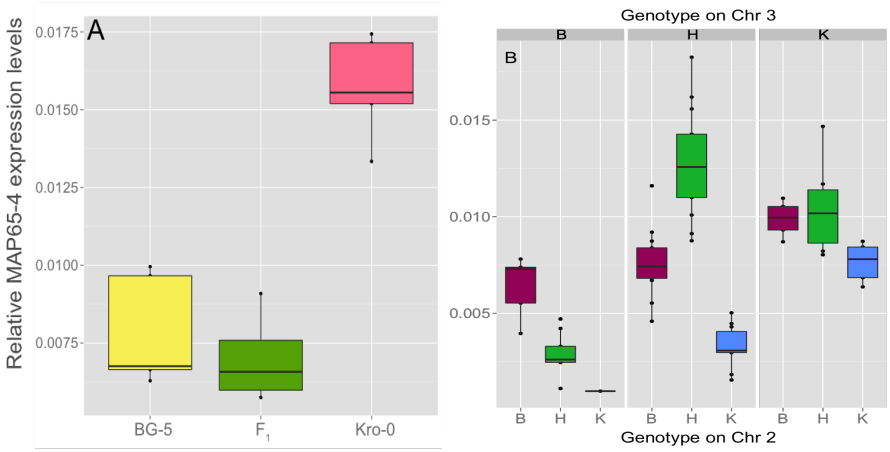

Figure 31: *Expression of MAP65-4 in 4-week old shoots in parents and hybrids. Transcript levels were calculated relative to ACTIN2 levels. At least four biological replicates were used for every genotype, except the double homozygous F_2 hybrid (K,B), of which only one sample could be tested for both genotype and expression levels. A total of 68 F_2 samples were tested for both genotype and expression levels.*

4.2.10 *Nucleotide polymorphisms in MAP65-4*

The nucleotide polymorphisms in the BG-5 and Kro-0 alleles of *MAP-65-4* were compared to the reference Col-0 to identify the causal polymorphism. I eliminated any polymorphisms relative to Col-0 that were shared between BG-5 and Kro-0. There were no non-synonymous codon changes in BG-5 and only one non-synonymous change in Kro-0 (a C to A change in exon 10 that leads to a conservative lysine to arginine change in a region that is not conserved among other MAP65 proteins). Since there were no amino acid changes unique to BG-5, the causal polymorphism is not likely to be a coding sequence change. Together with Beth Rowan, I then compared all of the SNPs in the BG-5 *MAP65-4* to 369 accessions that are a subgroup of the 1001 genomes dataset (www.1001genomes.org). There were two SNPs in BG-5 that were present in less than 10% of sequenced *Arabidopsis* accessions (Figure 32). One change in the promoter was shared with the accession ICE49 and another change in the ninth intron was shared with accession # 9921 of the 1001 sequenced genomes.

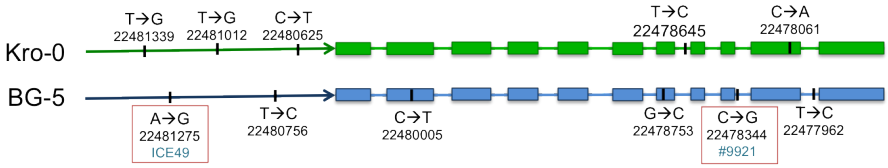

Figure 32: *Schematic diagram describing the single nucleotide polymorphisms in MAP65-4 between Kro-0 and BG-5. Arrows represent promoters, boxes exons and lines introns. Black vertical lines represent SNPs and red boxes surrounding the description of the SNP indicate that the SNP was present in less than 10% of sequenced Arabidopsis accessions. The names of accessions that share rare SNPs with BG-5 are in blue. Nucleotide numbers are in descending order from left to right since the MAP65-4 gene is encoded on the bottom strand of chromosome 3.*

If these rare SNPs are causal to the hybrid phenotype, then crossing Kro-0 with accessions that share them should recapitulate the hybrid phenotype. The accession #9921 was not available at the time of experimentation as there were doubts regarding its source and/or authenticity. It is now known that it is the accession FOR-23 from France. I crossed Kro-0 with ICE49 and examined the F_1 progeny at 16°C. The F_1 progeny displayed a wild-type phenotype (Fig. 33), indicating that this SNP was not responsible for the Kro-0 x BG-5 hybrid phenotype. Considering also that *MAP65-4* does not appear to be sufficient to recapitulate the hybrid phenotypes, it is difficult to say which nucleotide differences, if any, could be involved in the phenotype.

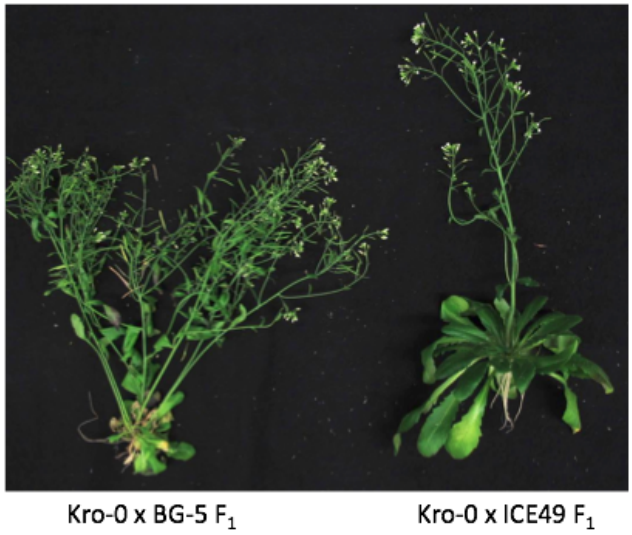

Figure 33: *Crossing Kro-0 with ICE49 does not recapitulate the bushy phenotype.*

4.2.11 *Testing long-distance effects in the hybrid*

A phenotype similar to that of the F_1 hybrid phenotype is seen in mutants of the strigolactone biosynthesis pathway, *max1* (*MORE AXILLARY GROWTH1*) and *max3* (Stirnberg et al., 2002). These mutants could be rescued when their shoots were grafted onto roots of wild-type plants. This is due to movement of a strigolactone precursor from root to shoot.

To determine if similar non-autonomous effects contribute to the increased branching of Kro-0 x BG-5 hybrids, I grafted hybrid shoot scions onto parental root stocks. However, the phenotypes of the scions were not rescued upon grafting (Fig. 34). This indicates that the hybrid phenotype is not caused by deficiency in the synthesis or movement of substances such as strigolactones from root to shoot.

4.2.12 *Testing the role of auxin*

To further investigate the possible roles of hormones in the hybrid phenotype, I exogenously added auxin since it is known to affect plant stature and apical dominance and also acts upstream of both cytokinins and strigolactones. The synthetic auxin analogs 2,4-D and 2,4-D methyl ester (ME) have different requirements for transport than the natural auxins. While 2,4-D can be exported from cells with-

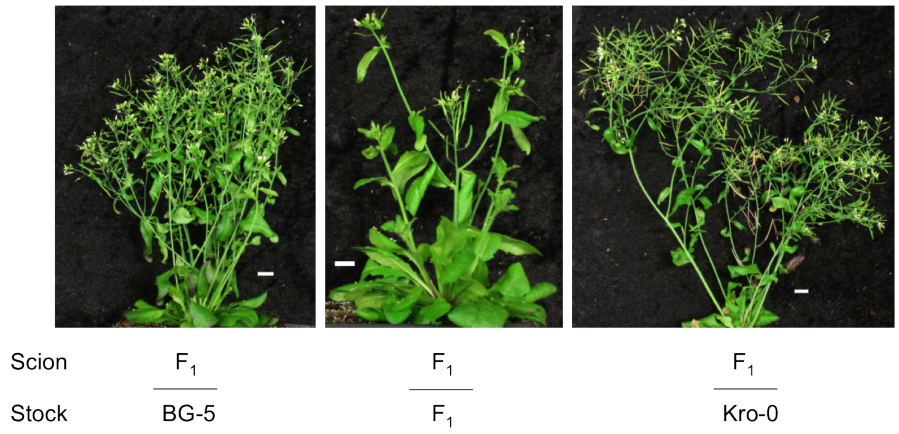

Figure 34: *Grafts between hybrids and parents did not rescue the bushy hybrid phenotype. Scale bars are 1 cm. Experiments were repeated twice with similar results.*

out auxin efflux transporters, 2,4-D ME can enter cells without requiring an influx transporter (Schenck et al., 2010; Savaldi-Goldstein et al., 2008). Therefore, the experiment could reveal if the hybrid has lower auxin production or if the transport of auxin by one or the other kind of auxin transporters is reduced.

There were significant differences in the way each genotype responded to the different treatments (Kruskal-Wallis test $X^2 = 44.3514$, df=8, p-value = 4.88e-07). The stem height of the F_1 hybrid was reduced upon treatment with 2,4-D (post-hoc Tukey's HSD p-value < 10^{-7}) as well as 2,4-D ME (post-hoc Tukey's HSD p-value < 10^{-7}). There was no difference in the main stem height of the the Kro-0 plants treated with 2,4-D (Tukey's HSD p-value = 1) or 2,4-D ME (Tukey's HSD p-value = 0.99997). The BG-5 plants experienced a small increase in stem height with 2,4-D ME, which was significantly different from the BG-5 plants treated with 2,4-D (Tukey's HSD p-value < 10^{-7}), but not different from the control (Tukey's HSD p-value =0.39341).

The results showed that the parents had slightly different responses to exogenous auxin and that the F_1 hybrid displayed enhanced sensitivity to increased auxin levels. This suggests that the phenotype is not due to a lack of auxin synthesis, but that it may be due to an imbalance in the ratios of auxin and cytokinin in the shoot apex, leading to the increased sensitivity. More work is needed in this direction before any conclusions can be made. Experiments with different concentrations of auxin and cytokinin will be very important to ensure that the hybrid phenotype is not being enhanced due to the relatively high

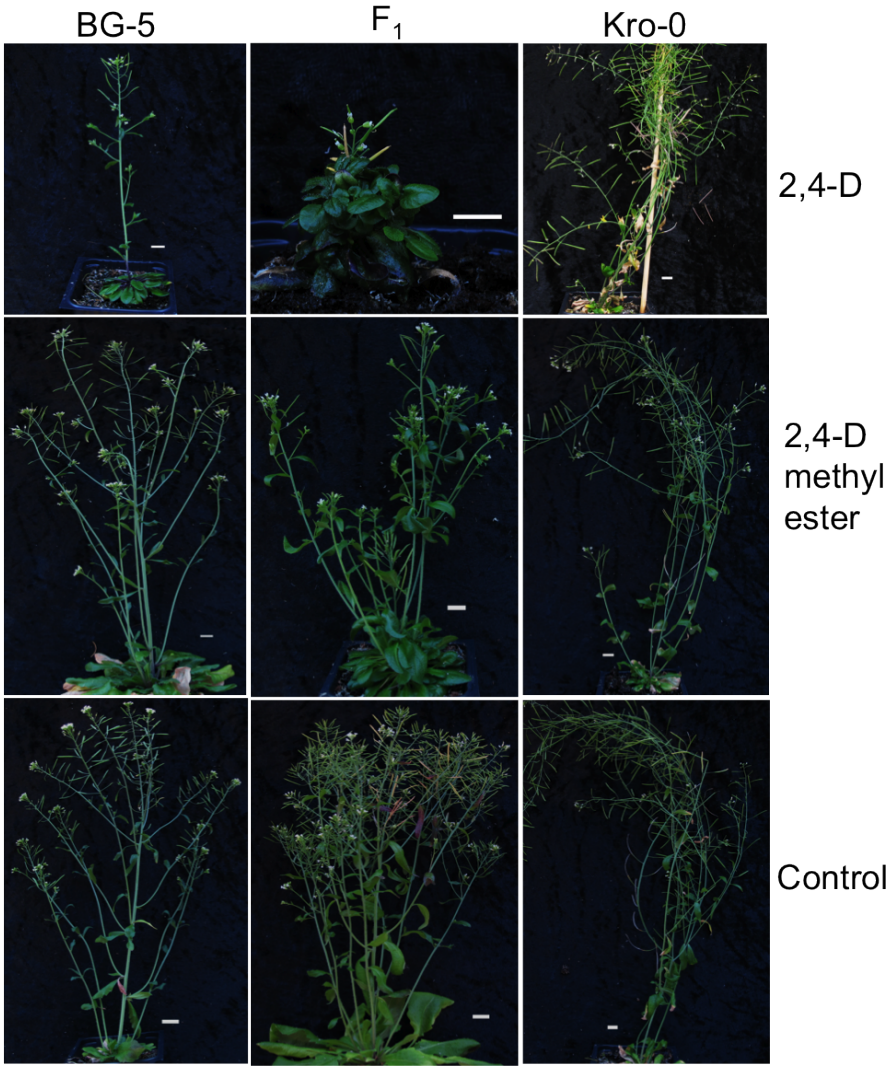

Figure 35: *Effect of treating Kro-0, BG-5 and their F_1 hybrid with 5µM 2,4-D and its methyl ester. Control plants were sprayed with the equivalent concentration of DMSO. Scale bars are 1 cm.*

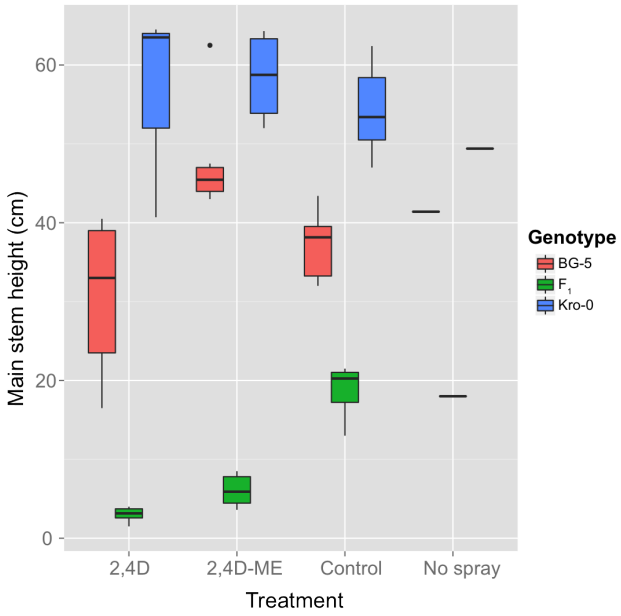

Figure 36: *Main stem heights of plants treated with synthetic auxins 2,4-D and 2,4-D methyl ester (ME). Each treatment and genotype combination had 6 biological replicates at the start of the experiment; some of the plants did not bolt, presumably due to the toxic effects of auxins. The control plants were sprayed with equivalent concentration of DMSO. One plant of each genotype was not sprayed with any chemicals to ensure that the spray of auxins did not spread by air to untreated plants.*

concentration of auxins (5µM sprayed once every four days) used in this experiment. To determine if auxin homeostasis is disturbed in the hybrids, its levels can be measured at the apex and at the nodes of the main stem. Since one of the genes involved in the hybrid phenotype is a microtubule-associated gene, it would also be interesting to see if auxin transport is somehow affected.

4.2.13 *Competency of the shoot apical meristem to divide*

To check whether the meristem of the hybrids had reduced competency to grow by division, I carried out scanning electron microscopy of the parents and hybrids grown at 16°C and 23°C. Apices were collected when 5-6 siliques had already formed on the main stem. At this stage, the axillary meristems of the F_1 hybrids are already growing and the apical meristem has lost its dominance.

In all genotypes, the SAM still contained dividing cells, evidenced by the growing primordia in the micrographs (Fig. 36). Therefore, the

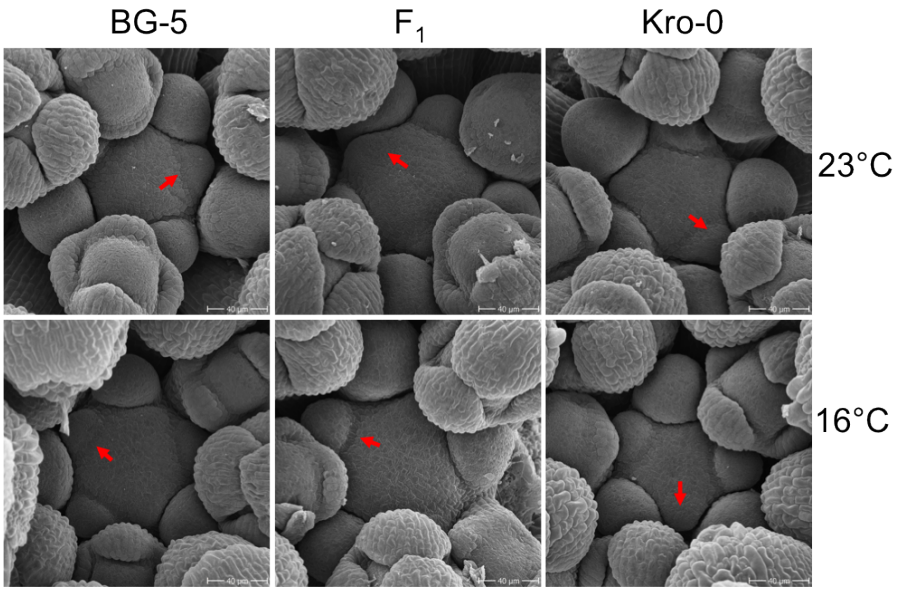

Figure 37: *Scanning electron micrographs of shoot apical meristems of BG-5, BG-5 x Kro-o F_1 hybrids and Kro-o grown at 23°C and 16°C. Red arrows indicate growing primordia, suggesting that the meristem is still dividing in all the genotypes at both temperatures.*

loss of apical dominance is not simply due to a growth termination of the main stem. However, examination of the meristem by expression analyses of stem cell markers may prove to be more informative. This may provide fine-scale details about the size of the stem cell population in the hybrid meristem, which cannot be inferred from SEM observations.

4.3 DISCUSSION

4.3.1 *Hybrid breakdown*

The Kro-o x BG-5 hybrid reveals aspects of hybrid vigor and hybrid breakdown not seen in other hybrids of *A. thaliana*. The F_1 generation produced more siliques than the parents and the F_2 generation on average. The F_1s also had a slightly larger shoot biomass than the parents, though the effect size is small, especially when compared to the BG-5 parent. As with silique number, the F_1 plants had a significantly higher biomass than the F_2 generation. Both shoot biomass and silique number are proxies for measuring plant fitness. On both

counts, the F_2 generation fared worse than the F_1 generation, pointing to hybrid breakdown. This kind of hybrid breakdown has been observed before and studied in crop species (Matsubara et al., 2003, 2007). In contrast to other cases of hybrid breakdown (Li et al., 2001b; Matsubara et al., 2015), the Kro-0 x BG-5 hybrid has a simple genetic basis. The bushy phenotype (hybrid vigor) is caused by the double heterozygous genotype at the loci on chromosomes two and three. The plants with the purple phenotype are homozygous for one or both of the "harmful" alleles (Kro-0 at the locus on chromosome two, and BG-5 at the locus on chromosome three). This is a typical example of transgressive phenotypes produced due to recombination of parental alleles in the F_2 generation. Such transgressive segregation of phenotypes is an important mechanism by which novel adaptations can arise in hybrid species or ecotypes (Rieseberg et al., 1999; Dittrich-Reed and Fitzpatrick, 2013). When these phenotypes respond to environmental variables like temperature, as they do in the case of the Kro-0 x BG-5 hybrids, they become important factors for the hybrids' success in different niches. Transgressive phenotypes are also important in the context of evolution in that the extreme or novel phenotypes produced in the hybrid may serve to reproductively isolate the hybrid from the parents.

4.3.2 *Chromosome 3 locus: MAPped?*

Knocking down the *MAP65-4* gene restored the phenotype of the double heterozygotes to normal, whereas knocking it down in the purple plants produced the bushy phenotype. This points to a hierarchy of phenotypes corresponding to the dosage of the causal loci. The purple plants in the F_2 generation that had increased levels of anthocyanins also showed reduced vigor in terms of biomass and silique number. It was not clear at the start of the study whether this phenotype was functionally related to the loss of apical dominance that led to the bushy phenotype. The identification of *MAP65-4* as a necessary factor for both the bushy phenotype and the purple phenotype established that the two phenotypes are linked functionally as well as genetically. This indicates that the purple phenotype is a more severe manifestation of the bushy phenotype.

Although *MAP65-4* was necessary for both the phenotypes, it was not sufficient for either phenotype. When the BG-5 allele of *MAP65-4* was introduced as a transgene, under the control of the endogenous promoter or expressed constitutively, it did not recapitulate the bushy or purple phenotypes. Additionally, in the most severe class of purple plants caused by double homozygosity of the causal loci, knocking down this gene did not rescue the phenotype. Together, these findings suggest that an additional gene in the chromosome 3 mapping interval might be involved.

The chromosome 3 locus experiences decreased meiotic recombination, due to a translocation from within the mapping interval. It is likely that if there are two causal genes in this interval, they were not broken up by recombination in the F_2 population. Of all the genes that I have tested so far, only *MAP65-4* was able to rescue the phenotype. However, there are some genes that I have not tested yet (Table 1) and it is possible that one of these might be necessary for the phenotype. Six out of these eleven genes do not have any SNPs in the coding region in BG-5 (compared to the reference genome of Col-0). However, there may be SNPs in the promoter regions of these genes that may be causal to the phenotype. Therefore, it would be useful to test the eleven genes, giving a higher priority to the five genes carrying SNPs, using the artificial miRNA approach.

Gene ID	SNPs in BG-5	Gene function
AT3G60720	No SNPs in coding region	Plasmodesmatal protein PLP8
AT3G60730	Intronic changes	Pectin methyl esterase
AT3G60750	3'UTR	Transketolase
AT3G60870	No SNPs in coding region	AT hook motif protein
AT3G60890	No SNPs in coding region	Little Zipper2
AT3G60900	No SNPs in coding region	Fasciclin-like arabinogalactan protein
AT3G60966	No SNPs in coding region	RING/U-box superfamily protein
AT3G60970	Synonymous amino acid changes	Multidrug-resistance protein associated protein
AT3G61010	Non-synonymous change to stop codon	Ferritin ribonucleotide reductase
AT3G61035	No SNPs in coding region	Cytochrome P450 protein
AT3G61070	Intronic changes	Peroxin11 gene family

Figure 38: *List of genes in the chromosome 3 mapping interval that have not yet been tested. The complete list of substitutions and small indels in the non-coding regions of the mapping interval can be found in the Appendix.*

MAP65-4 belongs to the microtubule associated protein family, encoded by nine different genes in *Arabidopsis* (Hussey et al., 2002). In vitro, these proteins function in bundling microtubules (MTs) by forming cross-bridges between tubulin strands at the growing ends (Gaillard et al., 2008; Li et al., 2009). At the onset of mitosis, plant cells arrange a MT bundle called the preprophase band, which defines the future division plane of the cell. The bundling of MTs is important for the stabilization of MT arrays during the cell cycle.

MAP65-4 forms shorter cross-bridges between adjacent microtubules than those generated by other MAP65 proteins (Fache et al., 2010). It localises preferentially at microtubules that orient towards the poles. Although it does not have an effect on the growth rate or shrinkage rate of microtubules, it decreases the occurrence of catastrophe events (when the microtubule switches from growth to shrinkage) and increases the rate of rescue (switching from shrinkage to rescue). Thus, it contributes to the stability of microtubule arrays.

From this known function of *MAP65-4*, it is difficult to imagine a role for this protein in producing the bushy phenotype or the purple phenotype of the Kro-0 x BG-5 hybrids. However, one other member of this gene family has been implicated in a similar phenotype: *map65-3* mutants display reduced stem height (Fig. 38). The MAP65-3 gene is expressed in tissues that have a large number of dividing cells, such as in the root meristem, lateral root meristems, buds and developing leaves (Caillaud et al., 2008). Therefore, it is possible that *MAP65-4* in BG-5 or Kro-0 has an as-yet unidentified function, which leads it to interact with the Kro-0 locus to produce the bushy and purple phenotypes.

4.3.3 *Chromosome two locus: found and lost*

From previous work, it appeared as though the *MMSDH* gene in the chromosome two interval was required for the hybrid phenotype (Boldt, 2009). However, recapitulation experiments were not successful, and I eventually discovered that the supposedly positive results with an artificial miRNA were due to seed contamination.

Figure 39: *Shoot architecture of a wildtype plant (left) and a map65-3 mutant (right). Figure from Caillaud et al. (2008). Copyright American Society of Plant Biologists. Reprinted with permission.*

The chromosome two mapping interval is fortunately not as gene-dense as the chromosome three locus. Of the 14 protein-coding loci in this mapping interval, 13 have non-synonymous SNPs (Table 40). Of these genes, AT2G14120 encodes a dynamin-related protein (*DRP3B*) and is a promising candidate. In Col-0, this gene is expressed at high levels at the shoot apical meristem during the floral transition and is also expressed in the 1st internode and root tissue (data from *Arabidopsis* eFP browser; Winter et al., 2007). Its annotated function is in mitochondrial fission; *drp3B-2* mutants display elongated mitochondria that were also reduced in number compared to wildtype. The *drp3A-2 drp3B-2* double mutants are small relative to wild type or either of the single mutants (Fujimoto et al., 2009; Zhang and Hu, 2009). Other dynamin family members, such as DRP1A and DRP1C, form transient complexes with PIN proteins on growing cell plates, contributing to their internalization from the plasma membrane and polar redistribution (Mravec et al., 2011). Therefore, it would be interesting to test if the *DRP3B* gene is also involved in these processes, thus producing the hybrid phenotype.

Another untested possibility is that the Kro-0 genome also contains gene rearrangements that cannot be easily inferred from short-read based resequencing techniques. Testing a few hundred F_2 generation progeny for recombination within the chromosome 2 mapping inter-

val should provide some first clues regarding any structural variations in Kro-0.

Gene ID	# of non-synonymous SNPs	Gene function
AT2G14080	>100	TIR-NBS-LRR protein
AT2G14095	3	Unknown protein
AT2G14100	2	Cytochrome P450
AT2G14120	2	Dynamin related protein3B
AT2G14160	1	RNA-binding family protein
AT2G14255	1	Ankyrin repeat family protein
AT2G14260	1	Proline iminopeptidase
AT2G14282	1	SCR-like 18
AT2G14288	1	Unknown protein
AT2G14290	3	F-box domain, cyclin-like
AT2G14365	1	Low molecular weight cysteine-rich 84
AT2G14390	15	Unknown protein
AT2G14440	17	LRR kinase family protein

Figure 40: *Genes in the chromosome 2 mapping interval that contain non-synonymous SNPs.*

4.3.4 *Hypothesis regarding mechanism*

Flavonoids have been implicated in interfering with auxin transport. It is possible that the increased amount of anthocyanin produced in the hybrids interferes with auxin transport, leading to the reduced apical dominance and the decreased stature. The excess auxin in the apex would decrease the production of cytokinin by repressing the biosynthesis genes. This would lead to a reduction of cell division and increased cell differentiation. This could lead to reduced stem height as the stem cells are not maintained for as long a duration as in the parents.

From preliminary experiments with exogenous application of auxin, it seems that the hybrids have an increased sensitivity to auxin. Synthetic auxins do not require efflux transporters to exit cells and are therefore expected to be transported basipetally to repress axillary

bud outgrowth. However, the addition of auxin to a plant that already contains excess auxin at the SAM could cause the enhancement of the phenotype that I observed, if it is not exported efficiently. Further experiments with a range of concentrations of auxin and cytokinin will prove useful in determining what kind of hormonal imbalance brings about the hybrid phenotype. From the SEM observations, there did not appear to be any change in the size of the F_1 meristems between 23°C and 16°C. However, this was not a quantitative assessment of meristem function. It can be tested in more detail by measuring the levels and domains of expression of meristem markers such as *WUS*, *CLV3* and *STM*. Generating transgenic lines in Kro-0 and BG-5 of *PIN1:GFP*, *IPT5:GUS*, *IPT7:GUS*, may also help in clarifying if their expression domains are changed in the hybrid.

It is not clear how *MAP65-4* operates in bringing about the phenotype. One hypothesis is that it may function in the continuous cycling of PIN proteins between the endosomes and the plasma membrane, which is responsible for the direction of auxin transport. Determination of the gene responsible on the chromosome two locus will be more useful in predicting the precise mechanism of action of *MAP65-4*.

4.3.5 *Outlook*

In order to suggest a plausible mechanism of action for the Kro-0 x BG-5 hybrid breakdown, it is most important to correctly identify the causal gene on chromosome 2. Apart from this, several other experiments can be conducted to tease out what pathways are responsible for the phenotypes. First, auxin transport assays using radiolabeled IAA can be conducted to confirm and complement the experiments with exogenous addition of auxin. Second, measuring the levels of auxin, cytokinin and strigolactone at the apices and at internodes and buds will give insights into which of these are altered in the hybrids relative to the parents.
A metabolomic analysis of the flavonoid contents in F_1 and F_2 generation will provide a deeper understanding of which type of flavonoids are involved and whether the change in metabolic flux in their synthesis is a cause of the hybrid breakdown. The current working hypothesis is that the *MAP65-4* gene on chromosome 3 along with a

gene on chromosome 2 and possibly a third gene on chromosome 3 acts in a semi-dominant manner to give rise to the bushy phenotype in the F_1 hybrid. This may be due to reduced auxin transport, leading to release of axillary meristems from dormancy.

4.4 CONCLUSION

In sum, I have phenotypically characterised the Kro-0 x BG-5 hybrid breakdown. I have discovered that its genetic basis is caused in part by MAP65-4, a protein that has not yet been implicated in control of shoot branching or anthocyanin accumulation. Hence, this study opens up the possibility of identifying novel genes or pathways that may be involved in the organization of plant body plans. I have also carried out tests to discern the mechanistic basis of the hybrid phenotype. Although there is not yet a clear picture of the mechanism, I have formulated a working hypothesis that can be tested in future.

5

CONCLUSIONS

5.1 GENERAL DISCUSSION AND CONCLUSION

I began this thesis by setting out some of the most important findings from work related to plant hybridisation and evolution. The coming together of scientists and discoveries in the fields of genetics, evolution and ecology in the 20th century has been instrumental in the major leaps of knowledge regarding the mechanisms operating in speciation. With the development of tools for genome sequencing and facile genetic manipulation of a wide range of organisms, it has become easier than before to test several hypotheses about incipient speciation.

Work for more than a decade has shown that diverging plant lineages can become incompatible with each other due to differences in their defence-related proteins. This is not surprising given the huge diversity of immunity genes and the co-evolution between plants and their pathogens. The temperature-sensitivity of plant immunity has already been studied in the context of mutants that display differential growth-defence trade-offs at different temperatures and in the context of plant-pathogen interactions at different temperatures (Alcazar and Parker, 2011). Both kinds of studies usually involved two specific temperatures and no clear reaction norms were fleshed out. My work with the necrotic Uk-1 x Uk-3 hybrids and KZ-10 x Mrk-0 hybrids fills this important gap. It is the first systematic study of induced defence responses varied by temperature. This study examined activated immune responses in the absence of pathogens; the hybrids therefore provided a useful tool to study the temperature sensitivity of plant immunity components in the absence of the confounding effects of temperature on pathogen growth and virulence.

In addition to discovering reaction norms, this was the first study that looked at both molecular and morphological readouts of induced defence over a wide range of temperatures. This enabled me to identify temperatures at which defence-related genes are expressed, but with-

out the morphological defects associated with the cost of immunity. Most studies concerned with growth and defence discuss these tradeoffs in a binary manner, as if these traits get turned either on or off. This view of plant life histories potentially disregards any intermediate metabolic conditions in which the plants are able to maintain a certain level of immunity without compromising growth and development. Indeed, Arabidopsis mutants have been identified that uncouple this tradeoff between growth and defence (reviewed in Alcazar and Parker, 2011; Hua, 2013; Huot et al., 2014). My study points to the presence of sweet spots in the temperature gradient, where just such a balance between the two traits is possible. Further investigation into how these sweet spots modulate the defence versus growth tradeoff may enable scientists to engineer plants that achieve this balance at any temperature. This would be a very useful application in agriculture, given climate change.

The second part of my thesis concerns the Kro-0 x BG-5 hybrid, which displays a very atypical hybrid incompatibility phenotype. The loss of apical dominance and accompanying bushy habit appear in the F_1 hybrids at 16°C, but not at 23°C. The additional phenotype of increased anthocyanin accumulation in the F_2 generation was caused by an increased dosage of the incompatible alleles.

Natural variation in shoot architecture exists in *Arabidopsis* and its genetic basis has previously been investigated (Ungerer et al., 2002, 2003; Ehrenreich et al., 2007). Variation in genes involved in regulating levels of strigolactones and cytokinins were associated with variations in shoot architecture. Differences in shoot architecture have been studied in the context of the domestication of maize (*Zea mays*) from its wild progenitor, teosinte (*Zea mays ssp. parviglumis*). Changes in the gene *TB1* (*TEOSINTE BRANCHED1*, encoding a TCP transcription factor) were associated with the suppression of axillary shoots (Doebley et al., 1995), that led to the shoot architecture seen in present day maize. Studies on plant height have also been conducted with the aim of increasing crop yields. The semi-dwarf varieties of rice and wheat, introduced during the Green Revolution, were either deficient in or insensitive to gibberellic acid. The reduced stature led to an increased proportion of photosynthetic produce being allocated to grains rather than to leaves. Studies in the last few years have identi-

fied many other genes that modulate the shoot architecture of plants, leading to increased yields (Yang and Hwa, 2008).

Identification of *MAP65-4* as a player in the control of shoot architecture and anthocyanin accumulation opens up exciting new avenues of study. The genes present in the Kro-0 chromosome two interval are also not obviously associated with shoot architecture. The novelty of this study lies in the fact that it brings together three things: (i) an environmentally plastic response in the form of an altered body plan, (ii) which results in increased vigour in the F1 generation followed by a breakdown of this vigour in successive generations and (iii) identification of at least one genetic factor, and possibly more, that were previously not known to be involved in this phenotype. Identification of the other genetic factors involved in this phenomenon and elucidation of the mechanistic bases are sure to bring new and interesting knowledge to the fore.

J. A. Aguilar-Martinez, C. Poza-Carrion, and P. Cubas. Arabidopsis branched1 acts as an integrator of branching signals within axillary buds. *Plant Cell*, 19(2):458–72, 2007. ISSN 1040-4651 (Print) 1040-4651 (Linking). doi: 10.1105/tpc.106.048934. URL http://www.ncbi.nlm.nih.gov/pubmed/17307924.

R. Alcazar and J. E. Parker. The impact of temperature on balancing immune responsiveness and growth in arabidopsis. *Trends Plant Sci*, 16(12):666–75, 2011. ISSN 1878-4372 (Electronic) 1360-1385 (Linking). doi: 10.1016/j.tplants.2011.09.001. URL http://www.ncbi.nlm.nih.gov/pubmed/21963982.

R. Alcazar, A.V. Garcia, I. Kronholm, J. de Meaux, M. Koornneef, J.E. Parker, and M. Reymond. Natural variation at strubbelig receptor kinase 3 drives immune-triggered incompatibilities between arabidopsis thaliana accessions. *Nature Genetics*, 42 (12):1135–1139, 2010.

R. Alcazar, M. von Reth, J. Bautor, E. Chae, D. Weigel, M. Koornneef, and J.E. and Parker. Analysis of a plant complex resistance gene locus underlying immune-related hybrid incompatibility and its occurrence in nature. *PloS Genetics*, 10(12):e1004848, 2014.

E. Anderson. A morphological comparison of triploid and tetraploid interspecific hybrids in tradescantia. *Genetics*, 21(1):61–5, 1936. ISSN 0016-6731 (Print) 0016-6731 (Linking). URL http://www.ncbi.nlm.nih.gov/pubmed/17246783.

E. Anderson and L. Hubricht. Hybridization in tradescantia. iii. the evidence for introgressive hybridization. *American Journal of Botany*, 25(6):396–402, 1938.

M. J. Axtell and B. J. Staskawicz. Initiation of rps2-specified disease resistance in arabidopsis is coupled to the avrrpt2-directed elimination of rin4. *Cell*, 112(3):369–77, 2003. ISSN 0092-8674 (Print) 0092-8674 (Linking). URL http://www.ncbi.nlm.nih.gov/pubmed/12581526.

J. Balla, P. Kalousek, V. Reinohl, J. Friml, and S. Prochazka. Competitive canalization of pin-dependent auxin flow from axillary buds controls pea bud outgrowth. *Plant J*, 65(4):571–7, 2011. ISSN 1365-313X (Electronic) 0960-7412 (Linking). doi: 10.1111/j.1365-313X.2010.04443.x. URL http://www.ncbi.nlm.nih.gov/pubmed/21219506.

D. A. Barbash and M. Ashburner. A novel system of fertility rescue in drosophila hybrids reveals a link between hybrid lethality and female sterility. *Genetics*, 163(1):217–26, 2003. ISSN 0016-6731 (Print) 0016-6731 (Linking). URL http://www.ncbi.nlm.nih.gov/pubmed/12586709.

M.K. Barton and R.S. Poethig. Formation of the shoot apical meristem in arabidopsis thaliana: an analysis of development in the wild type and in the shoot meristemless mutant. *Development*, 119:823–831, 1993.

William Bateson. *Heredity and Variation in Modern Lights*, book section Heredity and Variation in Modern Lights. Cambridge University Press, Cambrige, UK, 1909.

William Bateson and Gregor Mendel. *Mendel's principles of heredity*. At the University press, Cambridge,, 1909.

P. M. Beardsley, A. Yen, and R. G. Olmstead. Aflp phylogeny of mimulus section erythranthe and the evolution of hummingbird pollination. *Evolution*, 57(6):1397–410, 2003. ISSN 0014-3820 (Print) 0014-3820 (Linking). URL http://www.ncbi.nlm.nih.gov/pubmed/12894947.

D. Bikard, D. Patel, C. Le Metté, V. Giorgi, C. Camilleri, M.J. Bennett, and O. Loudet. Divergent evolution of duplicate genes leads to genetic incompatibilities within a. thaliana. *Science*, 323(5914):623–626, 2009.

H. Boldt. *Genetic and phenotypic characterization of the BG-5 x Kro-0 F1 hybrids of Arabidopsis thaliana*. Thesis, 2009.

K. Bomblies, J. Lempe, P. Epple, N. Warthmann, C. Lanz, J.L. Dangl, and D. Weigel. Autoimmune response as a mechanism for a dobzhansky-muller type incompatibility syndrome in plants. *PLoS Biol*, 5(9):e236, 2007.

S. A. Bowling, J. D. Clarke, Y. Liu, D. F. Klessig, and X. Dong. The cpr5 mutant of arabidopsis expresses both npr1-dependent and npr1-independent resistance. *Plant Cell*, 9(9):1573–84, 1997. ISSN 1040-4651 (Print) 1040-4651 (Linking). doi: 10.1105/tpc.9.9.1573. URL http://www.ncbi.nlm.nih.gov/pubmed/9338960.

M. S. Box, V. Coustham, C. Dean, and J. S. Mylne. Protocol: A simple phenol-based method for 96-well extraction of high quality rna from arabidopsis. *Plant Methods*, 7:7, 2011. ISSN 1746-4811 (Electronic) 1746-4811 (Linking). doi: 10.1186/1746-4811-7-7. URL http://www.ncbi.nlm.nih.gov/pubmed/21396125.

P. B. Brewer, E. A. Dun, B. J. Ferguson, C. Rameau, and C. A. Beveridge. Strigolactone acts downstream of auxin to regulate bud outgrowth in pea and arabidopsis. *Plant Physiol*, 150(1):482–93, 2009. ISSN 0032-0889 (Print) 0032-0889 (Linking). doi: 10.1104/pp.108.134783. URL http://www.ncbi.nlm.nih.gov/pubmed/19321710.

N. J. Brideau, H. A. Flores, J. Wang, S. Maheshwari, X. Wang, and D. A. Barbash. Two dobzhansky-muller genes interact to cause hybrid lethality in drosophila. *Science*, 314(5803):1292–5, 2006. ISSN 1095-9203 (Electronic) 0036-8075 (Linking). doi: 10.1126/science.1133953. URL http://www.ncbi.nlm.nih.gov/pubmed/17124320.

D. E. Brown, A. M. Rashotte, A. S. Murphy, J. Normanly, B. W. Tague, W. A. Peer, L. Taiz, and G. K. Muday. Flavonoids act as negative regulators of auxin transport in vivo in arabidopsis. *Plant Physiol*, 126(2):524–35, 2001. ISSN 0032-0889 (Print) 0032-0889 (Linking). URL http://www.ncbi.nlm.nih.gov/pubmed/11402184.

R. L. Brown, K. Kazan, K. C. McGrath, D. J. Maclean, and J. M. Manners. A role for the gcc-box in jasmonate-mediated activation of the pdf1.2 gene of arabidopsis. *Plant Physiol*, 132(2):1020–32, 2003. ISSN 0032-0889 (Print) 0032-0889 (Linking). doi: 10.1104/pp.102.017814. URL http://www.ncbi.nlm.nih.gov/pubmed/12805630.

C. S. Buer and M. A. Djordjevic. Architectural phenotypes in the transparent testa mutants of arabidopsis thaliana. *J Exp Bot*, 60(3):751–63, 2009. ISSN 1460-2431 (Electronic) 0022-0957 (Linking). doi: 10.1093/jxb/ern323. URL http://www.ncbi.nlm.nih.gov/pubmed/19129166.

D. Burkart-Waco, C. Josefsson, B. Dilkes, N. Kozloff, O. Torjek, R. Meyer, T. Altmann, and L. Comai. Hybrid incompatibility in arabidopsis is determined by a multiple-locus genetic network. *Plant Physiol*, 158(2):801–12, 2012. ISSN 1532-2548 (Electronic) 0032-0889 (Linking). doi: 10.1104/pp.111.188706. URL http://www.ncbi.nlm.nih.gov/pubmed/22135429.

M. C. Caillaud, P. Lecomte, F. Jammes, M. Quentin, S. Pagnotta, E. Andrio, J. de Almeida Engler, N. Marfaing, P. Gounon, P. Abad, and B. Favery. Map65-3 microtubule-associated protein is essential for nematode-induced giant cell ontogenesis in arabidopsis. *Plant Cell*, 20(2):423–37, 2008. ISSN 1040-4651 (Print) 1040-4651 (Linking). doi: 10.1105/tpc.107.057422. URL http://www.ncbi.nlm.nih.gov/pubmed/18263774.

E. Chae, K. Bomblies, S-T. Kim, D. Karelina, M. Zaidem, S. Ossowski, C. Martin-Pizarro, R.A.E. Laitinen, B.A. Rowan, H. Tenenboim, S. Lechner, M. Demar, A. Habring-Müller, C. Lanz, G. Rätsch, and D. Weigel. Species-wide genetic incompatibility analysis identifies immune genes as hot spots of deleterious epistasis. *Cell*, 59(6):1341–1351, 2014.

G. Charron, J. B. Leducq, and C. R. Landry. Chromosomal variation segregates within incipient species and correlates with reproductive isolation. *Mol Ecol*, 23(17):4362–72, 2014. ISSN 1365-294X (Electronic) 0962-1083 (Linking). doi: 10.1111/mec.12864. URL http://www.ncbi.nlm.nih.gov/pubmed/25039979.

S. P. Chatfield, P. Stirnberg, B. G. Forde, and O. Leyser. The hormonal regulation of axillary bud growth in arabidopsis. *Plant J*, 24(2):159–69, 2000. ISSN 0960-7412 (Print) 0960-7412 (Linking). URL http://www.ncbi.nlm.nih.gov/pubmed/11069691.

J. Chen, J. Ding, Y. Ouyang, H. Du, J. Yang, K. Cheng, J. Zhao, S. Qiu, X. Zhang, J. Yao, K. Liu, L. Wang, C. Xu, X. Li, Y. Xue, M. Xia, Q. Ji, J. Lu, M. Xu, and Q. Zhang. A triallelic system of s5 is a major regulator of the reproductive barrier and compatibility of indica-japonica hybrids in rice. *Proc Natl Acad Sci U S A*, 105(32):11436–41, 2008. ISSN 1091-6490 (Electronic) 0027-8424 (Linking). doi: 10.1073/pnas.0804761105. URL http://www.ncbi.nlm.nih.gov/pubmed/18678896.

S. E. Clark, S. E. Jacobsen, J. Z. Levin, and E. M. Meyerowitz. The clavata and shoot meristemless loci competitively regulate meristem activity in arabidopsis. *Development*, 122(5):1567–75, 1996. ISSN 0950-1991 (Print) 0950-1991 (Linking). URL http://www.ncbi.nlm.nih.gov/pubmed/8625843.

S. E. Clark, R. W. Williams, and E. M. Meyerowitz. The clavata1 gene encodes a putative receptor kinase that controls shoot and floral meristem size in arabidopsis. *Cell*, 89(4):575–85, 1997. ISSN 0092-8674 (Print) 0092-8674 (Linking). URL http://www.ncbi.nlm.nih.gov/pubmed/9160749.

M.G. Cline. Apical dominance. *Botanical Review*, 57(4):318–358, 1991.

S.J. Clough and A.F. Bent. Floral dip: a simplified method for agrobacterium-mediated transformation of arabidopsis thaliana. *The Plant Journal*, 16(6):735–743, 1994.

J.A. Coyne. Ernst mayr and the origin of species. *Evolution*, 48(1):19–30, 1994.

J.A. Coyne and H.A. Orr. *Speciation*. Sinauer Associates, Inc., 2004. ISBN 978-0-87893-089-0.

S. Crawford, N. Shinohara, T. Sieberer, L. Williamson, G. George, J. Hepworth, D. Muller, M. A. Domagalska, and O. Leyser. Strigolactones enhance competition between shoot branches by dampening auxin transport. *Development*, 137(17):2905–13, 2010. ISSN 1477-9129 (Electronic) 0950-1991 (Linking). doi: 10.1242/dev.051987. URL http://www.ncbi.nlm.nih.gov/pubmed/20667910.

A. D. Cutter. The polymorphic prelude to bateson-dobzhansky-muller incompatibilities. *Trends Ecol Evol*, 27(4):209–18, 2012. ISSN 1872-8383 (Electronic) 0169-5347 (Linking). doi: 10.1016/j.tree.2011.11.004. URL http://www.ncbi.nlm.nih.gov/pubmed/22154508.

T. N. Cuykendall, P. Satyaki, S. Ji, D. M. Clay, N. B. Edelman, A. Kimchy, L. H. Li, E. A. Nuzzo, N. Parekh, S. Park, and D. A. Barbash. A screen for f1 hybrid male rescue reveals no major-effect hybrid lethality loci in the drosophila melanogaster autosomal genome. *G3 (Bethesda)*, 4(12):2451–60, 2014. ISSN 2160-1836 (Electronic) 2160-1836 (Linking). doi: 10.1534/g3.114.014076. URL http://www.ncbi.nlm.nih.gov/pubmed/25352540.

Charles Darwin. *On the origin of species by means of natural selection*. J. Murray, London,, 1859.

D. R. Dittrich-Reed and B. M. Fitzpatrick. Transgressive hybrids as hopeful monsters. *Evol Biol*, 40(2):310–315, 2013. ISSN 0071-3260 (Print) 0071-3260 (Linking). doi: 10.1007/s11692-012-9209-0. URL http://www.ncbi.nlm.nih.gov/pubmed/23687396.

Theodosius Dobzhansky. *Genetics and the origin of species*. Columbia biological series,. Columbia Univ. Press, New York,, 1937.

J. Doebley, A. Stec, and C. Gustus. teosinte branched1 and the origin of maize: evidence for epistasis and the evolution of dominance. *Genetics*, 141(1):333–46, 1995. ISSN 0016-6731 (Print) 0016-6731 (Linking). URL http://www.ncbi.nlm.nih.gov/pubmed/8536981.

M. A. Domagalska and O. Leyser. Signal integration in the control of shoot branching. *Nat Rev Mol Cell Biol*, 12(4):211–21, 2011. ISSN 1471-0080 (Electronic) 1471-0072 (Linking). doi: 10.1038/nrm3088. URL http://www.ncbi.nlm.nih.gov/pubmed/21427763.

L. Du, G. S. Ali, K. A. Simons, J. Hou, T. Yang, A. S. Reddy, and B. W. Poovaiah. Ca(2+)/calmodulin regulates salicylic-acid-mediated plant immunity. *Nature*, 457(7233):1154–8, 2009. ISSN 1476-4687 (Electronic) 0028-0836 (Linking). doi: 10.1038/nature07612. URL http://www.ncbi.nlm.nih.gov/pubmed/19122675.

E. A. Dun, A. de Saint Germain, C. Rameau, and C. A. Beveridge. Antagonistic action of strigolactone and cytokinin in bud outgrowth control. *Plant Physiol*, 158(1):487–98, 2012. ISSN 1532-2548 (Electronic) 0032-0889 (Linking). doi: 10.1104/pp.111.186783. URL http://www.ncbi.nlm.nih.gov/pubmed/22042819.

S. Durand, N. Bouché, E.P. Strand, O. Loudet, and C. Camilleri. Rapid establishment of genetic incompatibility through natural epigenetic variation. *Curr Biol*, 22(4):326–331, 2012.

I. M. Ehrenreich, P. A. Stafford, and M. D. Purugganan. The genetic architecture of shoot branching in arabidopsis thaliana: a comparative assessment of candidate gene associations vs. quantitative trait locus mapping. *Genetics*, 176(2):1223–36, 2007. ISSN 0016-6731 (Print) 0016-6731 (Linking). doi: 10.1534/genetics.107.071928. URL http://www.ncbi.nlm.nih.gov/pubmed/17435248.

C. K. Ellison and R. S. Burton. Disruption of mitochondrial function in interpopulation hybrids of tigriopus californicus. *Evolution*, 60(7):1382–91, 2006. ISSN 0014-3820 (Print) 0014-3820 (Linking). URL http://www.ncbi.nlm.nih.gov/pubmed/16929655.

K. Endrizzi, B. Moussian, A. Haecker, J. Z. Levin, and T. Laux. The shoot meristemless gene is required for maintenance of undifferentiated cells in arabidopsis shoot and floral meristems and acts at a different regulatory level than the meristem genes wuschel and zwille. *Plant J*, 10(6):967–79, 1996. ISSN 0960-7412 (Print) 0960-7412 (Linking). URL http://www.ncbi.nlm.nih.gov/pubmed/9011081.

M. Estelle. Polar auxin transport. new support for an old model. *Plant Cell*, 10(11):1775–8, 1998. ISSN 1532-298X (Electronic) 1040-4651 (Linking). URL http://www.ncbi.nlm.nih.gov/pubmed/9811787.

V. Fache, J. Gaillard, D. Van Damme, D. Geelen, E. Neumann, V. Stoppin-Mellet, and M. Vantard. Arabidopsis kinetochore fiber-associated map65-4 cross-links microtubules and promotes microtubule bundle elongation. *Plant Cell*, 22(11):3804–15, 2010. ISSN 1532-298X (Electronic) 1040-4651 (Linking). doi: 10.1105/tpc.110.080606. URL http://www.ncbi.nlm.nih.gov/pubmed/21119057.

M. Faiss, J. Zalubilova, M. Strnad, and T. Schmulling. Conditional transgenic expression of the ipt gene indicates a function for cytokinins in paracrine signaling in whole tobacco plants. *Plant J*, 12(2):401–15, 1997. ISSN 0960-7412 (Print) 0960-7412 (Linking). URL http://www.ncbi.nlm.nih.gov/pubmed/9301091.

A. Falk, B. J. Feys, L. N. Frost, J. D. Jones, M. J. Daniels, and J. E. Parker. Eds1, an essential component of r gene-mediated disease resistance in arabidopsis has homology to eukaryotic lipases. *Proc Natl Acad Sci U S A*, 96(6):3292–7, 1999. ISSN 0027-8424 (Print) 0027-8424 (Linking). URL http://www.ncbi.nlm.nih.gov/pubmed/10077677.

R.A. Fisher. The correlation between relatives on the supposition of mendelian inheritance. *Philosophical Transactions of the Royal Society of Edinburgh*, 52(399-433), 1918.

J. C. Fletcher. Shoot and floral meristem maintenance in arabidopsis. *Annu Rev Plant Biol*, 53:45–66, 2002. ISSN 1543-5008 (Print) 1543-5008 (Linking). doi: 10.1146/annurev.arplant.53.092701.143332. URL http://www.ncbi.nlm.nih.gov/pubmed/12221985.

J. C. Fletcher, U. Brand, M. P. Running, R. Simon, and E. M. Meyerowitz. Signaling of cell fate decisions by clavata3 in arabidopsis shoot meristems. *Science*, 283(5409):1911–4, 1999. ISSN 0036-8075 (Print) 0036-8075 (Linking). URL http://www.ncbi.nlm.nih.gov/pubmed/10082464.

Wilhelm Olbers Focke. *Die pflanzen-mischlinge; ein beitrag zur biologie der gewächse*. Gebrüder Borntraeger, Berlin,, 1881.

R.S. Fritz, C. Moulia, and G. Newcombe. Resistance of hybrid plants and animals to herbivores, pathogens, and parasites. *Annual Review of Ecology and Systematics*, 30:565–591, 1999.

M. Fujimoto, S. Arimura, S. Mano, M. Kondo, C. Saito, T. Ueda, M. Nakazono, A. Nakano, M. Nishimura, and N. Tsutsumi. Arabidopsis dynamin-related proteins drp3a and drp3b are functionally redundant in mitochondrial fission, but have distinct roles in peroxisomal fission. *Plant J*, 58(3):388–400, 2009. ISSN 1365-313X (Electronic) 0960-7412 (Linking). doi: 10.1111/j.1365-313X.2009.03786.x. URL http://www.ncbi.nlm.nih.gov/pubmed/19144001.

J. Gaillard, E. Neumann, D. Van Damme, V. Stoppin-Mellet, C. Ebel, E. Barbier, D. Geelen, and M. Vantard. Two microtubule-associated proteins of arabidopsis map65s promote antiparallel microtubule bundling. *Mol Biol Cell*, 19(10):4534–44, 2008. ISSN 1939-4586 (Electronic) 1059-1524 (Linking). doi: 10.1091/mbc.E08-04-0341. URL http://www.ncbi.nlm.nih.gov/pubmed/18667529.

P. R. Gerard and D. C. Presgraves. Abundant genetic variability in drosophila simulans for hybrid female lethality in interspecific crosses to drosophila melanogaster. *Genet Res (Camb)*, 94(1):1–7, 2012. ISSN 1469-5073 (Electronic). doi: 10.1017/S0016672312000031. URL http://www.ncbi.nlm.nih.gov/pubmed/22353244.

J. M. Good, M. A. Handel, and M. W. Nachman. Asymmetry and polymorphism of hybrid male sterility during the early stages of speciation in house mice. *Evolution*, 62(1):50–65, 2008. ISSN 0014-3820 (Print) 0014-3820 (Linking). doi: 10.1111/j.1558-5646.2007.00257.x. URL http://www.ncbi.nlm.nih.gov/pubmed/18005156.

S. P. Gordon, V. S. Chickarmane, C. Ohno, and E. M. Meyerowitz. Multiple feedback loops through cytokinin signaling control stem cell number within the arabidopsis shoot meristem. *Proc Natl Acad Sci U S A*, 106(38):16529–34, 2009. ISSN 1091-6490 (Electronic) 0027-8424 (Linking). doi: 10.1073/pnas.0908122106. URL http://www.ncbi.nlm.nih.gov/pubmed/19717465.

D. Greig. Reproductive isolation in saccharomyces. *Heredity (Edinb)*, 102(1):39–44, 2009. ISSN 1365-2540 (Electronic) 0018-067X (Linking). doi: 10.1038/hdy.2008.73. URL http://www.ncbi.nlm.nih.gov/pubmed/18648383.

L. Gälweiler, C. Guan, A. Muller, E. Wisman, K. Mendgen, A. Yephremov, and K. Palme. Regulation of polar auxin transport by atpin1 in arabidopsis vascular tissue. *Science*, 282(5397):2226–30, 1998. ISSN 0036-8075 (Print) 0036-8075 (Linking). URL http://www.ncbi.nlm.nih.gov/pubmed/9856939.

J. B. S. Haldane. *The causes of evolution*. Longmans, Green and co., London, New York etc., 1932.

O. Hamant, F. Nogue, E. Belles-Boix, D. Jublot, O. Grandjean, J. Traas, and V. Pautot. The knat2 homeodomain protein interacts with ethylene and cytokinin signaling. *Plant Physiol*, 130(2):657–65, 2002. ISSN 0032-0889 (Print) 0032-0889 (Linking). doi: 10.1104/pp.004564. URL http://www.ncbi.nlm.nih.gov/pubmed/12376633.

J. S. Harrison and R. S. Burton. Tracing hybrid incompatibilities to single amino acid substitutions. *Mol Biol Evol*, 23(3):559–64, 2006. ISSN 0737-4038 (Print) 0737-4038 (Linking). doi: 10.1093/molbev/msj058. URL http://www.ncbi.nlm.nih.gov/pubmed/16280539.

A. Hay, H. Kaur, A. Phillips, P. Hedden, S. Hake, and M. Tsiantis. The gibberellin pathway mediates knotted1-type homeobox function in plants with different body plans. *Curr Biol*, 12(18):1557–65, 2002. ISSN 0960-9822 (Print) 0960-9822 (Linking). URL http://www.ncbi.nlm.nih.gov/pubmed/12372247.

A. Hayward, P. Stirnberg, C. Beveridge, and O. Leyser. Interactions between auxin and strigolactone in shoot branching control. *Plant Physiol*, 151(1):400–12, 2009. ISSN 0032-0889 (Print) 0032-0889 (Linking). doi: 10.1104/pp.109.137646. URL http://www.ncbi.nlm.nih.gov/pubmed/19641034.

M. Heil and I. T. Baldwin. Fitness costs of induced resistance: emerging experimental support for a slippery concept. *Trends Plant Sci*, 7(2):61–7, 2002. ISSN 1360-1385 (Print) 1360-1385 (Linking). URL http://www.ncbi.nlm.nih.gov/pubmed/11832276.

M. G. Heisler, C. Ohno, P. Das, P. Sieber, G. V. Reddy, J. A. Long, and E. M. Meyerowitz. Patterns of auxin transport and gene expression during primordium development revealed by live imaging of the arabidopsis inflorescence meristem. *Curr Biol*, 15(21):1899–911, 2005. ISSN 0960-9822 (Print) 0960-9822 (Linking). doi: 10.1016/j.cub.2005.09.052. URL http://www.ncbi.nlm.nih.gov/pubmed/16271866.

R. Hopkins and M. D. Rausher. Identification of two genes causing reinforcement in the texas wildflower phlox drummondii. *Nature*, 469(7330):411–4, 2011. ISSN 1476-4687 (Electronic) 0028-0836 (Linking). doi: 10.1038/nature09641. URL http://www.ncbi.nlm.nih.gov/pubmed/21217687.

R. Hopkins, R. F. Guerrero, M. D. Rausher, and M. Kirkpatrick. Strong reinforcing selection in a texas wildflower. *Curr Biol*, 24(17):1995–9, 2014. ISSN 1879-0445 (Electronic) 0960-9822 (Linking). doi: 10.1016/j.cub.2014.07.027. URL http://www.ncbi.nlm.nih.gov/pubmed/25155503.

J. Hua. Modulation of plant immunity by light, circadian rhythm, and temperature. *Curr Opin Plant Biol*, 16(4):406–13, 2013. ISSN 1879-0356 (Electronic) 1369-5266 (Linking). doi: 10.1016/j.pbi.2013.06.017. URL http://www.ncbi.nlm.nih.gov/pubmed/23856082.

B. Huot, J. Yao, B. L. Montgomery, and S. Y. He. Growth-defense tradeoffs in plants: a balancing act to optimize fitness. *Mol Plant*, 7(8):1267–87, 2014. ISSN 1752-9867 (Electronic) 1674-2052 (Linking). doi: 10.1093/mp/ssu049. URL http://www.ncbi.nlm.nih.gov/pubmed/24777989.

P. J. Hussey, T. J. Hawkins, H. Igarashi, D. Kaloriti, and A. Smertenko. The plant cytoskeleton: recent advances in the study of the plant microtubule-associated proteins map-65, map-190 and the xenopus map215-like protein, mor1. *Plant Mol Biol*, 50 (6):915–24, 2002. ISSN 0167-4412 (Print) 0167-4412 (Linking). URL http://www.ncbi.nlm.nih.gov/pubmed/12516862.

Julian Huxley. *Evolution, the modern synthesis*. G. Allen & Unwin ltd, London,, 1942.

S. Jasinski, P. Piazza, J. Craft, A. Hay, L. Woolley, I. Rieu, A. Phillips, P. Hedden, and M. Tsiantis. Knox action in arabidopsis is mediated by coordinate regulation of cytokinin and gibberellin activities. *Curr Biol*, 15(17):1560–5, 2005. ISSN 0960-9822 (Print) 0960-9822 (Linking). doi: 10.1016/j.cub.2005.07.023. URL http://www.ncbi.nlm.nih.gov/pubmed/16139211.

S. Jeong, A. E. Trotochaud, and S. E. Clark. The arabidopsis clavata2 gene encodes a receptor-like protein required for the stability of the clavata1 receptor-like kinase. *Plant Cell*, 11(10):1925–34, 1999. ISSN 1040-4651 (Print) 1040-4651 (Linking). URL http://www.ncbi.nlm.nih.gov/pubmed/10521522.

M. J. Jeuken, N. W. Zhang, L. K. McHale, K. Pelgrom, E. den Boer, P. Lindhout, R. W. Michelmore, R. G. Visser, and R. E. Niks. Rin4 causes hybrid necrosis and race-specific resistance in an interspecific lettuce hybrid. *Plant Cell*, 21(10):3368–78, 2009. ISSN 1532-298X (Electronic) 1040-4651 (Linking). doi: 10.1105/tpc.109.070334. URL http://www.ncbi.nlm.nih.gov/pubmed/19855048.

P. Kalousek, D. Buchtova, J. Balla, V. Reinöhl, and S. Procházka. Cytokinins and polar transport of auxin in axillary pea buds. *Magazine Acta Universitatis Agriculturae et Silviculturae Mendeleianae Brunensis.*, 58:79–88, 2010.

K.C. Kao, K. Schwartz, and G. Sherlock. A genome-wide analysis reveals no nuclear dobzhansky-muller pairs of determinants of speciation between s. cerevisiae and s. paradoxus, but suggests more complex incompatibilities. *PloS Genetics*, 6(7): e1001038, 2010.

H. S. Kim, D. Desveaux, A. U. Singer, P. Patel, J. Sondek, and J. L. Dangl. The pseudomonas syringae effector avrrpt2 cleaves its c-terminally acylated target, rin4, from arabidopsis membranes to block rpm1 activation. *Proc Natl Acad Sci U S A*, 102(18):6496–501, 2005a. ISSN 0027-8424 (Print) 0027-8424 (Linking). doi: 10.1073/pnas.0500792102. URL http://www.ncbi.nlm.nih.gov/pubmed/15845764.

M. G. Kim, L. da Cunha, A. J. McFall, Y. Belkhadir, S. DebRoy, J. L. Dangl, and D. Mackey. Two pseudomonas syringae type iii effectors inhibit rin4-regulated basal defense in arabidopsis. *Cell*, 121(5):749–59, 2005b. ISSN 0092-8674 (Print) 0092-8674 (Linking). doi: 10.1016/j.cell.2005.03.025. URL http://www.ncbi.nlm.nih.gov/pubmed/15935761.

M. Kirkpatrick and N. Barton. Chromosome inversions, local adaptation and speciation. *Genetics*, 173(1):419–34, 2006. ISSN 0016-6731 (Print) 0016-6731 (Linking). doi: 10.1534/genetics.105.047985. URL http://www.ncbi.nlm.nih.gov/pubmed/16204214.

T. Korves and J. Bergelson. A novel cost of r gene resistance in the presence of disease. *Am Nat*, 163(4):489–504, 2004. ISSN 1537-5323 (Electronic) 0003-0147 (Linking). doi: 10.1086/382552. URL http://www.ncbi.nlm.nih.gov/pubmed/15122498.

J. L. Kozlowska, A. R. Ahmad, E. Jahesh, and A. D. Cutter. Genetic variation for postzygotic reproductive isolation between caenorhabditis briggsae and caenorhabditis sp. 9. *Evolution*, 66(4):1180–95, 2012. ISSN 1558-5646 (Electronic) 0014-3820 (Linking). doi: 10.1111/j.1558-5646.2011.01514.x. URL http://www.ncbi.nlm.nih.gov/pubmed/22486697.

J. Krüger, C.M. Thomas, C. Golstein, M.S. Dixon, M. Smoker, S. Tang, L. Mulder, and J.D.G. Jones. A tomato cysteine protease required for cf-2-dependent disease resistance and suppression of autonecrosis. *Science*, 296(5568):744–747, 2002.

A. Lampropoulos, Z. Sutikovic, C. Wenzl, I. Maegele, J. U. Lohmann, and J. Forner. Greengate—a novel, versatile, and efficient cloning system for plant transgenesis. *PLoS One*, 8(12):e83043, 2013. ISSN 1932-6203 (Electronic) 1932-6203 (Linking). doi: 10.1371/journal.pone.0083043. URL http://www.ncbi.nlm.nih.gov/pubmed/24376629.

H.Y. Lee, J.Y. Chou, L. Cheong, N.H. Chang, S.Y. Yang, and J.Y. Leu. Incompatibility of nuclear and mitochondrial genomes causes hybrid sterility between two yeast species. *Cell*, 135(6):1065–1073, 2008.

A. Leibfried, J. P. To, W. Busch, S. Stehling, A. Kehle, M. Demar, J. J. Kieber, and J. U. Lohmann. Wuschel controls meristem function by direct regulation of cytokinin-inducible response regulators. *Nature*, 438(7071):1172–5, 2005. ISSN 1476-4687 (Electronic) 0028-0836 (Linking). doi: 10.1038/nature04270. URL http://www.ncbi.nlm.nih.gov/pubmed/16372013.

A. Leon-Reyes, D. Van der Does, E. S. De Lange, C. Delker, C. Wasternack, S. C. Van Wees, T. Ritsema, and C. M. Pieterse. Salicylate-mediated suppression of jasmonate-responsive gene expression in arabidopsis is targeted downstream of the jasmonate biosynthesis pathway. *Planta*, 232(6):1423–32, 2010. ISSN 1432-2048 (Electronic) 0032-0935 (Linking). doi: 10.1007/s00425-010-1265-z. URL http://www.ncbi.nlm.nih.gov/pubmed/20839007.

D.A. Levin. Reproductive character displacement in phlox. *Evolution*, 39(6):1275–1281, 1985.

C-J. Li and F. Bangerth. Autoinhibition of indoleacetic acid transport in the shoots of two-branched pea (pisum sativum) plants and its relationship to correlative dominance. *Physiologia Plantarum*, 106(4):415–420, 1999.

H. Li, X. Zeng, Z. Q. Liu, Q. T. Meng, M. Yuan, and T. L. Mao. Arabidopsis microtubule-associated protein atmap65-2 acts as a microtubule stabilizer. *Plant Mol Biol*, 69(3):313–24, 2009. ISSN 0167-4412 (Print) 0167-4412 (Linking). doi: 10.1007/s11103-008-9426-1. URL http://www.ncbi.nlm.nih.gov/pubmed/19002591.

L. Li, C. Li, and G. A. Howe. Genetic analysis of wound signaling in tomato. evidence for a dual role of jasmonic acid in defense and female fertility. *Plant Physiol*, 127(4):1414–7, 2001a. ISSN 0032-0889 (Print) 0032-0889 (Linking). URL http://www.ncbi.nlm.nih.gov/pubmed/11743083.

Z-K. Li, L.J Luo, H.W. Mei, D.L. Wang, Q.Y. Shu, R. Tabien, D.B. Zhong, C.S. Ying, J.W. Stansel, G.S. Khush, and A.H. Paterson. Overdominant epistatic loci are the primary genetic basis of inbreeding depression and heterosis in rice. i. biomass and grain yield. *Genetics*, 158:1737–1753, 2001b.

K. Lin, S. Smit, G. Bonnema, G. Sanchez-Perez, and D. de Ridder. Making the difference: integrating structural variation detection tools. *Brief Bioinform*, 2014. ISSN 1477-4054 (Electronic) 1467-5463 (Linking). doi: 10.1093/bib/bbu047. URL http://www.ncbi.nlm.nih.gov/pubmed/25504367.

T.L. Lomax, G.K. Muday, and P.H. Rubery. *Auxin transport.*, pages 509–530. Kluwer Academic Publishers, Dordrecht, The Netherlands, 1995.

J. A. Long and M. K. Barton. The development of apical embryonic pattern in arabidopsis. *Development*, 125(16):3027–35, 1998. ISSN 0950-1991 (Print) 0950-1991 (Linking). URL http://www.ncbi.nlm.nih.gov/pubmed/9671577.

J. A. Long, E. I. Moan, J. I. Medford, and M. K. Barton. A member of the knotted class of homeodomain proteins encoded by the stm gene of arabidopsis. *Nature*, 379(6560):66–9, 1996. ISSN 0028-0836 (Print) 0028-0836 (Linking). doi: 10.1038/379066a0. URL http://www.ncbi.nlm.nih.gov/pubmed/8538741.

Y. Long, L. Zhao, B. Niu, J. Su, H. Wu, Y. Chen, Q. Zhang, J. Guo, C. Zhuang, M. Mei, J. Xia, L. Wang, H. Wu, and Y. G. Liu. Hybrid male sterility in rice controlled by interaction between divergent alleles of two adjacent genes. *Proc Natl Acad Sci U S A*, 105(48):18871–6, 2008. ISSN 1091-6490 (Electronic) 0027-8424 (Linking). doi: 10.1073/pnas.0810108105. URL http://www.ncbi.nlm.nih.gov/pubmed/19033192.

O. Lorenzo, R. Piqueras, J. J. Sanchez-Serrano, and R. Solano. Ethylene response factor1 integrates signals from ethylene and jasmonate pathways in plant defense. *Plant Cell*, 15(1):165–78, 2003. ISSN 1040-4651 (Print) 1040-4651 (Linking). URL http://www.ncbi.nlm.nih.gov/pubmed/12509529.

D. Mackey, Y. Belkhadir, J. M. Alonso, J. R. Ecker, and J. L. Dangl. Arabidopsis rin4 is a target of the type iii virulence effector avrrpt2 and modulates rps2-mediated resistance. *Cell*, 112(3):379–89, 2003. ISSN 0092-8674 (Print) 0092-8674 (Linking). URL http://www.ncbi.nlm.nih.gov/pubmed/12581527.

M.R. Macnair and P. Christie. Reproductive isolation as a pleiotropic effect of copper tolerance in mimulus guttatus? *Heredity (Edinb)*, 50(3):295–302, 1983.

S. Maheshwari and D. A. Barbash. The genetics of hybrid incompatibilities. *Annu Rev Genet*, 45:331–55, 2011. ISSN 1545-2948 (Electronic) 0066-4197 (Linking). doi: 10.1146/annurev-genet-110410-132514. URL http://www.ncbi.nlm.nih.gov/pubmed/21910629.

J. Mallet. Hybrid speciation. *Nature*, 446(7133):279–83, 2007. ISSN 1476-4687 (Electronic) 0028-0836 (Linking). doi: 10.1038/nature05706. URL http://www.ncbi.nlm.nih.gov/pubmed/17361174.

G. S. Maloney, K. T. DiNapoli, and G. K. Muday. The anthocyanin reduced tomato mutant demonstrates the role of flavonols in tomato lateral root and root hair development. *Plant Physiol*, 166(2):614–31, 2014. ISSN 1532-2548 (Electronic) 0032-0889 (Linking). doi: 10.1104/pp.114.240507. URL http://www.ncbi.nlm.nih.gov/pubmed/25006027.

K. Matsubara, Thidar Khin, and Y. Sano. A gene block causing cross-incompatibility hidden in wild and cultivated rice. *Genetics*, 165(1):343–52, 2003. ISSN 0016-6731 (Print) 0016-6731 (Linking). URL http://www.ncbi.nlm.nih.gov/pubmed/14504241.

K. Matsubara, T. Ando, T. Mizubayashi, S. Ito, and M. Yano. Identification and linkage mapping of complementary recessive genes causing hybrid breakdown in an intraspecific rice cross. *Theor Appl Genet*, 115(2):179–86, 2007. ISSN 0040-5752 (Print) 0040-5752 (Linking). doi: 10.1007/s00122-007-0553-x. URL http://www.ncbi.nlm.nih.gov/pubmed/17486310.

K. Matsubara, E. Yamamoto, R. Mizobuchi, J. Yonemaru, T. Yamamoto, H. Kato, and M. Yano. Hybrid breakdown caused by epistasis-based recessive incompatibility in a cross of rice (oryza sativa l.). *J Hered*, 106(1):113–22, 2015. ISSN 1465-7333 (Electronic) 0022-1503 (Linking). doi: 10.1093/jhered/esu065. URL http://www.ncbi.nlm.nih.gov/pubmed/25429024.

D. R. Matute, I. A. Butler, D. A. Turissini, and J. A. Coyne. A test of the snowball theory for the rate of evolution of hybrid incompatibilities. *Science*, 329(5998):1518–21, 2010. ISSN 1095-9203 (Electronic) 0036-8075 (Linking). doi: 10.1126/science.1193440. URL http://www.ncbi.nlm.nih.gov/pubmed/20847270.

R. Mauricio. Costs of resistance to natural enemies in field populations of the annual plant arabidopsis thaliana. *Am Nat*, 151(1):20–8, 1998. ISSN 0003-0147 (Print) 0003-0147 (Linking). doi: 10.1086/286099. URL http://www.ncbi.nlm.nih.gov/pubmed/18811421.

K. F. Mayer, H. Schoof, A. Haecker, M. Lenhard, G. Jurgens, and T. Laux. Role of wuschel in regulating stem cell fate in the arabidopsis shoot meristem. *Cell*, 95(6):805–15, 1998. ISSN 0092-8674 (Print) 0092-8674 (Linking). URL http://www.ncbi.nlm.nih.gov/pubmed/9865698.

Ernst Mayr. *Systematics and the origin of species from the viewpoint of a zoologist*. Columbia biological series. Columbia University Press, New York,, 1942.

Y. Mizuta, Y. Harushima, and N. Kurata. Rice pollen hybrid incompatibility caused by reciprocal gene loss of duplicated genes. *Proc Natl Acad Sci U S A*, 107(47):20417–20422, 2010.

T. H. Morgan. Localization of the hereditary material in the germ cells. *Proc Natl Acad Sci U S A*, 1(7):420–9, 1915. ISSN 0027-8424 (Print) 0027-8424 (Linking). URL http://www.ncbi.nlm.nih.gov/pubmed/16576035.

L. C. Moyle and T. Nakazato. Hybrid incompatibility "snowballs" between solanum species. *Science*, 329(5998):1521–3, 2010. ISSN 1095-9203 (Electronic) 0036-8075 (Linking). doi: 10.1126/science.1193063. URL http://www.ncbi.nlm.nih.gov/pubmed/20847271.

J. Mravec, J. Petrasek, N. Li, S. Boeren, R. Karlova, S. Kitakura, M. Parezova, S. Naramoto, T. Nodzynski, P. Dhonukshe, S. Y. Bednarek, E. Zazimalova, S. de Vries, and J. Friml. Cell plate restricted association of drp1a and pin proteins is required for cell polarity establishment in arabidopsis. *Curr Biol*, 21(12):1055–60, 2011. ISSN 1879-0445 (Electronic) 0960-9822 (Linking). doi: 10.1016/j.cub.2011.05.018. URL http://www.ncbi.nlm.nih.gov/pubmed/21658946.

H.J. Muller. Isolating mechanisms, evolution and temperature. *Biology Symposium*, 6:71–125, 1942.

H.J. Muller and G. Pontecorvo. Recombinants between drosophila species the f1 hybrids of which are sterile. *Nature*, 146: 199–200, 1940.

A. Murphy, W. A. Peer, and L. Taiz. Regulation of auxin transport by aminopeptidases and endogenous flavonoids. *Planta*, 211 (3):315–24, 2000. ISSN 0032-0935 (Print) 0032-0935 (Linking). URL http://www.ncbi.nlm.nih.gov/pubmed/10987549.

A. Müntzing. Outlines to a genetic monograph of the genus galeopsis with special reference to the nature and inheritance of partial sterility. *Hereditas*, 13(2-3):185–341, 1930. doi: 10.1111/j.1601-5223.1930.tb02522.x.

A. Nordstrom, P. Tarkowski, D. Tarkowska, R. Norbaek, C. Astot, K. Dolezal, and G. Sandberg. Auxin regulation of cytokinin biosynthesis in arabidopsis thaliana: a factor of potential importance for auxin-cytokinin-regulated development. *Proc Natl Acad Sci U S A*, 101(21):8039–44, 2004. ISSN 0027-8424 (Print) 0027-8424 (Linking). doi: 10.1073/pnas.0402504101. URL http://www.ncbi.nlm.nih.gov/pubmed/15146070.

P. Nosil and D. Schluter. The genes underlying the process of speciation. *Trends Ecol Evol*, 26(4):160–7, 2011. ISSN 0169-5347 (Print) 0169-5347 (Linking). doi: 10.1016/j.tree.2011.01.001. URL http://www.ncbi.nlm.nih.gov/pubmed/21310503.

H. A. Orr. Dobzhansky, bateson, and the genetics of speciation. *Genetics*, 144(4):1331–5, 1996. ISSN 0016-6731 (Print) 0016-6731 (Linking). URL http://www.ncbi.nlm.nih.gov/pubmed/8978022.

H. A. Orr and M. Turelli. The evolution of postzygotic isolation: accumulating dobzhansky-muller incompatibilities. *Evolution*, 55(6):1085–94, 2001. ISSN 0014-3820 (Print) 0014-3820 (Linking). URL http://www.ncbi.nlm.nih.gov/pubmed/11475044.

S. P. Otto and J. Whitton. Polyploid incidence and evolution. *Annu Rev Genet*, 34:401–437, 2000. ISSN 0066-4197 (Print) 0066-4197 (Linking). doi: 10.1146/annurev.genet.34.1.401. URL http://www.ncbi.nlm.nih.gov/pubmed/11092833.

Y. Ouyang and Q. Zhang. Understanding reproductive isolation based on the rice model. *Annu Rev Plant Biol*, 64:111–35, 2013. ISSN 1545-2123 (Electronic) 1543-5008 (Linking). doi: 10.1146/annurev-arplant-050312-120205. URL http://www.ncbi.nlm.nih.gov/pubmed/23638826.

N. Phadnis and H. S. Malik. Speciation via autoimmunity: a dangerous mix. *Cell*, 159(6):1247–9, 2014. ISSN 1097-4172 (Electronic) 0092-8674 (Linking). doi: 10.1016/j.cell.2014.11.028. URL http://www.ncbi.nlm.nih.gov/pubmed/25480288.

G. Pontecorvo. Viability interactions between chromosomes ofdrosophila melanogaster anddrosophila simulans. *Journal of Genetics*, 45(1):51–66, 1943.

D. C. Presgraves. The molecular evolutionary basis of species formation. *Nat Rev Genet*, 11(3):175–80, 2010. ISSN 1471-0064 (Electronic) 1471-0056 (Linking). doi: 10.1038/nrg2718. URL http://www.ncbi.nlm.nih.gov/pubmed/20051985.

S. Q. Qiu, K. Liu, J. X. Jiang, X. Song, C. G. Xu, X. H. Li, and Q. Zhang. Delimitation of the rice wide compatibility gene s5 (n) to a 40-kb dna fragment. *Theor Appl Genet*, 111(6):1080–6, 2005. ISSN 0040-5752 (Print) 0040-5752 (Linking). doi: 10.1007/s00122-005-0033-0. URL http://www.ncbi.nlm.nih.gov/pubmed/16177904.

D. Reinhardt, E. R. Pesce, P. Stieger, T. Mandel, K. Baltensperger, M. Bennett, J. Traas, J. Friml, and C. Kuhlemeier. Regulation of phyllotaxis by polar auxin transport. *Nature*, 426(6964):255–60, 2003. ISSN 1476-4687 (Electronic) 0028-0836 (Linking). doi: 10.1038/nature02081. URL http://www.ncbi.nlm.nih.gov/pubmed/14628043.

L. H. Rieseberg. Crossing relationships among ancient and experimental sunflower hybrid lineages. *Evolution*, 54(3):859–65, 2000. ISSN 0014-3820 (Print) 0014-3820 (Linking). URL http://www.ncbi.nlm.nih.gov/pubmed/10937259.

L. H. Rieseberg. Chromosomal rearrangements and speciation. *Trends Ecol Evol*, 16(7):351–358, 2001. ISSN 1872-8383 (Electronic) 0169-5347 (Linking). URL http://www.ncbi.nlm.nih.gov/pubmed/11403867.

L. H. Rieseberg and B. K. Blackman. Speciation genes in plants. *Ann Bot*, 106(3):439–55, 2010. ISSN 1095-8290 (Electronic) 0305-7364 (Linking). doi: 10.1093/aob/mcq126. URL http://www.ncbi.nlm.nih.gov/pubmed/20576737.

L. H. Rieseberg and J. H. Willis. Plant speciation. *Science*, 317(5840):910–4, 2007. ISSN 1095-9203 (Electronic) 0036-8075 (Linking). doi: 10.1126/science.1137729. URL http://www.ncbi.nlm.nih.gov/pubmed/17702935.

L. H. Rieseberg, M. A. Archer, and R. K. Wayne. Transgressive segregation, adaptation and speciation. *Heredity (Edinb)*, 83 (Pt 4):363–72, 1999. ISSN 0018-067X (Print) 0018-067X (Linking). URL http://www.ncbi.nlm.nih.gov/pubmed/10583537.

L.H. Rieseberg and S.E. Carney. Plant hybridization. *New Phytologist*, 140:599–624, 1998.

H. F. Roberts. The contribution of carl friedrich von gartner to the history of plant hybridisation. *The American Naturalist*, 53 (628):431–445, 1919. URL http://www.jstor.org/stable/2456184.

H. F. Roberts. *Plant hybridization before Mendel*. Princeton University Press, Princeton,, 1929.

E. E. Rogers and F. M. Ausubel. Arabidopsis enhanced disease susceptibility mutants exhibit enhanced susceptibility to several bacterial pathogens and alterations in pr-1 gene expression. *Plant Cell*, 9(3):305–16, 1997. ISSN 1040-4651 (Print) 1040-4651 (Linking). doi: 10.1105/tpc.9.3.305. URL http://www.ncbi.nlm.nih.gov/pubmed/9090877.

H. C. Rooney, J. W. Van't Klooster, R. A. van der Hoorn, M. H. Joosten, J. D. Jones, and P. J. de Wit. Cladosporium avr2 inhibits tomato rcr3 protease required for cf-2-dependent disease resistance. *Science*, 308(5729):1783–6, 2005. ISSN 1095-9203 (Electronic) 0036-8075 (Linking). doi: 10.1126/science.1111404. URL http://www.ncbi.nlm.nih.gov/pubmed/15845874.

H. M. Rupp, M. Frank, T. Werner, M. Strnad, and T. Schmulling. Increased steady state mrna levels of the stm and knat1 homeobox genes in cytokinin overproducing arabidopsis thaliana indicate a role for cytokinins in the shoot apical meristem. *Plant J*, 18(5):557–63, 1999. ISSN 0960-7412 (Print) 0960-7412 (Linking). URL http://www.ncbi.nlm.nih.gov/pubmed/10417706.

T. Sachs and K.V. Thimann. The role of auxins and cytokinins in the release of buds from dominance. *American Journal of Botany*, 54(1):136–144, 1967.

P. A. Salome, K. Bomblies, J. Fitz, R. A. Laitinen, N. Warthmann, L. Yant, and D. Weigel. The recombination landscape in arabidopsis thaliana f2 populations. *Heredity (Edinb)*, 108(4):447–55, 2012. ISSN 1365-2540 (Electronic) 0018-067X (Linking). doi: 10.1038/hdy.2011.95. URL http://www.ncbi.nlm.nih.gov/pubmed/22072068.

P. R. Satyaki, T. N. Cuykendall, K. H. Wei, N. J. Brideau, H. Kwak, S. Aruna, P. M. Ferree, S. Ji, and D. A. Barbash. The hmr and lhr hybrid incompatibility genes suppress a broad range of heterochromatic repeats. *PLoS Genet*, 10(3):e1004240, 2014. ISSN 1553-7404 (Electronic) 1553-7390 (Linking). doi: 10.1371/journal.pgen.1004240. URL http://www.ncbi.nlm.nih.gov/pubmed/24651406.

S. Savaldi-Goldstein, T. J. Baiga, F. Pojer, T. Dabi, C. Butterfield, G. Parry, A. Santner, N. Dharmasiri, Y. Tao, M. Estelle, J. P. Noel, and J. Chory. New auxin analogs with growth-promoting effects in intact plants reveal a chemical strategy to improve hormone delivery. *Proc Natl Acad Sci U S A*, 105(39):15190–5, 2008. ISSN 1091-6490 (Electronic) 0027-8424 (Linking). doi: 10.1073/pnas.0806324105. URL http://www.ncbi.nlm.nih.gov/pubmed/18818305.

D. W. Schemske and Jr. Bradshaw, H. D. Pollinator preference and the evolution of floral traits in monkeyflowers (mimulus). *Proc Natl Acad Sci U S A*, 96(21):11910–5, 1999. ISSN 0027-8424 (Print) 0027-8424 (Linking). URL http://www.ncbi.nlm.nih.gov/pubmed/10518550.

D. Schenck, M. Christian, A. Jones, and H. Luthen. Rapid auxin-induced cell expansion and gene expression: a four-decade-old question revisited. *Plant Physiol*, 152(3):1183–5, 2010. ISSN 1532-2548 (Electronic) 0032-0889 (Linking). doi: 10.1104/pp.109.149591. URL http://www.ncbi.nlm.nih.gov/pubmed/20071604.

K. Schneeberger, S. Ossowski, C. Lanz, T. Juul, A. H. Petersen, K. L. Nielsen, J. E. Jorgensen, D. Weigel, and S. U. Andersen. Shoremap: simultaneous mapping and mutation identification by deep sequencing. *Nat Methods*, 6(8):550–1, 2009. ISSN 1548-7105 (Electronic) 1548-7091 (Linking). doi: 10.1038/nmeth0809-550. URL http://www.ncbi.nlm.nih.gov/pubmed/19644454.

H. Schoof, M. Lenhard, A. Haecker, K. F. Mayer, G. Jurgens, and T. Laux. The stem cell population of arabidopsis shoot meristems in maintained by a regulatory loop between the clavata and wuschel genes. *Cell*, 100(6):635–44, 2000. ISSN 0092-8674 (Print) 0092-8674 (Linking). URL http://www.ncbi.nlm.nih.gov/pubmed/10761929.

R. Schwab, S. Ossowski, M. Riester, N. Warthmann, and D. Weigel. Highly specific gene silencing by artificial micrornas in arabidopsis. *Plant Cell*, 18(5):1121–33, 2006. ISSN 1040-4651 (Print) 1040-4651 (Linking). doi: 10.1105/tpc.105.039834. URL http://www.ncbi.nlm.nih.gov/pubmed/16531494.

I. M. Scott, S. M. Clarke, J. E. Wood, and L. A. Mur. Salicylate accumulation inhibits growth at chilling temperature in arabidopsis. *Plant Physiol*, 135(2):1040–9, 2004. ISSN 0032-0889 (Print) 0032-0889 (Linking). doi: 10.1104/pp.104.041293. URL http://www.ncbi.nlm.nih.gov/pubmed/15173571.

H. S. Seidel, M. V. Rockman, and L. Kruglyak. Widespread genetic incompatibility in c. elegans maintained by balancing selection. *Science*, 319(5863):589–94, 2008. ISSN 1095-9203 (Electronic) 0036-8075 (Linking). doi: 10.1126/science.1151107. URL http://www.ncbi.nlm.nih.gov/pubmed/18187622.

J. Shah, P. Kachroo, and D. F. Klessig. The arabidopsis ssi1 mutation restores pathogenesis-related gene expression in npr1 plants and renders defensin gene expression salicylic acid dependent. *Plant Cell*, 11(2):191–206, 1999. ISSN 1040-4651 (Print) 1040-4651 (Linking). URL http://www.ncbi.nlm.nih.gov/pubmed/9927638.

S. Shimizu-Sato, M. Tanaka, and H. Mori. Auxin-cytokinin interactions in the control of shoot branching. *Plant Mol Biol*, 69 (4):429–35, 2009. ISSN 0167-4412 (Print) 0167-4412 (Linking). doi: 10.1007/s11103-008-9416-3. URL http://www.ncbi.nlm.nih.gov/pubmed/18974937.

Y. Shirano, P. Kachroo, J. Shah, and D. F. Klessig. A gain-of-function mutation in an arabidopsis toll interleukin1 receptor-nucleotide binding site-leucine-rich repeat type r gene triggers defense responses and results in enhanced disease resistance. *Plant Cell*, 14(12):3149–62, 2002. ISSN 1040-4651 (Print) 1040-4651 (Linking). URL http://www.ncbi.nlm.nih.gov/pubmed/12468733.

George Gaylord Simpson. *Tempo and mode in evolution*. Columbia biological series. Columbia University Press, New York, 1944.

L.S. Smith, K. Bomblies, and D. Weigel. Complex evolutionary events at a tandem cluster of arabidopsis thaliana genes resulting in a single-locus genetic incompatibility. *PloS Genetics*, 7(7):e1002164, 2011.

K. Sorefan, J. Booker, K. Haurogne, M. Goussot, K. Bainbridge, E. Foo, S. Chatfield, S. Ward, C. Beveridge, C. Rameau, and O. Leyser. Max4 and rms1 are orthologous dioxygenase-like genes that regulate shoot branching in arabidopsis and pea. *Genes Dev*, 17(12):1469–74, 2003. ISSN 0890-9369 (Print) 0890-9369 (Linking). doi: 10.1101/gad.256603. URL http://www.ncbi.nlm.nih.gov/pubmed/12815068.

A. Stathos and L. Fishman. Chromosomal rearrangements directly cause underdominant f1 pollen sterility in mimulus lewisii-mimulus cardinalis hybrids. *Evolution*, 68(11):3109–19, 2014. ISSN 1558-5646 (Electronic) 0014-3820 (Linking). doi: 10.1111/evo.12503. URL http://www.ncbi.nlm.nih.gov/pubmed/25125144.

G. L. Stebbins. The synthetic approach to problems of organic evolution. *Cold Spring Harb Symp Quant Biol*, 24:305–11, 1959. ISSN 0091-7451 (Print) 0091-7451 (Linking). URL http://www.ncbi.nlm.nih.gov/pubmed/13833941.

G. Ledyard Stebbins. *Variation and evolution in plants*. Columbia biological series,. Columbia University Press, New York,, 1950.

P. Stirnberg, K. van De Sande, and H. M. Leyser. Max1 and max2 control shoot lateral branching in arabidopsis. *Development*, 129(5):1131–41, 2002. ISSN 0950-1991 (Print) 0950-1991 (Linking). URL http://www.ncbi.nlm.nih.gov/pubmed/11874909.

I. M. Sussex. Developmental programming of the shoot meristem. *Cell*, 56(2):225–9, 1989. ISSN 0092-8674 (Print) 0092-8674 (Linking). URL http://www.ncbi.nlm.nih.gov/pubmed/2643476.

S. Swain, S. Roy, J. Shah, S. Van Wees, C. M. Pieterse, and A. K. Nandi. Arabidopsis thaliana cdd1 mutant uncouples the constitutive activation of salicylic acid signalling from growth defects. *Mol Plant Pathol*, 12(9):855–65, 2011. ISSN 1364-3703 (Electronic) 1364-3703 (Linking). doi: 10.1111/j.1364-3703.2011.00717.x. URL http://www.ncbi.nlm.nih.gov/pubmed/21726384.

M. Tanaka, K. Takei, M. Kojima, H. Sakakibara, and H. Mori. Auxin controls local cytokinin biosynthesis in the nodal stem in apical dominance. *Plant J*, 45(6):1028–36, 2006. ISSN 0960-7412 (Print) 0960-7412 (Linking). doi: 10.1111/j.1365-313X.2006.02656.x. URL http://www.ncbi.nlm.nih.gov/pubmed/16507092.

L. P. Taylor and E. Grotewold. Flavonoids as developmental regulators. *Curr Opin Plant Biol*, 8(3):317–23, 2005. ISSN 1369-5266 (Print) 1369-5266 (Linking). doi: 10.1016/j.pbi.2005.03.005. URL http://www.ncbi.nlm.nih.gov/pubmed/15860429.

D. Tian, M. B. Traw, J. Q. Chen, M. Kreitman, and J. Bergelson. Fitness costs of r-gene-mediated resistance in arabidopsis thaliana. *Nature*, 423(6935):74–7, 2003. ISSN 0028-0836 (Print) 0028-0836 (Linking). doi: 10.1038/nature01588. URL http://www.ncbi.nlm.nih.gov/pubmed/12721627.

M. Todesco, S. Balasubramanian, T. T. Hu, M. B. Traw, M. Horton, P. Epple, C. Kuhns, S. Sureshkumar, C. Schwartz, C. Lanz, R. A. Laitinen, Y. Huang, J. Chory, V. Lipka, J. O. Borevitz, J. L. Dangl, J. Bergelson, M. Nordborg, and D. Weigel. Natural allelic variation underlying a major fitness trade-off in arabidopsis thaliana. *Nature*, 465(7298):632–6, 2010. ISSN 1476-4687 (Electronic) 0028-0836 (Linking). doi: 10.1038/nature09083. URL http://www.ncbi.nlm.nih.gov/pubmed/20520716.

M. Todesco, S-T. Kim, E. Chae, K. Bomblies, M. Zaidem, LM. Smith, D. Weigel, and R.A.E. Laitinen. Activation of the arabidopsis thaliana immune system by combinations of common acd6 alleles. *PloS Genetics*, 10(7):e1004459, 2014.

M. B. Traw and J. Bergelson. Plant immune system incompatibility and the distribution of enemies in natural hybrid zones. *Curr Opin Plant Biol*, 13(4):466–71, 2010. ISSN 1879-0356 (Electronic) 1369-5266 (Linking). doi: 10.1016/j.pbi.2010.04.009. URL http://www.ncbi.nlm.nih.gov/pubmed/20494612.

A. E. Trotochaud, S. Jeong, and S. E. Clark. Clavata3, a multimeric ligand for the clavata1 receptor-kinase. *Science*, 289(5479):613–7, 2000. ISSN 0036-8075 (Print) 0036-8075 (Linking). URL http://www.ncbi.nlm.nih.gov/pubmed/10915623.

D. J. Tucker and T. A. Mansfield. Effects of light quality on apical dominance in xanthium strumarium and the associated changes in endogenous levels of abscisic acid and cytokinins. *Planta*, 102(2):140–51, 1971. ISSN 0032-0935 (Print) 0032-0935 (Linking). doi: 10.1007/BF00384868. URL http://www.ncbi.nlm.nih.gov/pubmed/24482132.

C.G.N. Turnbull, M.A.A. Raymond, I.C. Dodd, and S.E. Morris. Rapid increases in cytokinin concentration in lateral buds of chickpea (cicer arietinum l.) during release of apical dominance. *Planta*, 202:271–276, 1997.

S. Uknes, B. Mauch-Mani, M. Moyer, S. Potter, S. Williams, S. Dincher, D. Chandler, A. Slusarenko, E. Ward, and J. Ryals. Acquired resistance in arabidopsis. *Plant Cell*, 4(6):645–56, 1992. ISSN 1040-4651 (Print) 1040-4651 (Linking). doi: 10.1105/tpc.4.6.645. URL http://www.ncbi.nlm.nih.gov/pubmed/1392589.

M. C. Ungerer, S. S. Halldorsdottir, J. L. Modliszewski, T. F. Mackay, and M. D. Purugganan. Quantitative trait loci for inflorescence development in arabidopsis thaliana. *Genetics*, 160(3):1133–51, 2002. ISSN 0016-6731 (Print) 0016-6731 (Linking). URL http://www.ncbi.nlm.nih.gov/pubmed/11901129.

M. C. Ungerer, S. S. Halldorsdottir, M. D. Purugganan, and T. F. Mackay. Genotype-environment interactions at quantitative trait loci affecting inflorescence development in arabidopsis thaliana. *Genetics*, 165(1):353–65, 2003. ISSN 0016-6731 (Print) 0016-6731 (Linking). URL http://www.ncbi.nlm.nih.gov/pubmed/14504242.

M. van Hulten, M. Pelser, L. C. van Loon, C. M. Pieterse, and J. Ton. Costs and benefits of priming for defense in arabidopsis. *Proc Natl Acad Sci U S A*, 103(14):5602–7, 2006. ISSN 0027-8424 (Print) 0027-8424 (Linking). doi: 10.1073/pnas.0510213103. URL http://www.ncbi.nlm.nih.gov/pubmed/16565218.

D. Vlad, F. Rappaport, M. Simon, and O. Loudet. Gene transposition causing natural variation for growth in arabidopsis thaliana. *PloS Genetics*, 6(5):e1000945, 2010.

A. C. Vlot, D. A. Dempsey, and D. F. Klessig. Salicylic acid, a multifaceted hormone to combat disease. *Annu Rev Phytopathol*, 47:177–206, 2009. ISSN 0066-4286 (Print) 0066-4286 (Linking). doi: 10.1146/annurev.phyto.050908.135202. URL http://www.ncbi.nlm.nih.gov/pubmed/19400653.

M. J. Wade, N. A. Johnson, R. Jones, V. Siguel, and M. McNaughton. Genetic variation segregating in natural populations of tribolium castaneum affecting traits observed in hybrids with t. freemani. *Genetics*, 147(3):1235–47, 1997. ISSN 0016-6731 (Print) 0016-6731 (Linking). URL http://www.ncbi.nlm.nih.gov/pubmed/9383066.

Y. Wang, Z. Bao, Y. Zhu, and J. Hua. Analysis of temperature modulation of plant defense against biotrophic microbes. *Mol Plant Microbe Interact*, 22(5):498–506, 2009. ISSN 0894-0282 (Print) 0894-0282 (Linking). doi: 10.1094/MPMI-22-5-0498. URL http://www.ncbi.nlm.nih.gov/pubmed/19348568.

T. K. Watanabe and M. Kawanishi. Mating preference and the direction of evolution in drosophila. *Science*, 205(4409):906–7, 1979. ISSN 0036-8075 (Print) 0036-8075 (Linking). doi: 10.1126/science.205.4409.906. URL http://www.ncbi.nlm.nih.gov/pubmed/17813085.

D. Weigel. Natural variation in arabidopsis: from molecular genetics to ecological genomics. *Plant Physiol*, 158(1):2–22, 2012. ISSN 1532-2548 (Electronic) 0032-0889 (Linking). doi: 10.1104/pp.111.189845. URL http://www.ncbi.nlm.nih.gov/pubmed/22147517.

A. Widmer, C. Lexer, and S. Cozzolino. Evolution of reproductive isolation in plants. *Heredity (Edinb)*, 102(1):31–38, 2009.

E. Wijnker, G. Velikkakam James, J. Ding, F. Becker, J. R. Klasen, V. Rawat, B. A. Rowan, D. F. de Jong, C. B. de Snoo, L. Zapata, B. Huettel, H. de Jong, S. Ossowski, D. Weigel, M. Koornneef, J. J. Keurentjes, and K. Schneeberger. The genomic landscape of meiotic crossovers and gene conversions in arabidopsis thaliana. *Elife*, 2:e01426, 2013. ISSN 2050-084X (Electronic) 2050-084X (Linking). doi: 10.7554/eLife.01426. URL http://www.ncbi.nlm.nih.gov/pubmed/24347547.

C. S. Willett and R. S. Burton. Viability of cytochrome c genotypes depends on cytoplasmic backgrounds in tigriopus californicus. *Evolution*, 55(8):1592–9, 2001. ISSN 0014-3820 (Print) 0014-3820 (Linking). URL http://www.ncbi.nlm.nih.gov/pubmed/11580018.

Øjvind Winge. *Studier over planterigets chromosomtal og chromosomernes betydning*. H. Hagerup, Københavnn,, 1917.

D. Winter, B. Vinegar, H. Nahal, R. Ammar, G. V. Wilson, and N. J. Provart. An "electronic fluorescent pictograph" browser for exploring and analyzing large-scale biological data sets. *PLoS One*, 2(8):e718, 2007. ISSN 1932-6203 (Electronic) 1932-6203 (Linking). doi: 10.1371/journal.pone.0000718. URL http://www.ncbi.nlm.nih.gov/pubmed/17684564.

K. M. Wright, D. Lloyd, D. B. Lowry, M. R. Macnair, and J. H. Willis. Indirect evolution of hybrid lethality due to linkage with selected locus in mimulus guttatus. *PLoS Biol*, 11(2):e1001497, 2013. ISSN 1545-7885 (Electronic) 1544-9173 (Linking). doi: 10.1371/journal.pbio.1001497. URL http://www.ncbi.nlm.nih.gov/pubmed/23468595.

S. Wright. The roles of mutation, interbreeding, crossbreeding and selection in evolution. In D.F. Jones, editor, *Proceedings of the Sixth International Congress of Genetics*. International Congress of Genetics, 1932.

C. A. Wu, D. B. Lowry, A. M. Cooley, K. M. Wright, Y. W. Lee, and J. H. Willis. Mimulus is an emerging model system for the integration of ecological and genomic studies. *Heredity (Edinb)*, 100(2):220–30, 2008. ISSN 1365-2540 (Electronic) 0018-067X (Linking). doi: 10.1038/sj.hdy.6801018. URL http://www.ncbi.nlm.nih.gov/pubmed/17551519.

N. Yalpani, P. Silverman, T. M. Wilson, D. A. Kleier, and I. Raskin. Salicylic acid is a systemic signal and an inducer of pathogenesis-related proteins in virus-infected tobacco. *Plant Cell*, 3(8):809–18, 1991. ISSN 1040-4651 (Print) 1040-4651 (Linking). URL http://www.ncbi.nlm.nih.gov/pubmed/1820820.

Y. Yamagata, E. Yamamoto, K. Aya, K. T. Win, K. Doi, Sobrizal, T. Ito, H. Kanamori, J. Wu, T. Matsumoto, M. Matsuoka, M. Ashikari, and A. Yoshimura. Mitochondrial gene in the nuclear genome induces reproductive barrier in rice. *Proc Natl Acad Sci U S A*, 107(4):1494–9, 2010. ISSN 1091-6490 (Electronic) 0027-8424 (Linking). doi: 10.1073/pnas.0908283107. URL http://www.ncbi.nlm.nih.gov/pubmed/20080642.

E. Yamamoto, T. Takashi, Y. Morinaka, S. Lin, J. Wu, T. Matsumoto, H. Kitano, M. Matsuoka, and M. Ashikari. Gain of deleterious function causes an autoimmune response and bateson-dobzhansky-muller incompatibility in rice. *Molecular Genetics Genomics*, 283:305–315, 2010.

O. Yanai, E. Shani, K. Dolezal, P. Tarkowski, R. Sablowski, G. Sandberg, A. Samach, and N. Ori. Arabidopsis knoxi proteins activate cytokinin biosynthesis. *Curr Biol*, 15(17):1566–71, 2005. ISSN 0960-9822 (Print) 0960-9822 (Linking). doi: 10.1016/j.cub.2005.07.060. URL http://www.ncbi.nlm.nih.gov/pubmed/16139212.

J. Yang, X. Zhao, K. Cheng, H. Du, Y. Ouyang, J. Chen, S. Qiu, J. Huang, Y. Jiang, L. Jiang, J. Ding, J. Wang, C. Xu, X. Li, and Q. Zhang. A killer-protector system regulates both hybrid sterility and segregation distortion in rice. *Science*, 337(6100):1336–40, 2012. ISSN 1095-9203 (Electronic) 0036-8075 (Linking). doi: 10.1126/science.1223702. URL http://www.ncbi.nlm.nih.gov/pubmed/22984070.

S. Yang and J. Hua. A haplotype-specific resistance gene regulated by bonzai1 mediates temperature-dependent growth control in arabidopsis. *Plant Cell*, 16(4):1060–71, 2004. ISSN 1040-4651 (Print) 1040-4651 (Linking). doi: 10.1105/tpc.020479. URL http://www.ncbi.nlm.nih.gov/pubmed/15031411.

X. C. Yang and C. M. Hwa. Genetic modification of plant architecture and variety improvement in rice. *Heredity (Edinb)*, 101(5):396–404, 2008. ISSN 1365-2540 (Electronic) 0018-067X (Linking). doi: 10.1038/hdy.2008.90. URL http://www.ncbi.nlm.nih.gov/pubmed/18716608.

S. E. Zanders, M. T. Eickbush, J. S. Yu, J. W. Kang, K. R. Fowler, G. R. Smith, and H. S. Malik. Genome rearrangements and pervasive meiotic drive cause hybrid infertility in fission yeast. *Elife*, 3:e02630, 2014. ISSN 2050-084X (Electronic) 2050-084X (Linking). doi: 10.7554/eLife.02630. URL http://www.ncbi.nlm.nih.gov/pubmed/24963140.

X. Zhang and J. Hu. Two small protein families, dynamin-related protein3 and fission1, are required for peroxisome fission in arabidopsis. *Plant J*, 57(1):146–59, 2009. ISSN 1365-313X (Electronic) 0960-7412 (Linking). doi: 10.1111/j.1365-313X.2008.03677.x. URL http://www.ncbi.nlm.nih.gov/pubmed/18785999.

N. Zhou, T. L. Tootle, F. Tsui, D. F. Klessig, and J. Glazebrook. Pad4 functions upstream from salicylic acid to control defense responses in arabidopsis. *Plant Cell*, 10(6):1021–30, 1998. ISSN 1040-4651 (Print) 1040-4651 (Linking). URL http://www.ncbi.nlm.nih.gov/pubmed/9634589.

Y. Zhu, B. Du, J. Qian, B. Zou, and J. Hua. Disease resistance gene-induced growth inhibition is enhanced by rcd1 independent of defense activation in arabidopsis. *Plant Physiol*, 161(4):2005–13, 2013. ISSN 1532-2548 (Electronic) 0032-0889 (Linking). doi: 10.1104/pp.112.213363. URL http://www.ncbi.nlm.nih.gov/pubmed/23365132.

T. Zust, B. Joseph, K. K. Shimizu, D. J. Kliebenstein, and L. A. Turnbull. Using knockout mutants to reveal the growth costs of defensive traits. *Proc Biol Sci*, 278(1718):2598–603, 2011. ISSN 1471-2954 (Electronic) 0962-8452 (Linking). doi: 10.1098/rspb.2010.2475. URL http://www.ncbi.nlm.nih.gov/pubmed/21270041.

A

APPENDIX

A.1 OLIGOS (CHAPTER 3)

These oligos were ordered at the Wigge lab in the Sainsbury Laboratory, Cambridge, UK. They do not appear in the Weigel lab oligo database and therefore, do not have an "oligo name".

Target gene	Sequence
PR1	TGATCCTCGTGGGAATTATGT
PR1	TGCATGATCACATCATTACTTCAT
EDS1	CTCAATGACCTTGGAGTGAGC
EDS1	TCTTCCTCTAATGCAGCTTGAA
EDS5	CGAACTCGCTGCTCTTGG
EDS5	GCAACCATATTGGATGTAGCC
PAD4	TGCCATACTCAAACTCTTTCTTCA
PAD4	CCAAAGTGCGGTGAAAGC
FRK1	GAGACTATTTGGCAGGTAAAAGGT
FRK1	AGGAGGCTTACAACCATTGTG
LOX2	CTTACCCGCGGATCTCATC
LOX2	ACTCCATGTTCTGCGGTCTT
PDF1.2	GTTCTCTTTGCTGCTTTCGAC
PDF1.2	GCAAACCCCTGACCATGT
UBC21	TCCTCTTAACTGCGACTCAGG
UBC21	GCGAGGCGTGTATACATTTG

A.2 OLIGOS (CHAPTER 4)

Table 2: *Oligos (Chapter 4)*

Oligo	Sequence	Purpose
G-4448	TGATTTTGAAGAGTTGAAACC	SSLP marker, chr 3: 21.96 Mb
G-4449	TTGAGCAAAGACACTACTGAA	SSLP marker, chr 3: 21.96 Mb
G-28201	TGGATTTCTTCCTCTCTTCAC	SSLP marker, chr 3: 23.01 Mb
G-28202	ATGGAGAAGCTTACACTGATC	SSLP marker, chr 3: 23.01 Mb
G-20875	CCGCGATCTGATTATTGGTT	CAPS marker, chr 3: 22.14 Mb, DraI
G-20876	ACAGTATCAAAGGCGGGTTG	CAPS marker, chr 3: 22.14 Mb, DraI
G-20877	CCTCAAGGTCGTGGCTTTAG	CAPS marker, chr 3: 22.27 Mb, ScaI
G-20878	CCGTTTTGTTTGGAGCAAAT	CAPS marker, chr 3: 22.27 Mb, ScaI
G-22507	TACTGTGGTCACCGTGAAGC	CAPS marker, chr 3: 22.69 Mb, BccI
G-22508	GAACCCCAGAGTTCCCTTTC	CAPS marker, chr 3: 22.69 Mb, BccI
G-25234	GGGGAGATTTCCTGATTTCAA	SNP marker, chr 3: 22.24 Mb
G-25235	AGAGGTTTTCGAGGCTGTCA	SNP marker, chr 3: 22.24 Mb
G-25243	CTGGCAAAGTGTTCCTGGTT	SNP marker, chr 3: 22.44 Mb
G-25244	GGAGACATTTTGGCACTGGT	SNP marker, chr 3: 22.44 Mb
G-26142	TTGACTTGTGTCTATAACCTAGAAAAA	SNP marker, chr 3: 22.49 Mb
G-26143	CAGTTTACACGGACGGTTTG	SNP marker, chr 3: 22.49 Mb
G-28231	TGTCGGGCAATTAGAACCTT	SNP marker, chr 3: 22.50 Mb
G-28232	TAGTCGAGGAGGACGAGGAG	SNP marker, chr 3: 22.50 Mb

Continued on next page

Table 2 – continued from previous page

Oligo	Sequence	Purpose
G-28337	CCGGAACGATGACGTTTACT	SNP marker, chr 3: 22.60 Mb
G-28338	GTTGCAGATCCTCCTTCCAA	SNP marker, chr 3: 22.60 Mb
G-26166	AAATGATGATAGTAATTTGTTTGGTTT	SNP marker, chr 3: 22.62 Mb
G-26167	TTCTCATTTCAATTACCATGCAA	SNP marker, chr 3: 22.62 Mb
G-27889	AATGCCAACGAAACAGAACC	SNP marker, chr 3: 22.69 Mb
G-27890	TGCCTCATCATCCCATTGTA	SNP marker, chr 3: 22.69 Mb
G-28506	GATAAAGAAAGCGCGTCTTGCAGTCTCTCTTTTGTATTCC	amiRAT3G60910
G-28507	GACTGCAAGACGCGCTTTCTTTATCAAAGAGAATCAATGA	amiRAT3G60910
G-28508	GACTACAAGACGCGCATTCTTTTTCACAGGTCGTGATATG	amiRAT3G60910
G-28509	GAAAAAGAATGCGCGTCTTGTAGTCTACATATATATTCCT	amiRAT3G60910
G-28510	GATAGCCTGCTAACTTCACGCAATCTCTCTTTTGTATTCC	amiRAT3G60910
G-28511	GATTGCGTGAAGTTAGCAGGCTATCAAAGAGAATCAATGA	amiRAT3G60910
G-28512	GATTACGTGAAGTTACCAGGCTTTCACAGGTCGTGATATG	amiRAT3G60910
G-28515	GAAAGCCTGGTAACTTCACGTAATCTACATATATATTCCT	amiRAT3G60910
G-28516	GATACATTTTCGAATGCGGTCCGTCTCTCTTTTGTATTCC	amiRAT3G60961
G-28517	GACGGACCGCATTCGAAAATGTATCAAAGAGAATCAATGA	amiRAT3G60961
G-28518	GACGAACCGCATTCGTAAATGTTTCACAGGTCGTGATATG	amiRAT3G60961
G-28519	GAAACATTTACGAATGCGGTTCGTCTACATATATATTCCT	amiRAT3G60961
G-28520	GATTACAAATAAGCATGAGTCGGTCTCTCTTTTGTATTCC	amiRAT3G60961
G-28521	GACCGACTCATGCTTATTTGTAATCAAAGAGAATCAATGA	amiRAT3G60961
G-28522	GACCAACTCATGCTTTTTTGTATTCACAGGTCGTGATATG	amiRAT3G60961
G-28523	GAATACAAAAAAGCATGAGTTGGTCTACATATATATTCCT	amiRAT3G60961
G-28524	GATGTAATAAACCATAGACGCGGTCTCTCTTTTGTATTCC	amiRAT3G60966
G-28525	GACCGCGTCTATGGTTTATTACATCAAAGAGAATCAATGA	amiRAT3G60966
G-28527	GACCACGTCTATGGTATATTACTTCACAGGTCGTGATATG	amiRAT3G60966
G-28529	GAAGTAATATACCATAGACGTGGTCTACATATATATTCCT	amiRAT3G60966
G-28530	GATATTAGAAAAAGACCCCGCCTTCTCTCTTTTGTATTCC	amiRAT3G60966
G-28531	GAAGGCGGGGTCTTTTTCTAATATCAAAGAGAATCAATGA	amiRAT3G60966
G-28532	GAAGACGGGGTCTTTATCTAATTTCACAGGTCGTGATATG	amiRAT3G60966
G-28533	GAAATTAGATAAAGACCCCGTCTTCTACATATATATTCCT	amiRAT3G60966
G-28534	GATGATACGTGAAAAGGAAACTCTCTCTCTTTTGTATTCC	amiRAT3G61035
G-28535	GAGAGTTTCCTTTTCACGTATCATCAAAGAGAATCAATGA	amiRAT3G61035
G-28536	GAGAATTTCCTTTTCTCGTATCTTCACAGGTCGTGATATG	amiRAT3G61035
G-28537	GAAGATACGAGAAAAGGAAATTCTCTACATATATATTCCT	amiRAT3G61035
G-28586	GATCAATACTCGTTAATCTGCGCTCTCTCTTTTGTATTCC	amiRAT3G61160
G-28587	GAGCGCAGATTAACGAGTATTGATCAAAGAGAATCAATGA	amiRAT3G61160
G-28588	GAGCACAGATTAACGTGTATTGTTCACAGGTCGTGATATG	amiRAT3G61160
G-28589	GAACAATACACGTTAATCTGTGCTCTACATATATATTCCT	amiRAT3G61160
G-28590	GATGATAATTCATAGCACGGCAATCTCTCTTTTGTATTCC	amiRAT3G61160
G-28591	GATTGCCGTGCTATGAATTATCATCAAAGAGAATCAATGA	amiRAT3G61160
G-28592	GATTACCGTGCTATGTATTATCTTCACAGGTCGTGATATG	amiRAT3G61160
G-28593	GAAGATAATACATAGCACGGTAATCTACATATATATTCCT	amiRAT3G61160
G-28594	GATTCTAGAGGTCAAAACGACTCTCTCTCTTTTGTATTCC	amiRAT3G61220
G-28595	GAGAGTCGTTTTGACCTCTAGAATCAAAGAGAATCAATGA	amiRAT3G61220
G-28596	GAGAATCGTTTTGACGTCTAGATTCACAGGTCGTGATATG	amiRAT3G61220
G-28597	GAATCTAGACGTCAAAACGATTCTCTACATATATATTCCT	amiRAT3G61220
G-28598	GATTATGTTCGACATTCAAGCGGTCTCTCTTTTGTATTCC	amiRAT3G61220
G-28599	GACCGCTTGAATGTCGAACATAATCAAAGAGAATCAATGA	amiRAT3G61220
G-28600	GACCACTTGAATGTCCAACATATTCACAGGTCGTGATATG	amiRAT3G61220
G-28601	GAATATGTTGGACATTCAAGTGGTCTACATATATATTCCT	amiRAT3G61220
G-28602	GATAACGCTTCGTCGTGACGCAATCTCTCTTTTGTATTCC	amiRAT3G61120
G-28603	GATTGCGTCACGACGAAGCGTTATCAAAGAGAATCAATGA	amiRAT3G61120
G-28604	GATTACGTCACGACGTAGCGTTTTCACAGGTCGTGATATG	amiRAT3G61120
G-28605	GAAAACGCTACGTCGTGACGTAATCTACATATATATTCCT	amiRAT3G61120
G-28606	GATTTACAGCGATAGTACCGCTCTCTCTCTTTTGTATTCC	amiRAT3G61120

Continued on next page

Table 2 – continued from previous page

Oligo	Sequence	Purpose
G-28607	GAGAGCGGTACTATCGCTGTAAATCAAAGAGAATCAATGA	amiRAT3G61120
G-28608	GAGAACGGTACTATCCCTGTAATTCACAGGTCGTGATATG	amiRAT3G61120
G-28609	GAATTACAGGGATAGTACCGTTCTCTACATATATATTCCT	amiRAT3G61120
G-28610	GATAATCTAGTGTAGTGATGCTTTCTCTCTTTTGTATTCC	amiRAT3G61070
G-28611	GAAAGCATCACTACACTAGATTATCAAAGAGAATCAATGA	amiRAT3G61070
G-28612	GAAAACATCACTACAGTAGATTTTCACAGGTCGTGATATG	amiRAT3G61070
G-28613	GAAAATCTACTGTAGTGATGTTTTCTACATATATATTCCT	amiRAT3G61070
G-28614	GATTGTATATGCCGGACCTACAATCTCTCTTTTGTATTCC	amiRAT3G61070
G-28615	GATTGTAGGTCCGGCATATACAATCAAAGAGAATCAATGA	amiRAT3G61070
G-28616	GATTATAGGTCCGGCTTATACATTCACAGGTCGTGATATG	amiRAT3G61070
G-28617	GAATGTATAAGCCGGACCTATAATCTACATATATATTCCT	amiRAT3G61070
G-32299	GATATATTGCCTTCGTTTCGCTCTCTCTCTTTTGTATTCC	amiRAT3G60830
G-32300	GAGAGCGAAACGAAGGCAATATATCAAAGAGAATCAATGA	amiRAT3G60830
G-32301	GAGAACGAAACGAAGCCAATATTTCACAGGTCGTGATATG	amiRAT3G60830
G-32302	GAAATATTGGCTTCGTTTCGTTCTCTACATATATATTCCT	amiRAT3G60830
G-32303	GATGTACTACATAATCGGGTCAATCTCTCTTTTGTATTCC	amiRAT3G60830
G-32304	GATTGACCCGATTATGTAGTACATCAAAGAGAATCAATGA	amiRAT3G60830
G-32305	GATTAACCCGATTATCTAGTACTTCACAGGTCGTGATATG	amiRAT3G60830
G-32306	GAAGTACTAGATAATCGGGTTAATCTACATATATATTCCT	amiRAT3G60830
G-32307	GATTAATTTAGTCTACACCCCAGTCTCTCTTTTGTATTCC	amiRAT3G60750
G-32308	GACTGGGGTGTAGACTAAATTAATCAAAGAGAATCAATGA	amiRAT3G60750
G-32309	GACTAGGGTGTAGACAAAATTATTCACAGGTCGTGATATG	amiRAT3G60750
G-32310	GAATAATTTTGTCTACACCCTAGTCTACATATATATTCCT	amiRAT3G60750
G-32311	GATCAGAAATTGTATATCGACCCTCTCTCTTTTGTATTCC	amiRAT3G60750
G-32312	GAGGGTCGATATACAATTTCTGATCAAAGAGAATCAATGA	amiRAT3G60750
G-32313	GAGGATCGATATACATTTTCTGTTCACAGGTCGTGATATG	amiRAT3G60750
G-32314	GAACAGAAAATGTATATCGATCCTCTACATATATATTCCT	amiRAT3G60750
G-32315	GATTAGTTCATATGGCAAGACGCTCTCTCTTTTGTATTCC	amiRAT3G60740
G-32316	GAGCGTCTTGCCATATGAACTAATCAAAGAGAATCAATGA	amiRAT3G60740
G-32317	GAGCATCTTGCCATAAGAACTATTCACAGGTCGTGATATG	amiRAT3G60740
G-32318	GAATAGTTCTTATGGCAAGATGCTCTACATATATATTCCT	amiRAT3G60740
G-32319	GATTTAGACGTGAAGTAACGCGATCTCTCTTTTGTATTCC	amiRAT3G60740
G-32320	GATCGCGTTACTTCACGTCTAAATCAAAGAGAATCAATGA	amiRAT3G60740
G-32321	GATCACGTTACTTCAGGTCTAATTCACAGGTCGTGATATG	amiRAT3G60740
G-32322	GAATTAGACCTGAAGTAACGTGATCTACATATATATTCCT	amiRAT3G60740
G-32323	GATATTCAACCGACTTTTACCGATCTCTCTTTTGTATTCC	amiRAT3G60730
G-32324	GATCGGTAAAAGTCGGTTGAATATCAAAGAGAATCAATGA	amiRAT3G60730
G-32325	GATCAGTAAAAGTCGCTTGAATTTCACAGGTCGTGATATG	amiRAT3G60730
G-32326	GAAATTCAAGCGACTTTTACTGATCTACATATATATTCCT	amiRAT3G60730
G-32327	GATATACAACGTCGACAAAGCGTTCTCTCTTTTGTATTCC	amiRAT3G60730
G-32328	GAACGCTTTGTCGACGTTGTATATCAAAGAGAATCAATGA	amiRAT3G60730
G-32329	GAACACTTTGTCGACCTTGTATTTCACAGGTCGTGATATG	amiRAT3G60730
G-32330	GAAATACAAGGTCGACAAAGTGTTCTACATATATATTCCT	amiRAT3G60730
G-32331	GATAATACGAAAAATCTGGGCGATCTCTCTTTTGTATTCC	amiRAT3G60860
G-32332	GATCGCCCAGATTTTTCGTATTATCAAAGAGAATCAATGA	amiRAT3G60860
G-32333	GATCACCCAGATTTTACGTATTTTCACAGGTCGTGATATG	amiRAT3G60860
G-32334	GAAAATACGTAAAATCTGGGTGATCTACATATATATTCCT	amiRAT3G60860
G-32335	GATATGTTATAATGCGCTAGCTCTCTCTCTTTTGTATTCC	amiRAT3G60860
G-32336	GAGAGCTAGCGCATTATAACATATCAAAGAGAATCAATGA	amiRAT3G60860
G-32337	GAGAACTAGCGCATTTTAACATTTCACAGGTCGTGATATG	amiRAT3G60860
G-32338	GAAATGTTAAAATGCGCTAGTTCTCTACATATATATTCCT	amiRAT3G60860
G-32340	GATTAACCATGGTCAAGTCGCTATCTCTCTTTTGTATTCC	amiRAT3G60900
G-32341	GATAGCGACTTGACCATGGTTAATCAAAGAGAATCAATGA	amiRAT3G60900
G-32342	GATAACGACTTGACCTTGGTTATTCACAGGTCGTGATATG	amiRAT3G60900
G-32343	GAATAACCAAGGTCAAGTCGTTATCTACATATATATTCCT	amiRAT3G60900

Continued on next page

Table 2 – continued from previous page

Oligo	Sequence	Purpose
G-32344	GATTAAATCGTATTTACCGGCTCTCTCTCTTTTGTATTCC	amiRAT3G60900
G-32345	GAGAGCCGGTAAATACGATTTAATCAAAGAGAATCAATGA	amiRAT3G60900
G-32346	GAGAACCGGTAAATAGGATTTATTCACAGGTCGTGATATG	amiRAT3G60900
G-32347	GAATAAATCCTATTTACCGGTTCTCTACATATATATTCCT	amiRAT3G60900
G-32348	GATGAGTAATCACGATCGCGCGTTCTCTCTTTTGTATTCC	amiRAT3G60940
G-32349	GAACGCGCGATCGTGATTACTCATCAAAGAGAATCAATGA	amiRAT3G60940
G-32350	GAACACGCGATCGTGTTTACTCTTCACAGGTCGTGATATG	amiRAT3G60940
G-32351	GAAGAGTAAACACGATCGCGTGTTCTACATATATATTCCT	amiRAT3G60940
G-32352	GATTACTAACTGTGGGTAACCTGTCTCTCTTTTGTATTCC	amiRAT3G60940
G-32353	GACAGGTTACCCACAGTTAGTAATCAAAGAGAATCAATGA	amiRAT3G60940
G-32354	GACAAGTTACCCACACTTAGTATTCACAGGTCGTGATATG	amiRAT3G60940
G-32355	GAATACTAAGTGTGGGTAACTTGTCTACATATATATTCCT	amiRAT3G60940
G-32356	GATTATGTAATAGGATGGCACGTTCTCTCTTTTGTATTCC	amiRAT3G61010
G-32357	GAACGTGCCATCCTATTACATAATCAAAGAGAATCAATGA	amiRAT3G61010
G-32358	GAACATGCCATCCTAATACATATTCACAGGTCGTGATATG	amiRAT3G61010
G-32359	GAATATGTATTAGGATGGCATGTTCTACATATATATTCCT	amiRAT3G61010
G-32360	GATAAATATATAGGTAGCGACGGTCTCTCTTTTGTATTCC	amiRAT3G61010
G-32361	GACCGTCGCTACCTATATATTTATCAAAGAGAATCAATGA	amiRAT3G61010
G-32362	GACCATCGCTACCTAAATATTTTTCACAGGTCGTGATATG	amiRAT3G61010
G-32363	GAAAAATATTTAGGTAGCGATGGTCTACATATATATTCCT	amiRAT3G61010
G-32364	GATATATGCTGTTTACATGCCTATCTCTCTTTTGTATTCC	amiRAT3G60970
G-32365	GATAGGCATGTAAACAGCATATATCAAAGAGAATCAATGA	amiRAT3G60970
G-32366	GATAAGCATGTAAACTGCATATTTCACAGGTCGTGATATG	amiRAT3G60970
G-32367	GAAATATGCAGTTTACATGCTTATCTACATATATATTCCT	amiRAT3G60970
G-32368	GATCGTTCTGATATACCGCGCGATCTCTCTTTTGTATTCC	amiRAT3G60970
G-32369	GATCGCGCGGTATATCAGAACGATCAAAGAGAATCAATGA	amiRAT3G60970
G-32370	GATCACGCGGTATATGAGAACGTTCACAGGTCGTGATATG	amiRAT3G60970
G-32371	GAACGTTCTCATATACCGCGTGATCTACATATATATTCCT	amiRAT3G60970
G-32736	GATATTGCTAAACGTTCTCGCCATCTCTCTTTTGTATTCC	amiRAT3G61130
G-32737	GATGGCGAGAACGTTTAGCAATATCAAAGAGAATCAATGA	amiRAT3G61130
G-32738	GATGACGAGAACGTTAAGCAATTTCACAGGTCGTGATATG	amiRAT3G61130
G-32739	GAAATTGCTTAACGTTCTCGTCATCTACATATATATTCCT	amiRAT3G61130
G-32740	GATGATACTCGGGTTATATGCAATCTCTCTTTTGTATTCC	amiRAT3G61130
G-32741	GATTGCATATAACCCGAGTATCATCAAAGAGAATCAATGA	amiRAT3G61130
G-32742	GATTACATATAACCCCAGTATCTTCACAGGTCGTGATATG	amiRAT3G61130
G-32743	GAAGATACTGGGGTTATATGTAATCTACATATATATTCCT	amiRAT3G61130
G-32744	GATACACGATAATTCGCAGGCATTCTCTCTTTTGTATTCC	amiRAT3G61060
G-32745	GAATGCCTGCGAATTATCGTGTATCAAAGAGAATCAATGA	amiRAT3G61060
G-32746	GAATACCTGCGAATTTTCGTGTTTCACAGGTCGTGATATG	amiRAT3G61060
G-32747	GAAACACGAAAATTCGCAGGTATTCTACATATATATTCCT	amiRAT3G61060
G-32748	GATGTATAGTGAATGTTTCGCTGTCTCTCTTTTGTATTCC	amiRAT3G61060
G-32749	GACAGCGAAACATTCACTATACATCAAAGAGAATCAATGA	amiRAT3G61060
G-32750	GACAACGAAACATTCTCTATACTTCACAGGTCGTGATATG	amiRAT3G61060
G-32751	GAAGTATAGAGAATGTTTCGTTGTCTACATATATATTCCT	amiRAT3G61060
G-32752	GATTTGAATAGTCGCGACTGCAGTCTCTCTTTTGTATTCC	amiRAT3G61028
G-32753	GACTGCAGTCGCGACTATTCAAATCAAAGAGAATCAATGA	amiRAT3G61028
G-32754	GACTACAGTCGCGACAATTCAATTCACAGGTCGTGATATG	amiRAT3G61028
G-32755	GAATTGAATTGTCGCGACTGTAGTCTACATATATATTCCT	amiRAT3G61028
G-32756	GATTAATCGATGTGATGGGCCCTTCTCTCTTTTGTATTCC	amiRAT3G61028
G-32757	GAAGGGCCCATCACATCGATTAATCAAAGAGAATCAATGA	amiRAT3G61028
G-32758	GAAGAGCCCATCACAACGATTATTCACAGGTCGTGATATG	amiRAT3G61028
G-32759	GAATAATCGTTGTGATGGGCTCTTCTACATATATATTCCT	amiRAT3G61028
G-32760	GATAAGTCGCAAATGCATAGCGATCTCTCTTTTGTATTCC	amiRAT3G60920
G-32761	GATCGCTATGCATTTGCGACTTATCAAAGAGAATCAATGA	amiRAT3G60920
G-32762	GATCACTATGCATTTCCGACTTTTCACAGGTCGTGATATG	amiRAT3G60920

Continued on next page

Table 2 – continued from previous page

Oligo	Sequence	Purpose
G-32763	GAAAAGTCGGAAATGCATAGTGATCTACATATATATTCCT	amiRAT3G60920
G-32764	GATAAAATATTTGGTCTGCACGCTCTCTCTTTTGTATTCC	amiRAT3G60920
G-32765	GAGCGTGCAGACCAAATATTTTATCAAAGAGAATCAATGA	amiRAT3G60920
G-32766	GAGCATGCAGACCAATTATTTTTTCACAGGTCGTGATATG	amiRAT3G60920
G-32767	GAAAAAATAATTGGTCTGCATGCTCTACATATATATTCCT	amiRAT3G60920
G-32768	GATAATTCGCTTTACCCCGACTCTCTCTCTTTTGTATTCC	amiRAT3G60840
G-32769	GAGAGTCGGGGTAAAGCGAATTATCAAAGAGAATCAATGA	amiRAT3G60840
G-32770	GAGAATCGGGGTAAACCGAATTTTCACAGGTCGTGATATG	amiRAT3G60840
G-32771	GAAAATTCGGTTTACCCCGATTCTCTACATATATATTCCT	amiRAT3G60840
G-32772	GATAACGGGCTTTTTATGCGCGCTCTCTCTTTTGTATTCC	amiRAT3G60840
G-32773	GAGCGCGCATAAAAAGCCCGTTATCAAAGAGAATCAATGA	amiRAT3G60840
G-32774	GAGCACGCATAAAAACCCCGTTTTCACAGGTCGTGATATG	amiRAT3G60840
G-32775	GAAAACGGGGTTTTTATGCGTGCTCTACATATATATTCCT	amiRAT3G60840
G-32776	GATCATGCTTAATTTAGGGGCTATCTCTCTTTTGTATTCC	amiRAT3G60790
G-32777	GATAGCCCCTAAATTAAGCATGATCAAAGAGAATCAATGA	amiRAT3G60790
G-32778	GATAACCCCTAAATTTAGCATGTTCACAGGTCGTGATATG	amiRAT3G60790
G-32779	GAACATGCTAAATTTAGGGGTTATCTACATATATATTCCT	amiRAT3G60790
G-32780	GATATTTGTTACGTGCTCCCCCATCTCTCTTTTGTATTCC	amiRAT3G60790
G-32781	GATGGGGGAGCACGTAACAAATATCAAAGAGAATCAATGA	amiRAT3G60790
G-32782	GATGAGGGAGCACGTTACAAATTTCACAGGTCGTGATATG	amiRAT3G60790
G-32783	GAAATTTGTAACGTGCTCCCTCATCTACATATATATTCCT	amiRAT3G60790
G-32784	GATAAAGCGTACAAACGGGTCAATCTCTCTTTTGTATTCC	amiRAT3G60710
G-32785	GATTGACCCGTTTGTACGCTTTATCAAAGAGAATCAATGA	amiRAT3G60710
G-32786	GATTAACCCGTTTGTTCGCTTTTTCACAGGTCGTGATATG	amiRAT3G60710
G-32787	GAAAAAGCGAACAAACGGGTTAATCTACATATATATTCCT	amiRAT3G60710
G-32788	GATAAGATGTAGTTAGCAAGCTCTCTCTCTTTTGTATTCC	amiRAT3G60710
G-32789	GAGAGCTTGCTAACTACATCTTATCAAAGAGAATCAATGA	amiRAT3G60710
G-32790	GAGAACTTGCTAACTTCATCTTTTCACAGGTCGTGATATG	amiRAT3G60710
G-32791	GAAAAGATGAAGTTAGCAAGTTCTCTACATATATATTCCT	amiRAT3G60710
G-32792	GATGAGTCTAAAACAGACGTCGTTCTCTCTTTTGTATTCC	amiRAT3G60630
G-32793	GAACGACGTCTGTTTTAGACTCATCAAAGAGAATCAATGA	amiRAT3G60630
G-32794	GAACAACGTCTGTTTAAGACTCTTCACAGGTCGTGATATG	amiRAT3G60630
G-32795	GAAGAGTCTTAAACAGACGTTGTTCTACATATATATTCCT	amiRAT3G60630
G-32796	GATGTATCGACGGTTACACGCAATCTCTCTTTTGTATTCC	amiRAT3G60630
G-32797	GATTGCGTGTAACCGTCGATACATCAAAGAGAATCAATGA	amiRAT3G60630
G-32798	GATTACGTGTAACCGACGATACTTCACAGGTCGTGATATG	amiRAT3G60630
G-32799	GAAGTATCGTCGGTTACACGTAATCTACATATATATTCCT	amiRAT3G60630
G-32800	GATAGATAAATTCCCTACCGCGTTCTCTCTTTTGTATTCC	amiRAT3G60580
G-32801	GAACGCGGTAGGGAATTTATCTATCAAAGAGAATCAATGA	amiRAT3G60580
G-32802	GAACACGGTAGGGAAATTATCTTTCACAGGTCGTGATATG	amiRAT3G60580
G-32803	GAAAGATAATTTCCCTACCGTGTTCTACATATATATTCCT	amiRAT3G60580
G-32804	GATTACGAAAATTTGGGCGACCCTCTCTCTTTTGTATTCC	amiRAT3G60580
G-32805	GAGGGTCGCCCAAATTTTCGTAATCAAAGAGAATCAATGA	amiRAT3G60580
G-32806	GAGGATCGCCCAAATATTCGTATTCACAGGTCGTGATATG	amiRAT3G60580
G-32807	GAATACGAATATTTGGGCGATCCTCTACATATATATTCCT	amiRAT3G60580
G-32808	GATTTGTTGTATACATGGCGCTATCTCTCTTTTGTATTCC	amiRAT3G60440
G-32809	GATAGCGCCATGTATACAACAAATCAAAGAGAATCAATGA	amiRAT3G60440
G-32810	GATAACGCCATGTATTCAACAATTCACAGGTCGTGATATG	amiRAT3G60440
G-32811	GAATTGTTGAATACATGGCGTTATCTACATATATATTCCT	amiRAT3G60440
G-32812	GATACTAAGACTTGTGATCACGTTCTCTCTTTTGTATTCC	amiRAT3G60440
G-32813	GAACGTGATCACAAGTCTTAGTATCAAAGAGAATCAATGA	amiRAT3G60440
G-32814	GAACATGATCACAAGACTTAGTTTCACAGGTCGTGATATG	amiRAT3G60440
G-32815	GAAACTAAGTCTTGTGATCATGTTCTACATATATATTCCT	amiRAT3G60440
G-33050	GATTTTCGTAACGTAAGACGCAGTCTCTCTTTTGTATTCC	amiRAT3G60720
G-33051	GACTGCGTCTTACGTTACGAAAATCAAAGAGAATCAATGA	amiRAT3G60720

Continued on next page

Table 2 – continued from previous page

Oligo	Sequence	Purpose
G-33052	GACTACGTCTTACGTAACGAAATTCACAGGTCGTGATATG	amiRAT3G60720
G-33053	GAATTTCGTTACGTAAGACGTAGTCTACATATATATTCCT	amiRAT3G60720
G-33054	GATAACATGTATAATGCATGCCGTCTCTCTTTTGTATTCC	amiRAT3G60720
G-33055	GACGGCATGCATTATACATGTTATCAAAGAGAATCAATGA	amiRAT3G60720
G-33056	GACGACATGCATTATTCATGTTTTCACAGGTCGTGATATG	amiRAT3G60720
G-33057	GAAAACATGAATAATGCATGTCGTCTACATATATATTCCT	amiRAT3G60720
G-33058	GATATTAAATTCGACGGCGCCCCTCTCTCTTTTGTATTCC	amiRAT3G60870
G-33059	GAGGGGCGCCGTCGAATTTAATATCAAAGAGAATCAATGA	amiRAT3G60870
G-33060	GAGGAGCGCCGTCGATTTTAATTTCACAGGTCGTGATATG	amiRAT3G60870
G-33061	GAAATTAAAATCGACGGCGCTCCTCTACATATATATTCCT	amiRAT3G60870
G-33062	GATTGACGTTTGTAATGGCCCGGTCTCTCTTTTGTATTCC	amiRAT3G60870
G-33063	GACCGGGCCATTACAAACGTCAATCAAAGAGAATCAATGA	amiRAT3G60870
G-33064	GACCAGGCCATTACATACGTCATTCACAGGTCGTGATATG	amiRAT3G60870
G-33065	GAATGACGTATGTAATGGCCTGGTCTACATATATATTCCT	amiRAT3G60870
G-33066	GATAACAATTTACAGTATGGCCCTCTCTCTTTTGTATTCC	amiRAT3G60880
G-33067	GAGGGCCATACTGTAAATTGTTATCAAAGAGAATCAATGA	amiRAT3G60880
G-33068	GAGGACCATACTGTATATTGTTTTCACAGGTCGTGATATG	amiRAT3G60880
G-33069	GAAAACAATATACAGTATGGTCCTCTACATATATATTCCT	amiRAT3G60880
G-33070	GATTCTAAGGGACCTTATGCCGTTCTCTCTTTTGTATTCC	amiRAT3G60880
G-33071	GAACGGCATAAGGTCCCTTAGAATCAAAGAGAATCAATGA	amiRAT3G60880
G-33072	GAACAGCATAAGGTCGCTTAGATTCACAGGTCGTGATATG	amiRAT3G60880
G-33073	GAATCTAAGCGACCTTATGCTGTTCTACATATATATTCCT	amiRAT3G60880
G-33074	GATTTTGATATGGTACGAAGCACTCTCTCTTTTGTATTCC	amiRAT3G60890
G-33075	GAGTGCTTCGTACCATATCAAAATCAAAGAGAATCAATGA	amiRAT3G60890
G-33076	GAGTACTTCGTACCAAATCAAATTCACAGGTCGTGATATG	amiRAT3G60890
G-33077	GAATTTGATTTGGTACGAAGTACTCTACATATATATTCCT	amiRAT3G60890
G-33078	GATTTATCACACAAAGCGAACTGTCTCTCTTTTGTATTCC	amiRAT3G60890
G-33079	GACAGTTCGCTTTGTGTGATAAATCAAAGAGAATCAATGA	amiRAT3G60890
G-33080	GACAATTCGCTTTGTCTGATAATTCACAGGTCGTGATATG	amiRAT3G60890
G-33081	GAATTATCAGACAAAGCGAATTGTCTACATATATATTCCT	amiRAT3G60890
G-33082	GATATTCCAAATTGTCACGTCTCTCTCTCTTTTGTATTCC	amiRAT3G60760
G-33083	GAGAGACGTGACAATTTGGAATATCAAAGAGAATCAATGA	amiRAT3G60760
G-33084	GAGAAACGTGACAATATGGAATTTCACAGGTCGTGATATG	amiRAT3G60760
G-33085	GAAATTCCATATTGTCACGTTTCTCTACATATATATTCCT	amiRAT3G60760
G-33086	GATCTGAAATGACAATAGTCCGATCTCTCTTTTGTATTCC	amiRAT3G60760
G-33087	GATCGGACTATTGTCATTTCAGATCAAAGAGAATCAATGA	amiRAT3G60760
G-33088	GATCAGACTATTGTCTTTTCAGTTCACAGGTCGTGATATG	amiRAT3G60760
G-33089	GAACTGAAAAGACAATAGTCTGATCTACATATATATTCCT	amiRAT3G60760
G-36778	AACAGGTCTCAACCTGGTTCGTCGTCCTTTATCCA	MAP65-4 promoter
G-36779	AACAGGTCTCTTGTTTTCATTCCATATTTCCTGATATCATCA	MAP65-4 promoter
G-36780	AACAGGTCTCAGGCTCAACAATGGGAGAGACTGAGGATG	MAP65-4 CDS
G-36781	ATCAGTCTCTTCAGCAGC	MAP65-4 CDS
G-37051	GCTGAAGAGACTGATCTTTCGC	MAP65-4 CDS
G-36783	CTTGGCCTCTGTTAAGTG	MAP65-4 CDS
G-36784	CAGAGGCCAAGAGAGAG	MAP65-4 CDS
G-36785	AACAGGTCTCTCTGAGCAAAAACCGGCCCTAACC	MAP65-4 CDS
G-37554	TTTTTCTGCACGCTTCAATG	MAP65-4 RT-PCR
G-37553	GGAAGAAGCTTGAGCTTGAGG	MAP65-4 RT-PCR
G-27290	GCCATCCAAGCTGTTCTCTC	ACTIN2 RT-PCR
G-27291	GCTCGTAGTCAACAGCAACAA	ACTIN2 RT-PCR
G-18783	ATGAGCCCAGAACGACG	BASTA RT-PCR
G-37569	GTCCAGTCGTAGGCGTTGC	BASTA RT-PCR
G-0426	TTGGAGAGAACACGGGGGACG	35S promoter, for testing presence of amiRNA transgene in plants
G-8732	AACTCAGTAGGATTCTGGTGTGTGC	rbcs terminator, for testing presence of amiRNA transgene in plants

A.3 ARTIFICIAL MIRNA CONSTRUCTS USED IN CANDIDATE GENE APPROACH

Table 3: *Artificial miRNA constructs used in candidate gene approach*

Plasmid name	amiRNA target	Vector backbone
pSM1	AT3G60440	pJLblue_rev
pSM2	AT3G60440	pGreenIIS_Basta
pSM3	AT3G60440	pGreenIIS_Basta
pSM4	AT3G60580	pGreenIIS_Basta
pSM5	AT3G60630	pGreenIIS_Basta
pSM6	AT3G60630	pGreenIIS_Basta
pSM7	AT3G60710	pJLblue_rev
pSM8	AT3G60710	pGreenIIS_Basta
pSM9	AT3G60710	pGreenIIS_Basta
pSM10	AT3G60710	pJLblue_rev
pSM11	AT3G60710	pGreenIIS_Basta
pSM12	AT3G60710	pGreenIIS_Basta
pSM13	AT3G60720	pGreenIIS_Basta
pSM14	AT3G60740	pGEM-Teasy
pSM15	AT3G60740	pGreenIIS_Basta
pSM16	AT3G60750	pJLblue_rev
pSM17	AT3G60750	pGreenIIS_Basta
pSM18	AT3G60760	pGreenIIS_Basta
pSM19	AT3G60840	pJLblue_rev
pSM20	AT3G60840	pGreenIIS_Basta
pSM21	AT3G60840	pGreenIIS_Basta
pSM22	AT3G60840	pJLblue_rev
pSM23	AT3G60840	pGreenIIS_Basta
pSM24	AT3G60840	pGreenIIS_Basta
pSM25	AT3G60860	pGEM-Teasy
pSM26	AT3G60860	pGreenIIS_Basta
pSM27	AT3G60880	pGreenIIS_Basta
pSM28	AT3G60890	pGreenIIS_Basta
pSM29	AT3G60900	pGEM-Teasy
pSM30	AT3G60910	pJLblue_rev
pSM31	AT3G60910	pGreenIIS_Basta
pSM32	AT3G60910	pJLblue_rev
pSM33	AT3G60910	pGreenIIS_Basta
pSM34	AT3G60920	pJLblue_rev
pSM35	AT3G60920	pGreenIIS_Basta
pSM36	AT3G60920	pGreenIIS_Basta
pSM37	AT3G60940	pGEM-Teasy
pSM38	AT3G60940	pGreenIIS_Basta
pSM39	AT3G60960	pGreenIIS_Basta
pSM40	AT3G60960	pGreenIIS_Basta
pSM41	AT3G60961	pJLblue_rev
pSM42	AT3G60961	pGreenIIS_Basta
pSM43	AT3G60961	pJLblue_rev
pSM44	AT3G60961	pGreenIIS_Basta
pSM45	AT3G60966	pGEM-Teasy
pSM46	AT3G60966	pGreenIIS_Basta
pSM47	AT3G61028	pGreenIIS_Basta
pSM48	AT3G61028	pGreenIIS_Basta
pSM49	AT3G61035	pGEM-Teasy

Continued on next page

Table 3 – continued from previous page

Plasmid name	amiRNA target	Vector backbone
pSM50	AT3G61060	pJLblue_rev
pSM51	AT3G61060	pGreenIIS_Basta
pSM52	AT3G61060	pGreenIIS_Basta
pSM53	AT3G61060	pJLblue_rev
pSM54	AT3G61070	pJLblue_rev
pSM55	AT3G61070	pGreenIIS_Basta
pSM56	AT3G61120	pJLblue_rev
pSM57	AT3G61120	pGreenIIS_Basta
pSM58	AT3G61160	pGEM-Teasy
pSM59	AT3G60790	pJLblue_rev
pSM60	AT3G60790	pGreenIIS_Basta
pSM61	AT3G60790	pGreenIIS_Basta
pSM62	AT3G60830	pGEM-Teasy
pSM63	AT3G60830	pGreenIIS_Basta
pSM64	AT3G60970	pGEM-Teasy
pSM65	AT3G61010	pGEM-Teasy
pSM66	AT3G60750	pGEM-Teasy
pSM67	AT3G60960	pGreenIIS_Basta
pSM68	AT3G60960	pGreenIIS_Basta

A.4 GENOMIC CONTRUCTS

Table 4: *Genomic contructs*

Plasmid name	Alias	Vector backbone
pSM108	pBMAP65:BMAP65:BASTA	pGreenIIS
pSM138	pBMAP65:BMAP65:BASTA	pGreenIIS
pSM141	pCMAP65:BMAP65:BASTA	pGreenIIS
pSM147	35S:BMAP65:BASTA	pGreenIIS
pSM150	35S:BMAP65:LinkermCherry:BASTA	pGreenIIS
pSM177	pBMAP65-4 entry	pUC19
pSM178	pCMAP65-4 entry	pUC19
pSM179	pKMAP65-4 entry	pUC19
pSM180	BMAP65-4 CDS entry	pUC19
pSM181	CMAP65-4 CDS entry	pUC19
pSM200	KMAP65-4 CDS IN pCR8 GW TOPO - reverse orientation	pCR8/GW-TOPO

A.5 STATISTICAL ANALYSES (CHAPTER 3)

Adjusted p-values after a post-hoc ANOVA Tukeys HSD test for multiple comparisons between transcript levels of various genes in UU and KM F1 hybrids grown at different temperatures.

Table 5: *Statistical Analyses (Chapter 3)*

Genotype	Transcript	Plant age	Temperatures compared	Adjusted p-value
UU	PR1	10 DAS	16-14	0.9996
			18-14	0.9825
			20-14	0.751
			22-14	0.0583
			24-14	0.0144
			26-14	0.0368
			18-16	0.9996

Continued on next page

Table 5 – continued from previous page

Genotype	Transcript	Plant age	Temperatures compared	Adjusted p-value
			20-16	0.9217
			22-16	0.115
			24-16	0.0295
			26-16	0.0739
			20-18	0.9909
			22-18	0.217
			24-18	0.0599
			26-18	0.1442
			22-20	0.5414
			24-20	0.1918
			26-20	0.4001
			24-22	0.9841
			26-22	1
			26-24	0.9982
UU	PR1	16 DAS	16-14	0.9999
			18-14	0.874
			20-14	0.7923
			22-14	0
			24-14	0
			26-14	0
			18-16	0.9587
			20-16	0.9113
			22-16	0
			24-16	0
			26-16	0
			20-18	1
			22-18	0
			24-18	0
			26-18	0
			22-20	0
			24-20	0
			26-20	0
			24-22	0.6812
			26-22	0.027
			26-24	0.3774
KM	PR1	10DAS	16-14	0.8265
			18-14	0.6604
			20-14	1
			22-14	0.0367
			24-14	0.0058
			26-14	0
			18-16	0.9999
			20-16	0.7328
			22-16	0.0033
			24-16	0.0006
			26-16	0
			20-18	0.5541
			22-18	0.0019
			24-18	0.0003
			26-18	0
			22-20	0.0508
			24-20	0.0081
			26-20	0
			24-22	0.942
			26-22	0

Continued on next page

Table 5 – continued from previous page

Genotype	Transcript	Plant age	Temperatures compared	Adjusted p-value
			26-24	0
KM	PR1	16 DAS	16-14	0.9997
			18-14	0.998
			20-14	0.6565
			22-14	0.0053
			24-14	0.0008
			26-14	0
			18-16	1
			20-16	0.8535
			22-16	0.0105
			24-16	0.0016
			26-16	0
			20-18	0.9101
			22-18	0.0138
			24-18	0.0021
			26-18	0
			22-20	0.1027
			24-20	0.016
			26-20	0
			24-22	0.9349
			26-22	0
			26-24	0.0002
KM	EDS1	10 DAS	16-14	1
			18-14	0.9998
			20-14	0.9997
			22-14	0.4191
			24-14	0.2853
			26-14	0
			18-16	0.9964
			20-16	0.9955
			22-16	0.3098
			24-16	0.2029
			26-16	0
			20-18	1
			22-18	0.6176
			24-18	0.4539
			26-18	0.0001
			22-20	0.6331
			24-20	0.4684
			26-20	0.0001
			24-22	0.9999
			26-22	0.0014
			26-24	0.0023
KM	EDS1	16 DAS	16-14	0.4537
			18-14	0.704
			20-14	0.1895
			22-14	0.1598
			24-14	0.0381
			26-14	0.0001
			18-16	0.9993
			20-16	0.9947
			22-16	0.0045
			24-16	0.001
			26-16	0
			20-18	0.9296

Continued on next page

Table 5 – continued from previous page

Genotype	Transcript	Plant age	Temperatures compared	Adjusted p-value
			22-18	0.01
			24-18	0.0022
			26-18	0
			22-20	0.0015
			24-20	0.0004
			26-20	0
			24-22	0.9772
			26-22	0.0135
			26-24	0.0606
KM	EDS5	10 DAS	16-14	0.9999
			18-14	0.8864
			20-14	0.761
			22-14	0.0048
			24-14	0.0018
			26-14	0
			18-16	0.9669
			20-16	0.8944
			22-16	0.0081
			24-16	0.0029
			26-16	0
			20-18	1
			22-18	0.0414
			24-18	0.0149
			26-18	0
			22-20	0.0671
			24-20	0.0245
			26-20	0
			24-22	0.997
			26-22	0.0007
			26-24	0.0019
KM	EDS5	16 DAS	16-14	0.3348
			18-14	1
			20-14	0.9957
			22-14	0
			24-14	0
			26-14	0
			18-16	0.2547
			20-16	0.662
			22-16	0
			24-16	0
			26-16	0
			20-18	0.9818
			22-18	0.0001
			24-18	0
			26-18	0
			22-20	0
			24-20	0
			26-20	0
			24-22	0.2088
			26-22	0.0004
			26-24	0.041
KM	PAD4	10 DAS	16-14	0.9665
			18-14	0.9999
			20-14	0.9925
			22-14	0.1286

Continued on next page

Table 5 – continued from previous page

Genotype	Transcript	Plant age	Temperatures compared	Adjusted p-value
			24-14	0.2313
			26-14	0.0001
			18-16	0.8866
			20-16	0.7027
			22-16	0.0265
			24-16	0.0515
			26-16	0
			20-18	0.9997
			22-18	0.2047
			24-18	0.3498
			26-18	0.0001
			22-20	0.3537
			24-20	0.5511
			26-20	0.0001
			24-22	0.9997
			26-22	0.0062
			26-24	0.0032
KM	PAD4	16 DAS	16-14	0.9229
			18-14	0.8826
			20-14	0.5341
			22-14	0.0672
			24-14	0.0003
			26-14	0
			18-16	1
			20-16	0.9838
			22-16	0.0095
			24-16	0.0001
			26-16	0
			20-18	0.993
			22-18	0.0077
			24-18	0
			26-18	0
			22-20	0.0024
			24-20	0
			26-20	0
			24-22	0.0841
			26-22	0.0002
			26-24	0.0391
KM	FRK1	10 DAS	16-14	0.9997
			18-14	0.9983
			20-14	0.9957
			22-14	0.0183
			24-14	0.0238
			26-14	0
			18-16	1
			20-16	1
			22-16	0.0355
			24-16	0.0462
			26-16	0
			20-18	1
			22-18	0.0456
			24-18	0.0591
			26-18	0
			22-20	0.0539
			24-20	0.0698

Continued on next page

Table 5 – continued from previous page

Genotype	Transcript	Plant age	Temperatures compared	Adjusted p-value
			26-20	0
			24-22	1
			26-22	0.0001
			26-24	0
KM	FRK1	16 DAS	16-14	1
			18-14	0.9972
			20-14	1
			22-14	0.0557
			24-14	0.0011
			26-14	0
			18-16	0.9805
			20-16	0.9985
			22-16	0.086
			24-16	0.0017
			26-16	0
			20-18	0.9999
			22-18	0.0204
			24-18	0.0004
			26-18	0
			22-20	0.0356
			24-20	0.0007
			26-20	0
			24-22	0.3582
			26-22	0.0029
			26-24	0.1449
KM	LOX2	10 DAS	16-14	0.9585
			18-14	0.9946
			20-14	1
			22-14	0.9606
			24-14	0.594
			26-14	0.2943
			18-16	0.7012
			20-16	0.9226
			22-16	0.525
			24-16	0.1693
			26-16	0.0639
			20-18	0.9987
			22-18	0.9999
			24-18	0.909
			26-18	0.624
			22-20	0.9823
			24-20	0.6769
			26-20	0.3579
			24-22	0.9782
			26-22	0.793
			26-24	0.9966
KM	LOX2	16 DAS	16-14	1
			18-14	0.9793
			20-14	1
			22-14	0.9535
			24-14	0.9149
			26-14	0.9849
			18-16	0.967
			20-16	1
			22-16	0.9329

Continued on next page

Table 5 – continued from previous page

Genotype	Transcript	Plant age	Temperatures compared	Adjusted p-value
			24-16	0.939
			26-16	0.9749
			20-18	0.9869
			22-18	1
			24-18	0.4971
			26-18	1
			22-20	0.9673
			24-20	0.8904
			26-20	0.9908
			24-22	0.4149
			26-22	1
			26-24	0.5255
KM	PDF1.2	10 DAS	16-14	0.9526
			18-14	1
			20-14	0.4475
			22-14	0.119
			24-14	0.9882
			26-14	1
			18-16	0.9375
			20-16	0.9345
			22-16	0.4862
			24-16	1
			26-16	0.868
			20-18	0.4147
			22-18	0.1072
			24-18	0.9822
			26-18	1
			22-20	0.9666
			24-20	0.8474
			26-20	0.3164
			24-22	0.3602
			26-22	0.0754
			26-24	0.9468
KM	PDF1.2	16 DAS	16-14	0.9992
			18-14	0.3039
			20-14	0.0215
			22-14	0.0002
			24-14	0.0124
			26-14	0.0348
			18-16	0.532
			20-16	0.0482
			22-16	0.0005
			24-16	0.0281
			26-16	0.0769
			20-18	0.7004
			22-18	0.0131
			24-18	0.5261
			26-18	0.8381
			22-20	0.2039
			24-20	0.9999
			26-20	1
			24-22	0.3173
			26-22	0.1333
			26-24	0.9969

Table 6: *Statistical Analyses (Chapter 4)*

Dataset	Fligner-Killeen	Kruskal-Wallis	Comparison	Tukey's HSD
Anthocyanin accumulation	χ^2=87.4052 df=4 p-value=2.2e-16	χ^2=37.9924 df=4 p-value=1.125e-07	BG-5 - Col-0 BG-5 - F1 BG-5 - F2 BG-5 - Kro-0 Col-0 - F1 Col-0 - F2 Col-0 - Kro-0 F1 - F2 F1 - Kro-0 F2 - Kro-0	0.00299 0.00716 0.01016 0.13396 0.00004 0.00000 0.00025 0.00344 0.99834 0.23850
Main stem height	χ^2=31.8527 df=3 p-value=5.621e-07	χ^2=16.3063 df=3 p-value=0.0009813	BG-5 - F1 BG-5 - Kro-0 BG-5 - F2 F1 - Kro-0 F1 - F2 Kro-0 - F2	0.00000 0.62908 0.00844 0.00000 0.99784 0.00731
# of RI branches	χ^2=25.1144 df=3 p-value=1.461e-05	χ^2=17.3854 df=3 p-value=0.0005888	BG-5 - F1 BG-5 - Kro-0 BG-5 - F2 F1 - Kro-0 F1 - F2 Kro-0 - F2	0.00111 0.01184 0.08189 0.27376 0.00197 0.43870
# of RII branches	χ^2=3.3144 df=3 p-value=0.3456	χ^2=26.7001 df=3 p-value=6.804e-06	BG-5 - F1 BG-5 - Kro-0 BG-5 - F2 F1 - Kro-0 F1 - F2 Kro-0 - F2	0.00000 0.18921 0.85674 0.00151 0.00024 0.61736
# of RIII branches	χ^2=43.0081 df=3 p-value=2.451e-09	χ^2=22.6907 df=3 p-value=4.684e-05	BG-5 - F1 BG-5 - Kro-0 BG-5 - F2 F1 - Kro-0 F1 - F2 Kro-0 - F2	0.01202 1.00000 0.00760 0.01186 0.04384 0.00743
# of CI branches	χ^2=4.5662 df=3 p-value=0.2065	χ^2=40.1316 df=3 p-value=9.992e-09	BG-5 - F1 BG-5 - Kro-0 BG-5 - F2 F1 - Kro-0 F1 - F2 Kro-0 - F2	0.00685 0.00162 0.00000 0.22081 0.00004 0.14201
# of CII branches	χ^2=2.5042 df=3 p-value=0.4745	χ^2=32.1157 df=3 p-value=4.948e-07	BG-5 - F1 BG-5 - Kro-0 BG-5 - F2 F1 - Kro-0 F1 - F2 Kro-0 - F2	0.00451 0.62153 0.00799 0.00000 0.00001 0.20396
# of CIII branches	χ^2=24.3448 df=3 p-value=2.116e-05	χ^2=33.2684 df=3 p-value=2.827e-07	BG-5 - F1 BG-5 - Kro-0 BG-5 - F2 F1 - Kro-0	0.00000 0.99999 0.11722 0.00166

Continued on next page

Table 6 – continued from previous page

Dataset	Fligner-Killeen	Kruskal-Wallis	Comparison	Tukey's HSD
			F1 - F2	0.00003
			Kro-0 - F2	0.35768
Silique Number	χ^2=5.3121	χ^2=11.7945	BG-5 - F1	0.40952
	df=3	df=3	BG-5 - Kro-0	0.38749
	p-value=0.1503	p-value=0.008121	BG-5 - F2	0.12516
			F1 - Kro-0	0.10197
			F1 - F2	0.00377
			Kro-0 - F2	0.29230
Biomass	χ^2=19.5452	χ^2=28.316	BG-5 - F1	0.65870
	df=3	df=3	BG-5 - Kro-0	0.00005
	p-value=0.0002109	p-value=3.118e-06	BG-5 - F2	0.00463
			F1 - Kro-0	0.00192
			F1 - F2	0.00296
			Kro-0 - F2	0.39733
MAP65-4	χ^2=0.2232	χ^2=9.4114	BG-5 - F1	0.78571
gene expression	df=2	df=2	BG-5 - Kro-0	0.00000
	p-value=0.8944	p-value=0.009043	F1 - Kro-0	0.00000

A.7 SNPs in the BG-5 mapping interval

Table 7: *SNPs in the BG-5 mapping interval*

Positon	Reference base	Alternative base	Read support	Type of DNA	Gene ID	Syn or Nonsyn?	Ref AA	Changed AA	Codon	Degeneracy of codon position
22338184	C	A	5	CDS	AT3G60440	Nonsyn	S	*	TAG	2
22345606	T	C	4	CDS	AT3G60470	Nonsyn	V	A	GCT	0
22345759	G	A	4	CDS	AT3G60470	Nonsyn	R	Q	CAG	0
22394034	T	G	9	CDS	AT3G60580	Nonsyn	F	V	GTT	0
22394439	A	-	6	CDS	AT3G60580	Nonsyn	N	X	-A-	-
22394441	T	-	6	CDS	AT3G60580	Nonsyn	N	X	-A-	-
22394443	A	C	6	CDS	AT3G60580	Nonsyn	K	T	ACA	0
22394445	G	-	6	CDS	AT3G60580	Nonsyn	E	X	#NAME?	-
22394748	G	A	6	CDS	AT3G60580	Nonsyn	V	I	ATA	0
22410886	G	T	5	CDS	AT3G60630	Nonsyn	C	*	GAA	2
22441176	T	C	4	CDS	AT3G60710	Nonsyn	C	R	CGT	0
22458704	C	A	5	CDS	AT3G60760	Nonsyn	R	I	GAG	0
22466005	T	A	9	CDS	AT3G60790	Nonsyn	V	D	GAT	0
22466007	A	T	9	CDS	AT3G60790	Nonsyn	I	F	TTC	0
22479213	C	T	7	CDS	AT3G60840	Nonsyn	R	K	AGG	0
22505634	T	G	6	CDS	AT3G60920	Nonsyn	E	D	CGA	4
22506157	A	T	6	CDS	AT3G60920	Nonsyn	M	K	AGG	0
22508469	A	G	4	CDS	AT3G60920	Nonsyn	C	R	AAC	0
22509562	T	A	11	CDS	AT3G60920	Nonsyn	E	V	AAA	0
22512191	T	C	7	CDS	AT3G60920	Nonsyn	S	G	AAA	0
22512380	G	A	6	CDS	AT3G60920	Nonsyn	P	S	ACA	0
22512381	T	A	7	CDS	AT3G60920	Nonsyn	E	D	AGA	2
22552056	C	T	6	CDS	AT3G60961	Nonsyn	T	I	ATC	0
22558498	G	C	7	CDS	AT3G60970	Nonsyn	E	Q	CAG	0
22560837	C	A	7	CDS	AT3G60970	Nonsyn	T	K	AAA	0

Continued on next page

Table 7 – continued from previous page

Positon	Reference base	Alternative base	Read support	Type of DNA	Gene ID	Syn or Nonsyn?	Ref AA	Changed AA	Codon	Degeneracy of codon position
22571960	G	A	12	CDS	AT3G61010	Nonsyn	R	*	GAA	0
22582981	C	T	7	CDS	AT3G61028	Nonsyn	E	K	GGG	0
22603220	T	A	11	CDS	AT3G61060	Nonsyn	Y	N	AAC	0
22603297	G	T	7	CDS	AT3G61060	Nonsyn	E	D	GAT	2
22603330	C	A	7	CDS	AT3G61060	Nonsyn	F	L	TTA	2
22603370	T	G	8	CDS	AT3G61060	Nonsyn	L	V	GTG	0
22603373	C	A	8	CDS	AT3G61060	Nonsyn	P	T	ACT	0
22603376	G	T	8	CDS	AT3G61060	Nonsyn	A	S	TCG	0
22603385	C	T	6	CDS	AT3G61060	Nonsyn	R	C	TGT	0
22623373	G	A	6	CDS	AT3G61130	Nonsyn	A	T	ACA	0
22641858	C	G	5	CDS	AT3G61172	Nonsyn	S	T	ACG	0
22682325	T	C	4	CDS	AT3G61280	Nonsyn	V	A	GCG	0
22682750	G	A	4	CDS	AT3G61280	Nonsyn	D	N	AAT	0
22684581	G	C	6	CDS	AT3G61290	Nonsyn	E	Q	CAA	0
22686250	A	T	6	CDS	AT3G61290	Nonsyn	K	N	AAT	2
22688097	T	C	4	CDS	AT3G61300	Nonsyn	S	P	CCT	0
22329843	T	C	6	CDS	AT3G60400	Syn	L	L	CTG	2
22330529	T	C	8	CDS	AT3G60400	Syn	D	D	GAC	2
22349667	G	A	5	CDS	AT3G60490	Syn	V	V	GTA	4
22355168	T	G	4	CDS	AT3G60500	Syn	T	T	ACG	4
22380396	C	T	5	CDS	AT3G60550	Syn	L	L	TTA	2
22394453	G	A	8	CDS	AT3G60580	Syn	V	V	GTA	4
22461047	T	C	6	CDS	AT3G60770	Syn	K	K	AGG	2
22486661	G	A	8	CDS	AT3G60860	Syn	L	L	TTA	2
22487096	C	T	6	CDS	AT3G60860	Syn	D	D	GAT	2
22502288	C	A	9	CDS	AT3G60910	Syn	S	S	TCA	4

Continued on next page

Table 7 – continued from previous page

Positon	Reference base	Alternative base	Read support	Type of DNA	Gene ID	Syn or Nonsyn?	Ref AA	Changed AA	Codon	Degeneracy of codon position
22503457	G	A	50	CDS	AT3G60920	Syn	T	T	ACG	4
22507086	A	G	5	CDS	AT3G60920	Syn	D	D	CGA	4
22511200	G	A	4	CDS	AT3G60920	Syn	L	L	GAA	0
22558038	T	A	8	CDS	AT3G60970	Syn	I	I	ATA	2
22558462	A	C	10	CDS	AT3G60970	Syn	R	R	CGA	2
22558506	C	T	7	CDS	AT3G60970	Syn	F	F	TTT	2
22559130	T	A	6	CDS	AT3G60970	Syn	T	T	ACA	4
22560416	G	A	13	CDS	AT3G60970	Syn	K	K	AAA	2
22560992	G	A	9	CDS	AT3G60970	Syn	L	L	CTA	4
22566231	A	G	7	CDS	AT3G60980	Syn	L	L	AAC	0
22603234	C	T	11	CDS	AT3G61060	Syn	L	L	CTT	4
22603252	T	G	9	CDS	AT3G61060	Syn	P	P	CCG	4
22623172	C	T	4	CDS	AT3G61130	Syn	T	T	ACT	4
22623926	A	G	7	CDS	AT3G61130	Syn	L	L	TTG	2
22623962	G	A	10	CDS	AT3G61130	Syn	R	R	CGA	4
22624431	T	C	5	CDS	AT3G61130	Syn	V	V	GTC	4
22624724	T	C	5	CDS	AT3G61130	Syn	R	R	CGC	4
22624796	A	G	6	CDS	AT3G61130	Syn	L	L	CTG	4
22624955	C	T	14	CDS	AT3G61130	Syn	V	V	GTT	4
22627644	T	C	4	CDS	AT3G61140	Syn	L	L	CTG	2
22640164	G	A	8	CDS	AT3G61170	Syn	T	T	ACG	4
22679873	A	G	4	CDS	AT3G61270	Syn	G	G	GGG	4
22435142	A	G	6	five_prime_UTR	AT3G60690					
22442028	A	G	9	five_prime_UTR	AT3G60720					
22603151	T	A	7	five_prime_UTR	AT3G61060					
22603156	G	A	8	five_prime_UTR	AT3G61060					

Continued on next page

Table 7 – continued from previous page

Positon	Reference base	Alternative base	Read support	Type of DNA	Gene ID	Syn or Nonsyn?	Ref AA	Changed AA	Codon	Degeneracy of codon position
22636011	T	-	8	five_prime_UTR	AT3G61160					
22676727	T	C	13	five_prime_UTR	AT3G61260					
22681005	A	T	12	five_prime_UTR	AT3G61280					
22681006	A	T	11	five_prime_UTR	AT3G61280					
22681069	T	C	7	five_prime_UTR	AT3G61280					
22692728	A	G	9	five_prime_UTR	AT3G61310					
22304007	G	A	7	intergenic						
22311492	A	T	13	intergenic						
22311573	G	A	15	intergenic						
22311839	T	A	9	intergenic						
22319518	A	G	11	intergenic						
22320468	T	G	9	intergenic						
22320469	T	C	8	intergenic						
22323418	G	A	6	intergenic						
22323707	T	A	16	intergenic						
22325236	T	A	6	intergenic						
22328578	T	A	7	intergenic						
22340671	C	T	5	intergenic						
22340679	A	G	5	intergenic						
22348736	G	A	6	intergenic						
22348771	G	C	7	intergenic						
22348773	T	-	6	intergenic						
22349177	A	-	9	intergenic						
22349178	T	-	9	intergenic						
22349179	A	-	9	intergenic						
22349180	T	-	9	intergenic						

Continued on next page

Table 7 – continued from previous page

Positon	Reference base	Alternative base	Read support	Type of DNA	Gene ID	Syn or Nonsyn?	Ref AA	Changed AA	Codon	Degeneracy of codon position
22351654	A	T	4	intergenic						
22351808	A	G	10	intergenic						
22351810	G	T	10	intergenic						
22351851	A	-	9	intergenic						
22351852	C	-	9	intergenic						
22351853	G	-	9	intergenic						
22352061	C	T	4	intergenic						
22352815	T	A	7	intergenic						
22352824	A	T	7	intergenic						
22360715	T	C	9	intergenic						
22362587	A	G	10	intergenic						
22362829	A	G	15	intergenic						
22362842	T	C	13	intergenic						
22365106	A	G	5	intergenic						
22365192	A	G	5	intergenic						
22366360	T	C	5	intergenic						
22366509	T	A	7	intergenic						
22366658	T	C	11	intergenic						
22366735	T	C	13	intergenic						
22367034	G	C	8	intergenic						
22368218	T	C	4	intergenic						
22368481	A	G	8	intergenic						
22369021	C	T	4	intergenic						
22369129	C	T	5	intergenic						
22370592	C	T	9	intergenic						
22370645	C	T	9	intergenic						

Continued on next page

Table 7 – continued from previous page

Positon	Reference base	Alternative base	Read support	Type of DNA	Gene ID	Syn or Nonsyn?	Ref AA	Changed AA	Codon	Degeneracy of codon position
22371786	G	C	9	intergenic						
22371790	T	C	9	intergenic						
22371944	G	A	9	intergenic						
22372045	C	G	11	intergenic						
22372066	A	G	9	intergenic						
22373041	G	A	6	intergenic						
22373067	A	T	6	intergenic						
22373068	A	T	6	intergenic						
22373074	G	T	6	intergenic						
22374436	G	T	4	intergenic						
22377257	A	G	4	intergenic						
22377290	C	T	4	intergenic						
22377587	T	A	4	intergenic						
22377607	T	C	5	intergenic						
22377617	G	A	5	intergenic						
22377669	C	T	7	intergenic						
22377705	C	-	4	intergenic						
22377707	T	-	4	intergenic						
22377708	T	-	4	intergenic						
22377726	C	T	4	intergenic						
22377996	C	T	10	intergenic						
22378048	T	A	8	intergenic						
22378073	T	A	4	intergenic						
22378074	A	T	4	intergenic						
22378085	A	G	4	intergenic						
22378092	T	C	5	intergenic						

Continued on next page

Table 7 – continued from previous page

Positon	Reference base	Alternative base	Read support	Type of DNA	Gene ID	Syn or Nonsyn?	Ref AA	Changed AA	Codon	Degeneracy of codon position
22378200	T	C	10	intergenic						
22378223	G	A	10	intergenic						
22378232	G	A	9	intergenic						
22378264	T	C	11	intergenic						
22378295	C	T	13	intergenic						
22378307	A	-	13	intergenic						
22379001	C	-	5	intergenic						
22379304	G	T	5	intergenic						
22379510	T	C	6	intergenic						
22381870	T	C	7	intergenic						
22382012	T	C	15	intergenic						
22382013	G	A	15	intergenic						
22393039	A	G	7	intergenic						
22395695	G	C	9	intergenic						
22396025	C	T	4	intergenic						
22396353	A	T	9	intergenic						
22396440	T	A	6	intergenic						
22397615	T	-	5	intergenic						
22397626	T	A	5	intergenic						
22399947	T	A	7	intergenic						
22405967	C	A	5	intergenic						
22406140	C	A	8	intergenic						
22412941	C	G	7	intergenic						
22413260	A	G	11	intergenic						
22413261	A	T	11	intergenic						
22413435	G	A	7	intergenic						

Continued on next page

Table 7 – continued from previous page

Positon	Reference base	Alternative base	Read support	Type of DNA	Gene ID	Syn or Nonsyn?	Ref AA	Changed AA	Codon	Degeneracy of codon position
22413649	T	-	7	intergenic						
22414546	A	T	7	intergenic						
22414965	T	C	7	intergenic						
22415295	A	T	4	intergenic						
22415355	C	T	8	intergenic						
22415370	T	G	10	intergenic						
22415527	C	-	6	intergenic						
22415528	G	A	6	intergenic						
22417801	C	T	7	intergenic						
22418368	G	T	12	intergenic						
22424015	A	-	7	intergenic						
22424020	C	-	7	intergenic						
22424052	T	A	19	intergenic						
22424053	T	A	19	intergenic						
22424163	T	A	13	intergenic						
22424223	C	A	18	intergenic						
22424231	A	C	20	intergenic						
22424237	A	-	18	intergenic						
22424238	A	G	18	intergenic						
22424297	C	A	4	intergenic						
22424373	T	A	5	intergenic						
22424378	G	A	5	intergenic						
22424394	T	G	8	intergenic						
22424408	A	-	10	intergenic						
22424409	A	-	10	intergenic						
22424481	C	G	6	intergenic						

Continued on next page

Table 7 – continued from previous page

Positon	Reference base	Alternative base	Read support	Type of DNA	Gene ID	Syn or Nonsyn?	Ref AA	Changed AA	Codon	Degeneracy of codon position
22426903	G	A	5	intergenic						
22427975	G	T	10	intergenic						
22428364	A	T	4	intergenic						
22428737	T	A	13	intergenic						
22433089	T	C	5	intergenic						
22433115	T	G	5	intergenic						
22433125	G	T	5	intergenic						
22433782	A	-	6	intergenic						
22433817	T	C	6	intergenic						
22433865	T	-	5	intergenic						
22433866	T	-	5	intergenic						
22436114	T	-	9	intergenic						
22437312	T	C	5	intergenic						
22439382	A	G	7	intergenic						
22439436	T	C	5	intergenic						
22439548	T	A	4	intergenic						
22439555	T	A	4	intergenic						
22439556	T	A	4	intergenic						
22439557	T	A	4	intergenic						
22441479	T	G	5	intergenic						
22441507	C	A	4	intergenic						
22444015	A	G	4	intergenic						
22444217	T	-	7	intergenic						
22444235	T	A	8	intergenic						
22444431	A	T	4	intergenic						
22444877	T	A	6	intergenic						

Continued on next page

Table 7 – continued from previous page

Positon	Reference base	Alternative base	Read support	Type of DNA	Gene ID	Syn or Nonsyn?	Ref AA	Changed AA	Codon	Degeneracy of codon position
22458187	T	-	7	intergenic						
22458299	A	G	10	intergenic						
22458390	C	G	8	intergenic						
22458427	A	C	9	intergenic						
22459337	C	A	7	intergenic						
22459575	A	T	6	intergenic						
22461864	G	C	5	intergenic						
22463953	A	G	12	intergenic						
22464001	T	C	7	intergenic						
22464091	G	T	6	intergenic						
22464093	G	T	6	intergenic						
22464385	T	-	5	intergenic						
22476450	G	T	9	intergenic						
22476478	A	C	6	intergenic						
22476574	A	-	9	intergenic						
22477118	G	A	5	intergenic						
22477122	T	A	6	intergenic						
22477170	G	A	8	intergenic						
22477289	T	C	12	intergenic						
22477348	G	A	12	intergenic						
22481275	A	G	7	intergenic						
22493068	C	A	5	intergenic						
22494627	A	G	6	intergenic						
22494638	G	A	6	intergenic						
22494670	A	G	8	intergenic						
22498833	C	T	8	intergenic						

Continued on next page

Table 7 – continued from previous page

Positon	Reference base	Alternative base	Read support	Type of DNA	Gene ID	Syn or Nonsyn?	Ref AA	Changed AA	Codon	Degeneracy of codon position
22513659	C	T	6	intergenic						
22513662	A	G	6	intergenic						
22513672	A	C	6	intergenic						
22514218	A	C	6	intergenic						
22514232	C	T	6	intergenic						
22514264	A	G	6	intergenic						
22514266	A	C	6	intergenic						
22514281	G	T	4	intergenic						
22514436	A	C	4	intergenic						
22514463	T	C	4	intergenic						
22514470	T	A	4	intergenic						
22514653	T	-	6	intergenic						
22514654	C	-	6	intergenic						
22514655	C	-	6	intergenic						
22514813	C	T	8	intergenic						
22515329	G	A	9	intergenic						
22515344	A	G	16	intergenic						
22515542	A	G	8	intergenic						
22515969	A	G	6	intergenic						
22515980	T	C	5	intergenic						
22516907	T	C	15	intergenic						
22520383	C	T	4	intergenic						
22520671	G	A	8	intergenic						
22520675	T	-	8	intergenic						
22520703	T	C	8	intergenic						
22520787	C	T	6	intergenic						

Continued on next page

Table 7 – continued from previous page

Positon	Reference base	Alternative base	Read support	Type of DNA	Gene ID	Syn or Nonsyn?	Ref AA	Changed AA	Codon	Degeneracy of codon position
22520811	C	T	9	intergenic						
22520882	G	A	8	intergenic						
22520937	T	C	4	intergenic						
22521063	G	T	4	intergenic						
22521145	C	T	4	intergenic						
22521177	A	G	4	intergenic						
22534244	G	T	5	intergenic						
22538780	G	A	9	intergenic						
22538919	G	T	7	intergenic						
22538981	A	G	11	intergenic						
22539007	G	A	11	intergenic						
22539018	T	G	13	intergenic						
22539019	A	T	13	intergenic						
22539043	G	A	12	intergenic						
22539064	C	A	5	intergenic						
22539073	A	G	5	intergenic						
22539146	G	A	10	intergenic						
22539237	C	A	17	intergenic						
22539437	T	A	7	intergenic						
22539470	A	G	6	intergenic						
22539520	C	T	6	intergenic						
22539749	A	G	8	intergenic						
22539953	G	A	14	intergenic						
22539980	A	G	15	intergenic						
22540404	C	T	5	intergenic						
22540788	G	A	10	intergenic						

Continued on next page

Table 7 – continued from previous page

Positon	Reference base	Alternative base	Read support	Type of DNA	Gene ID	Syn or Nonsyn?	Ref AA	Changed AA	Codon	Degeneracy of codon position
22540814	C	T	8	intergenic						
22540851	A	-	4	intergenic						
22541001	G	A	4	intergenic						
22541301	G	A	11	intergenic						
22554174	G	A	5	intergenic						
22554276	G	A	11	intergenic						
22555586	T	A	12	intergenic						
22561915	A	T	7	intergenic						
22563646	C	A	6	intergenic						
22563724	C	A	5	intergenic						
22567360	G	A	4	intergenic						
22567438	G	T	9	intergenic						
22568008	G	A	12	intergenic						
22570658	T	A	4	intergenic						
22570659	T	C	4	intergenic						
22570683	C	A	5	intergenic						
22570831	C	T	7	intergenic						
22570930	T	A	6	intergenic						
22577606	T	G	23	intergenic						
22577674	T	G	10	intergenic						
22577749	G	T	15	intergenic						
22577752	T	C	15	intergenic						
22577967	T	C	9	intergenic						
22577974	G	T	8	intergenic						
22577975	G	A	8	intergenic						
22578032	G	A	6	intergenic						

Continued on next page

Table 7 – continued from previous page

Positon	Reference base	Alternative base	Read support	Type of DNA	Gene ID	Syn or Nonsyn?	Ref AA	Changed AA	Codon	Degeneracy of codon position
22578250	G	C	8	intergenic						
22578251	T	A	8	intergenic						
22578277	A	T	6	intergenic						
22578363	A	T	12	intergenic						
22578379	G	A	13	intergenic						
22578510	G	T	13	intergenic						
22578556	A	T	13	intergenic						
22578840	T	C	17	intergenic						
22579936	C	-	5	intergenic						
22579937	C	-	4	intergenic						
22580007	A	G	10	intergenic						
22593939	A	C	4	intergenic						
22596943	A	C	18	intergenic						
22597041	A	C	4	intergenic						
22601557	A	G	10	intergenic						
22602380	G	T	7	intergenic						
22606823	C	G	7	intergenic						
22610204	T	C	4	intergenic						
22614222	T	-	4	intergenic						
22615936	A	G	6	intergenic						
22616258	A	-	8	intergenic						
22620578	C	T	7	intergenic						
22620590	A	-	6	intergenic						
22620748	A	T	5	intergenic						
22620893	G	C	11	intergenic						
22621039	A	-	9	intergenic						

Continued on next page

Table 7 – continued from previous page

Positon	Reference base	Alternative base	Read support	Type of DNA	Gene ID	Syn or Nonsyn?	Ref AA	Changed AA	Codon	Degeneracy of codon position
22621331	A	G	9	intergenic						
22621596	T	A	4	intergenic						
22625724	T	G	9	intergenic						
22625770	T	-	5	intergenic						
22625771	A	-	5	intergenic						
22625776	C	-	5	intergenic						
22625777	T	-	5	intergenic						
22625778	G	-	5	intergenic						
22625834	T	C	13	intergenic						
22625845	A	G	13	intergenic						
22625867	A	G	10	intergenic						
22625893	T	-	4	intergenic						
22625976	T	A	5	intergenic						
22625988	G	T	4	intergenic						
22626095	A	T	4	intergenic						
22626103	A	G	7	intergenic						
22626146	T	A	7	intergenic						
22641477	G	A	9	intergenic						
22642504	G	A	6	intergenic						
22643903	G	T	7	intergenic						
22645094	G	A	14	intergenic						
22653967	G	T	4	intergenic						
22657108	G	A	5	intergenic						
22660318	G	A	10	intergenic						
22660496	C	T	4	intergenic						
22661046	G	A	9	intergenic						

Continued on next page

Table 7 – continued from previous page

Positon	Reference base	Alternative base	Read support	Type of DNA	Gene ID	Syn or Nonsyn?	Ref AA	Changed AA	Codon	Degeneracy of codon position
22662559	A	G	7	intergenic						
22662814	A	G	5	intergenic						
22673003	G	T	8	intergenic						
22673996	C	T	6	intergenic						
22674109	A	G	6	intergenic						
22674110	G	T	6	intergenic						
22674175	A	G	5	intergenic						
22674270	T	-	4	intergenic						
22674780	C	T	8	intergenic						
22674881	G	A	7	intergenic						
22674884	A	G	7	intergenic						
22675087	T	C	11	intergenic						
22678042	G	T	12	intergenic						
22680940	G	T	7	intergenic						
22684091	A	-	5	intergenic						
22684259	T	C	7	intergenic						
22687278	G	A	5	intergenic						
22300343	A	C	8	intronic/noncoding	AT3G60330					
22315143	T	A	4	intronic/noncoding	AT3G60370					
22346284	A	C	6	intronic/noncoding	AT3G60470					
22346287	T	A	6	intronic/noncoding	AT3G60470					
22346319	A	-	4	intronic/noncoding	AT3G60470					
22346320	A	-	4	intronic/noncoding	AT3G60470					
22346321	G	-	4	intronic/noncoding	AT3G60470					
22346322	A	-	4	intronic/noncoding	AT3G60470					
22346323	C	T	4	intronic/noncoding	AT3G60470					

Continued on next page

Table 7 – continued from previous page

Positon	Reference base	Alternative base	Read support	Type of DNA	Gene ID	Syn or Nonsyn?	Ref AA	Changed AA	Codon	Degeneracy of codon position
22346335	T	C	6	intronic/noncoding	AT3G60470					
22346362	G	A	6	intronic/noncoding	AT3G60470					
22346378	C	T	5	intronic/noncoding	AT3G60470					
22346379	G	A	5	intronic/noncoding	AT3G60470					
22346390	T	C	5	intronic/noncoding	AT3G60470					
22346393	T	A	5	intronic/noncoding	AT3G60470					
22346396	G	-	6	intronic/noncoding	AT3G60470					
22346398	A	T	6	intronic/noncoding	AT3G60470					
22346425	T	C	6	intronic/noncoding	AT3G60470					
22346438	C	A	8	intronic/noncoding	AT3G60470					
22346493	T	G	8	intronic/noncoding	AT3G60470					
22401890	C	A	6	intronic/noncoding	AT3G60600					
22402155	T	A	4	intronic/noncoding	AT3G60600					
22402168	T	C	4	intronic/noncoding	AT3G60600					
22416044	A	G	18	intronic/noncoding	AT3G60640					
22416070	G	T	14	intronic/noncoding	AT3G60640					
22416632	A	T	9	intronic/noncoding	AT3G60640					
22416634	T	C	9	intronic/noncoding	AT3G60640					
22423068	A	C	7	intronic/noncoding	AT3G60660					
22425146	G	A	9	intronic/noncoding	AT3G60670					
22425852	T	A	8	intronic/noncoding	AT3G60670					
22438807	C	A	4	intronic/noncoding	AT3G60700					
22446590	A	T	10	intronic/noncoding	AT3G60730					
22446712	T	A	15	intronic/noncoding	AT3G60730					
22447692	G	C	11	intronic/noncoding	AT3G60740					
22448092	A	G	13	intronic/noncoding	AT3G60740					

Continued on next page

Table 7 – continued from previous page

Positon	Reference base	Alternative base	Read support	Type of DNA	Gene ID	Syn or Nonsyn?	Ref AA	Changed AA	Codon	Degeneracy of codon position
22450779	T	G	6	intronic/noncoding	AT3G60740					
22452107	A	G	8	intronic/noncoding	AT3G60740					
22452388	A	T	5	intronic/noncoding	AT3G60740					
22460890	C	-	7	intronic/noncoding	AT3G60770					
22460894	C	A	7	intronic/noncoding	AT3G60770					
22461119	T	C	9	intronic/noncoding	AT3G60770					
22462868	G	A	4	intronic/noncoding	AT3G60780					
22465099	T	C	8	intronic/noncoding	AT3G60790					
22465349	G	T	7	intronic/noncoding	AT3G60790					
22465436	A	C	5	intronic/noncoding	AT3G60790					
22465460	A	C	6	intronic/noncoding	AT3G60790					
22473510	T	G	9	intronic/noncoding	AT3G60820					
22478344	C	G	6	intronic/noncoding	AT3G60840					
22490818	A	-	11	intronic/noncoding	AT3G60860					
22502452	G	T	5	intronic/noncoding	AT3G60910					
22502570	T	A	4	intronic/noncoding	AT3G60910					
22504639	C	A	4	intronic/noncoding	AT3G60920					
22504650	T	C	4	intronic/noncoding	AT3G60920					
22507129	A	-	4	intronic/noncoding	AT3G60920					
22507146	T	C	5	intronic/noncoding	AT3G60920					
22507206	T	-	4	intronic/noncoding	AT3G60920					
22507443	A	G	5	intronic/noncoding	AT3G60920					
22507462	A	-	6	intronic/noncoding	AT3G60920					
22507463	A	-	6	intronic/noncoding	AT3G60920					
22507464	A	-	6	intronic/noncoding	AT3G60920					
22507466	G	-	6	intronic/noncoding	AT3G60920					

Continued on next page

Table 7 – continued from previous page

Positon	Reference base	Alternative base	Read support	Type of DNA	Gene ID	Syn or Nonsyn?	Ref AA	Changed AA	Codon	Degeneracy of codon position
22507583	T	C	5	intronic/noncoding	AT3G60920					
22507639	T	A	7	intronic/noncoding	AT3G60920					
22508293	A	G	5	intronic/noncoding	AT3G60920					
22508305	A	T	6	intronic/noncoding	AT3G60920					
22508775	G	T	6	intronic/noncoding	AT3G60920					
22508780	G	-	6	intronic/noncoding	AT3G60920					
22509123	T	A	5	intronic/noncoding	AT3G60920					
22509288	G	A	9	intronic/noncoding	AT3G60920					
22509426	C	T	6	intronic/noncoding	AT3G60920					
22510188	C	T	7	intronic/noncoding	AT3G60920					
22537000	T	C	12	intronic/noncoding	AT3G60960					
22537059	G	A	7	intronic/noncoding	AT3G60960					
22537556	G	A	8	intronic/noncoding	AT3G60960					
22537672	G	A	15	intronic/noncoding	AT3G60960					
22537807	C	T	9	intronic/noncoding	AT3G60960					
22537852	G	A	8	intronic/noncoding	AT3G60960					
22548892	A	T	13	intronic/noncoding	AT3G60961					
22548892	A	T	13	intronic/noncoding	AT3G60961					
22548947	A	G	5	intronic/noncoding	AT3G60961					
22548947	A	G	5	intronic/noncoding	AT3G60961					
22549669	T	A	8	intronic/noncoding	AT3G60961					
22549669	T	A	8	intronic/noncoding	AT3G60961					
22549688	G	A	5	intronic/noncoding	AT3G60961					
22549688	G	A	5	intronic/noncoding	AT3G60961					
22549693	A	T	5	intronic/noncoding	AT3G60961					
22549693	A	T	5	intronic/noncoding	AT3G60961					

Continued on next page

Table 7 – continued from previous page

Positon	Reference base	Alternative base	Read support	Type of DNA	Gene ID	Syn or Nonsyn?	Ref AA	Changed AA	Codon	Degeneracy of codon position
22549995	C	A	4	intronic/noncoding	AT3G60961					
22549995	C	A	4	intronic/noncoding	AT3G60961					
22550863	A	C	6	intronic/noncoding	AT3G60961					
22550863	A	C	6	intronic/noncoding	AT3G60961					
22550971	A	T	4	intronic/noncoding	AT3G60961					
22550971	A	T	4	intronic/noncoding	AT3G60961					
22551394	T	C	7	intronic/noncoding	AT3G60961					
22573526	C	A	6	intronic/noncoding	AT3G61010					
22573749	C	T	9	intronic/noncoding	AT3G61010					
22574423	A	G	6	intronic/noncoding	AT3G61010					
22583476	G	A	5	intronic/noncoding	AT3G61028					
22583494	A	C	7	intronic/noncoding	AT3G61028					
22583510	A	T	7	intronic/noncoding	AT3G61028					
22583704	C	G	6	intronic/noncoding	AT3G61028					
22583717	G	A	7	intronic/noncoding	AT3G61028					
22583761	C	A	6	intronic/noncoding	AT3G61028					
22598223	G	A	10	intronic/noncoding	AT3G61050					
22598350	T	A	8	intronic/noncoding	AT3G61050					
22598450	T	C	5	intronic/noncoding	AT3G61050					
22598732	C	G	4	intronic/noncoding	AT3G61050					
22599458	G	T	12	intronic/noncoding	AT3G61050					
22600293	G	C	9	intronic/noncoding	AT3G61050					
22600510	C	T	8	intronic/noncoding	AT3G61050					
22601109	T	C	9	intronic/noncoding	AT3G61050					
22601314	C	T	6	intronic/noncoding	AT3G61050					
22606517	T	-	7	intronic/noncoding	AT3G61070					

Continued on next page

Table 7 – continued from previous page

Positon	Reference base	Alternative base	Read support	Type of DNA	Gene ID	Syn or Nonsyn?	Ref AA	Changed AA	Codon	Degeneracy of codon position
22606519	C	-	7	intronic/noncoding	AT3G61070					
22606520	C	-	7	intronic/noncoding	AT3G61070					
22606521	A	-	7	intronic/noncoding	AT3G61070					
22606522	A	-	7	intronic/noncoding	AT3G61070					
22612098	A	G	11	intronic/noncoding	AT3G61110					
22612331	A	T	7	intronic/noncoding	AT3G61110					
22620251	G	T	5	intronic/noncoding	AT3G61120					
22620254	T	G	5	intronic/noncoding	AT3G61120					
22621995	A	-	4	intronic/noncoding	AT3G61130					
22621996	A	-	4	intronic/noncoding	AT3G61130					
22622979	T	-	5	intronic/noncoding	AT3G61130					
22622980	T	-	5	intronic/noncoding	AT3G61130					
22622981	T	-	5	intronic/noncoding	AT3G61130					
22622982	T	-	5	intronic/noncoding	AT3G61130					
22622983	T	-	5	intronic/noncoding	AT3G61130					
22622988	G	-	5	intronic/noncoding	AT3G61130					
22622995	T	G	5	intronic/noncoding	AT3G61130					
22622997	G	-	5	intronic/noncoding	AT3G61130					
22623098	G	C	8	intronic/noncoding	AT3G61130					
22623120	C	T	8	intronic/noncoding	AT3G61130					
22623293	C	T	4	intronic/noncoding	AT3G61130					
22623296	A	G	4	intronic/noncoding	AT3G61130					
22623352	C	A	6	intronic/noncoding	AT3G61130					
22623497	T	C	5	intronic/noncoding	AT3G61130					
22623642	T	-	6	intronic/noncoding	AT3G61130					
22624008	A	C	16	intronic/noncoding	AT3G61130					

Continued on next page

Table 7 – continued from previous page

Positon	Reference base	Alternative base	Read support	Type of DNA	Gene ID	Syn or Nonsyn?	Ref AA	Changed AA	Codon	Degeneracy of codon position
22624029	T	A	16	intronic/noncoding	AT3G61130					
22624039	T	C	13	intronic/noncoding	AT3G61130					
22624069	A	G	11	intronic/noncoding	AT3G61130					
22624088	T	C	5	intronic/noncoding	AT3G61130					
22625161	T	C	7	intronic/noncoding	AT3G61130					
22625181	A	C	4	intronic/noncoding	AT3G61130					
22627912	T	C	9	intronic/noncoding	AT3G61140					
22628695	A	T	4	intronic/noncoding	AT3G61140					
22628925	A	G	5	intronic/noncoding	AT3G61140					
22629661	A	T	4	intronic/noncoding	AT3G61140					
22632392	G	A	11	intronic/noncoding	AT3G61150					
22632419	A	C	6	intronic/noncoding	AT3G61150					
22636799	A	T	5	intronic/noncoding	AT3G61160					
22638120	A	G	5	intronic/noncoding	AT3G61160					
22639651	G	-	9	intronic/noncoding	AT3G61170					
22639659	T	C	10	intronic/noncoding	AT3G61170					
22641982	A	G	4	intronic/noncoding	AT3G61172					
22642029	T	C	4	intronic/noncoding	AT3G61172					
22682651	T	G	5	intronic/noncoding	AT3G61280					
22684969	A	C	6	intronic/noncoding	AT3G61290					
22685058	G	C	5	intronic/noncoding	AT3G61290					
22685066	C	A	6	intronic/noncoding	AT3G61290					
22685068	G	A	6	intronic/noncoding	AT3G61290					
22685071	A	G	7	intronic/noncoding	AT3G61290					
22685080	T	-	7	intronic/noncoding	AT3G61290					
22685081	A	C	6	intronic/noncoding	AT3G61290					

Continued on next page

Table 7 – continued from previous page

Positon	Reference base	Alternative base	Read support	Type of DNA	Gene ID	Syn or Nonsyn?	Ref AA	Changed AA	Codon	Degeneracy of codon position
22685237	C	T	8	intronic/noncoding	AT3G61290					
22685290	C	T	6	intronic/noncoding	AT3G61290					
22691716	A	C	4	intronic/noncoding	AT3G61310					
22617256	G	A	8	ncRNA	AT3G61118					
22403853	T	C	4	pseudogene	AT3G60610					
22404402	C	A	4	pseudogene	AT3G60610					
22404891	G	A	7	pseudogene	AT3G60610					
22404893	G	-	5	pseudogene	AT3G60610					
22575822	T	C	5	pseudogene	AT3G61020					
22575827	A	T	5	pseudogene	AT3G61020					
22576127	C	T	7	pseudogene	AT3G61020					
22577480	G	A	14	pseudogene	AT3G61020					
22649150	A	C	5	pseudogene	AT3G61185					
22306552	G	T	9	three_prime_UTR	AT3G60350					
22306553	A	T	9	three_prime_UTR	AT3G60350					
22320737	A	G	6	three_prime_UTR	AT3G60390					
22333644	G	A	6	three_prime_UTR	AT3G60410					
22342292	C	A	4	three_prime_UTR	AT3G60450					
22346964	G	C	4	three_prime_UTR	AT3G60470					
22356513	C	T	4	three_prime_UTR	AT3G60500					
22374330	A	T	7	three_prime_UTR	AT3G60530					
22374979	A	C	14	three_prime_UTR	AT3G60540					
22435790	A	T	4	three_prime_UTR	AT3G60690					
22456879	G	T	6	three_prime_UTR	AT3G60750					
22456880	G	T	6	three_prime_UTR	AT3G60750					
22467201	T	C	6	three_prime_UTR	AT3G60800					

Continued on next page

Table 7 – continued from previous page

Positon	Reference base	Alternative base	Read support	Type of DNA	Gene ID	Syn or Nonsyn?	Ref AA	Changed AA	Codon	Degeneracy of codon position
22521512	G	A	6	three_prime_UTR	AT3G60940					
22521556	G	A	6	three_prime_UTR	AT3G60940					
22565332	G	A	5	three_prime_UTR	AT3G60980					
22625574	C	T	11	three_prime_UTR	AT3G61130					
22625621	T	G	12	three_prime_UTR	AT3G61130					
22625638	T	-	13	three_prime_UTR	AT3G61130					
22625640	C	-	13	three_prime_UTR	AT3G61130					
22625668	A	C	11	three_prime_UTR	AT3G61130					
22629871	T	C	5	three_prime_UTR	AT3G61140					
22629945	G	A	7	three_prime_UTR	AT3G61140					
22630005	G	A	7	three_prime_UTR	AT3G61140					
22630036	A	T	6	three_prime_UTR	AT3G61140					
22634992	C	-	5	three_prime_UTR	AT3G61150					
22647557	T	A	8	three_prime_UTR	AT3G61180					
22658749	A	T	8	three_prime_UTR	AT3G61210					
22675370	G	A	9	three_prime_UTR	AT3G61260					
22686853	C	A	4	three_prime_UTR	AT3G61290					
22516501	T	C	7	transposon	AT3G60930					
22516510	T	C	7	transposon	AT3G60930					
22516580	T	G	6	transposon	AT3G60930					
22516597	C	T	5	transposon	AT3G60930					
22516614	C	T	4	transposon	AT3G60930					
22516682	A	G	5	transposon	AT3G60930					
22516695	G	A	6	transposon	AT3G60930					
22516844	A	G	10	transposon	AT3G60930					
22517386	T	A	4	transposon	AT3G60935					

Continued on next page

Table 7 – continued from previous page

Positon	Reference base	Alternative base	Read support	Type of DNA	Gene ID	Syn or Nonsyn?	Ref AA	Changed AA	Codon	Degeneracy of codon position
22519121	C	G	6	transposon	AT3G60935					

Table 8: *Indels in the BG-5 mapping interval*

Start position	End position	Min Size	Max Size	p-value
Insertion				
23414664	23414664	85	1	1.15E-05
Deletions				
22397091	22397436	295	346	5.22E-05
22553612	22553979	311	368	3.48E-05
22568559	22570719	2148	2161	0
22576292	22576640	313	349	1.18E-05
22578916	22582846	3932	3931	0
22660407	22660696	292	290	3.75E-05
22989719	22989851	279	133	7.56E-05
23255548	23255878	280	331	7.42E-05